Ivanna Hrynchak

Studies towards the synthesis of metabolites of mitoxantrone

Dissertação do 2º Ciclo de Estudos Conducente ao Grau de Mestre em Química Farmacêutica, Faculdade de Farmácia, Universidade do Porto

Trabalho realizado sob a orientação de:

Professora Doutora Emília Sousa

Professora Doutora Vera Marisa Costa

Setembro de 2017

(Assinatura do autor)

AUTHOR'S DECLARATION

Under the terms of the Decree-Law nº 216/92, of October 13th, is hereby declared that the author afforded a major contribution to the conceptual design and technical execution of the work and interpretation of the results included in this dissertation. Under the terms of the referred Decree-Law, is hereby declared that the following articles/communications were prepared in the scope of this dissertation.

The results presented in this dissertation are part of the following scientific publications/communications:

Review article published

I. Hrynchak, E. Sousa, M. Pinto, and V.M. Costa, "The importance of drug metabolites synthesis: the case-study of cardiotoxic anticancer drugs". *Drug Metabolism Review*, 2017, *49* (2), 158-196.

Poster communications

I. Hrynchak*****, E. Sousa, M.L. Bastos, M. Pinto, and V.M. Costa, "The main metabolites of mitoxantrone: Synthesis and Structure Elucidation". *Escola de Inverno de Farmácia* (**EIF2017**), Porto, Portugal, January 19-27, 2017.

I. Hrynchak*****; E. Sousa, M.L. Bastos, M. Pinto, and V.M. Costa, "Synthesis and Characterization of Main Metabolites of Mitoxantrone". 10º *Encontro de Jovens Investigadores da Universidade do Porto* (**IJUP17**), Porto, Portugal, February 8-10, 2017.

Accepted for Poster communication

I. Hrynchak*****, E. Sousa, M.L. Bastos, M. Pinto, and V.M. Costa, "Studies towards the synthesis of dicarboxylic acid metabolite of mitoxantrone". 12th Young Environmental Scientists Meeting (**YES2017**) Porto, Portugal, September, 14-17, 2017.

Oral communications

I. Hrynchak**,** A. Reis-Mendes, M.L. Bastos, M. Pinto, V.M. Costa, and E. Sousa*, "Old Sources for New Drugs: Challenges and Opportunities. *XXV* Encontro Nacional da Sociedade Portuguesa de Química (**XXV-EN**), Lisboa, Portugal, July, 16-19, 2017.

Course TOX-OER

Participation in Intense Learners Course on Cardiopulmonary toxicity in Hradec Kralové, Czech Republic, May, 8-14, 2017.

*presenting author

Acknowledgements

A realização desta tese de Mestrado em Química Farmacêutica contou, directa e indirectamente, com importantes apoios e incentivos sem os quais não seria possível cumprir os meus objectivos e concretizar esta etapa da minha formação académica. Este espaço é dedicado aos que deram o seu contributo para que esta dissertação fosse uma realidade. A todos eles deixo aqui o meu agradecimento sincero.

Quero agradecer em primeiro lugar à minha orientadora, professora Doutora Emília Sousa, pela sua orientação, apoio e total disponibilidade, pelo saber que transmitiu, pelas opiniões e críticas, pela colaboração no solucionar de dúvidas e problemas que foram surgindo ao longo da realização deste trabalho e por todas as palavras de incentivo.

À professora Doutora Vera Marisa Costa, minha co-orientadora, pela clareza e rigor, pelo apoio e toda a disponibilidade que sempre revelou para comigo, conselhos e sugestões, pelas oportunidades e desafios propostos além das palavras de ânimo e boa disposição.

À Professora Doutora Madalena Pinto, Diretora do Laboratório de Química Orgânica e Farmacêutica da Faculdade de Farmácia da Universidade do Porto, pela oportunidade e recetividade para desenvolver o meu trabalho neste grupo.

À Dra. Sara Cravo quero agradecer todo o apoio técnico, simpatia, preocupação, paciência e conhecimento transmitido. Muito obrigada!

À Gisela e Liliana pelo suporte técnico do laboratório.

À Filipa Mendes pela companhia e diversão durante o curso na República Checa, simpatia e por toda a ajuda laboratorial.

Aos meus amigos e colegas de laboratório, pela companhia nas horas extras, por todos os momentos de diversão, apoio, entreajuda, confiança, incentivo, companheirismo, e principalmente, pela amizade!

Aos meus amigos de Viseu, pelos curtos mas restauradores cafés, por durante certos momentos me permitirem olvidar as preocupações e receios da faculdade, por toda a amizade e confiança.

Um especial obrigada ao Luís por acreditar em mim e nas minhas capacidades, por todo o carinho diário, dedicação e confiança, pelo apoio incondicional em todos os momentos, pela inspiração e companhia, pela generosidade e por tudo o que representa para mim.

Aos meus manos, Marya e Miguel, pelo apoio prestado, pela compreensão e claro por estarem sempre a torcer por mim. A eles dedico este trabalho para que lhes possa servir de estímulo para fazerem mais e melhor!

Finalmente, gostaria de deixar um agradecimento muito especial aos meus pais, Halyna e Volodymyr, pela forma como me incutiram os valores e capacidades para ultrapassar todos os obstáculos ao longo deste percurso, pelo incentivo, força, inspiração e amor. Espero que esta etapa, que agora termino, possa de alguma forma retribuir e compensar todo o carinho, apoio e dedicação que constantemente me oferecem.

This work was developed in Laboratório de Química Orgânica e Farmacêutica, Departamento de Ciências Químicas, Faculdade de Farmácia da Universidade do Porto. We thank FCT/MCTES and ERDF through the COMPETE–POFC programme, under the Strategic Funding UID/Multi/04423/2013, the project PTDC/MAR-BIO/4694/2014 (POCI-01-0145-FEDER-016790; 3599-PPCDT) and PTDC/DTP-FTO/1489/2014 (POCI-01-0145-FEDER-016537) in the framework of PT2020, to INNOVMAR (NORTE-01-0145-FEDER-000035, NOVELMAR), supported by NORTE 2020, under PORTUGAL 2020, through ERDF. To Dr. S Cravo for technical assistance.

Index

Index of figures

Index of tables

Index of schemes

Abstract

Anticancer drugs currently enable more survivors as a result of more powerful drugs or combinations of drugs used in therapy. Thus, it is increasingly more important to study and overcome the side effects of these therapies. Mitoxantrone (MTX, **1**) has been used in patients with advanced breast cancer, prostate cancer, acute leukaemia, lymphoma, and in multiple sclerosis. One of the most relevant side effects on the long-term cancer survivors treated with MTX (**1**) is cardiotoxicity. The metabolites of this anticancer drugs are possible culprits of cardiotoxicity; however, data regarding the synthesis and toxicological evaluation of its metabolites are scarcely available. Therefore, the work aims to synthetize cyclic naphtoquinoxaline (NAPHT, **2**) metabolite, the main human metabolite, dicarboxylic acid derivative (**3**) of MTX (**1**), through total synthesis, and to synthetize possible MTX (**1**) acetylated metabolites, mono (**4**)- and di-acetoxy (**5**), to assess in the future their possible toxicity.

The synthesis of NAPHT (**2**) was accomplished by the horseradish peroxidase (HRP) catalyzed H_2O_2 oxidation. This derivative was isolated by high-performance liquid chromatography with diode array detector (HPLC-DAD) with a purity of 95% and 42% yield.

The total synthesis of the dicarboxylic acid (**3**) was performed via six steps starting from chrysazin (**7**). With this synthetic pathway, many by-products were obtained and the intermediates were all quite polar. Therefore, efficient processes of purification were not possible and consequently, this derivative has been obtained in 1.7% overall yield. The structure elucidation of dicarboxylic acid (**3**) was established by infrared (IR) and ^{1}H nuclear magnetic resonance (NMR) techniques.

To investigate the possibility of obtaining derivative **3** from commercial available MTX (**1**), several oxidative conditions were tested. Five reactions (oxidation catalyzed by tungstate, oxidation with sodium nitrite, oxidation with chromic acid, oxidation with potassium permanganate and, oxidation with potassium ferrocyanide) were investigated to try to obtain the dicarboxylic acid (**3**) derivative in a single step with improved yield. Unfortunately, none of the reactions provided the desirable compound. Many by-products were formed, some of which correspond to degradation products of MTX (**1**).

Finally, the synthesis of the mono (**4**)- and di-acetoxy (**5**) derivatives was performed with acetic anhydride (Ac_2O). The yields after purification of these compounds were 38 and 21% for mono (**4**)- and di-acetoxy (**5**) derivatives, respectively. These new derivatives were also characterized using IR and ^1H NMR techniques.

In the future, it would be important to improve the yield of the obtained products and to study the cardiotoxicity of the synthesized derivatives **2-5**, in order to verify if MTX (**1**) metabolites can influence the clinical cardiotoxicity of the drug.

Keywords: anticancer drugs, metabolites, mitoxantrone, synthesis, toxicity.

Resumo

A terapêutica anticancerígena atualmente permite assegurar mais sobreviventes como resultado de fármacos mais poderosos ou através do uso de combinações de fármacos. Assim, tornou-se, cada vez mais importante estudar e evitar os efeitos adversos dessas terapêuticas. A mitoxantrona (MTX, **1**) tem sido utilizada em pacientes com cancro de mama avançado, cancro de próstata, leucemia aguda, linfoma ou com esclerose múltipla. A cardiotoxicidade é um dos efeitos colaterais mais relevantes para os sobreviventes ao cancro submetidos a tratamentos com MTX (**1**). Os metabolitos deste fármaco anticancerígeno são possíveis causadores de cardiotoxicidade; no entanto, são escassos os dados, quer relativamente à sua síntese, quer à avaliação toxicológica dos seus metabolitos. Este trabalho teve como objectivo principal sintetizar o metabolito naftoquinoxalina cíclica (NAPHT, **2**); sintetizar o principal metabolito humano da MTX (**1**), o derivado ácido dicarboxílico **3**; e, por último, sintetizar os derivados mono- (**4**) e di-acetoxi (**5**) como possíveis metabolitos acetilados da MTX (**1**) para, futuramente, avaliar a possível toxicidade destes.

A síntese da NAPHT (**2**) foi concretizada através da oxidação catalisada pela peroxidase do rábano (HRP) na presença de H_2O_2. Este metabolito foi isolado por cromatografia líquida de alta resolução com detector de sistema de díodos (HPLC-DAD) com uma pureza de 95% e num rendimento de 42%.

A síntese total do ácido dicarboxílico (**3**) foi realizada através de seis passos reacionais tendo como ponto de partida a crisazina (**7**). Nesta síntese, vários subprodutos foram obtidos e devido à elevada polaridade dos intermediários, os processos de purificação foram comprometidos. Portanto, este derivado foi obtido num rendimento global de 1,7%. A elucidação estrutural do ácido dicarboxílico (**3**) foi conseguida por técnicas de infravermelho e ressonância magnética nuclear de protão.

No sentido de investigar a possibilidade de obter o derivado **3** a partir da MTX (**1**) comercialmente disponível, várias condições oxidativas de reação foram testadas. Foram investigadas cinco reações, por forma a obter o derivado do ácido dicarboxílico **3** num único passo e com maior rendimento. Infelizmente, nenhuma das reações permitiu obter o derivado pretendido. Foram encontrados muitos subprodutos, alguns dos quais correspondentes a produtos de degradação da MTX (**1**).

Finalmente, a síntese dos derivados mono (**4**)- e di-acetoxi (**5**) foi realizada com anidrido acético (Ac_2O). O rendimento após a purificação destes compostos foi cerca de 38 e 21% para os derivados mono (**4**)- e di-acetoxi (**5**), respectivamente. Estes novos derivados foram também caracterizados utilizando técnicas de infravermelho e ressonância magnética nuclear de protão.

Seria importante, no futuro, melhorar o rendimento dos produtos obtidos e estudar a cardiotoxicidade dos derivados sintetizados **2-5** de forma a verificar se os metabolitos da MTX (**1**) influenciam a sua cardiotoxicidade clínica.

Palavras-chave: anticancerígenos, metabolitos, mitoxantrona, síntese, toxicidade.

Abbreviations

Ac_2O	Acetic anhydride
AcOH	Acetic acid
AcONa	Sodium acetate
calc	Calculated
CYP	Cytochrome
deg	Degradation
DMF	*N*,*N*-dimethylformamide
DMS	Dimethyl sulfate
DNA	Deoxyribonucleic acid
d	Doublet
dd	Doublet doublet
FDA	Food and Drug Administration
h	hours
HPLC-DAD	High performance liquid chromatography – diode array detector
HRMS	High resolution mass spectrometry
HRP	Horseradish peroxidase
IR	Infrared
m	Multiplet
MTX	Mitoxantrone
NAPHT	Naphtoquinoxaline
NMR	Nuclear magnetic resonance
Py	Pyridine
ROS	Reactive oxygen species
r.t.	Room temperature
s	Singlet
SPE	Solid phase extraction
t	Triplet
TFA	Trifluoroacetic acid
TLC	Thin layer chromatography
TMS	Tetramethylsilane
UV-Vis	Ultraviolet-visible

Outline of the dissertation

CHAPTER 1 – INTRODUCTION

Chapter 1 includes a brief introduction to the importance of studying drug metabolism, methods to study metabolism and a brief description of synthesis, pharmacokinetics, and adverse effects of the anticancer drug, mitoxantrone (MTX, **1**).

CHAPTER 2 – AIMS

In this chapter, the main objectives are described.

CHAPTER 3 – RESULTS AND DISCUSSION

Results and discussion are divided into four topics. The first topic describes the synthesis and structure elucidation of NAPHT (**2**, Figure 1), the second topic describes the studies towards the synthesis of dicarboxylic acid (**3**). The third topic concerns the MTX (**1**) oxidation studies, and finally, the fourth topic describes the synthesis and the structure elucidation of the acetoxy metabolites, mono (**4**)- and di-acetoxy (**5**) derivatives.

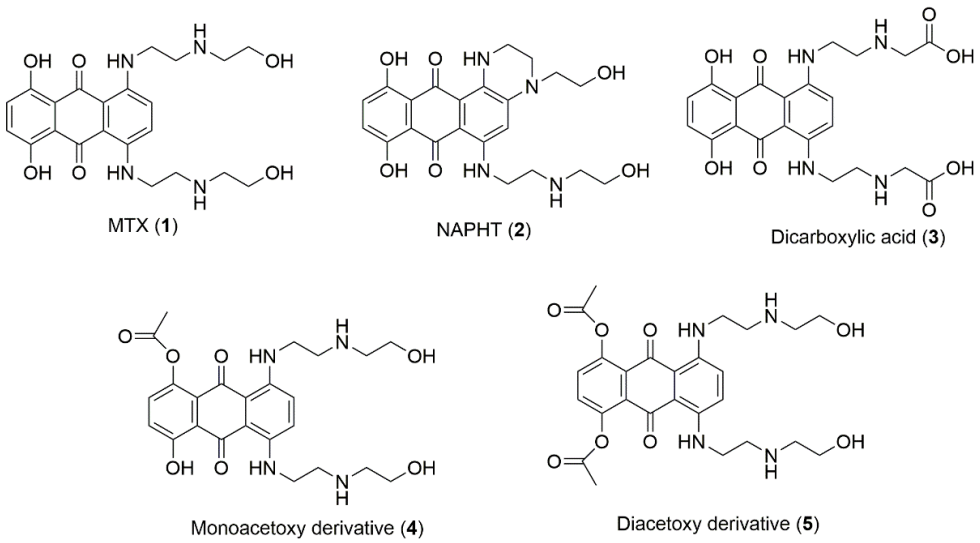

Figure 1 – Chemical structure of MTX (**1**), NAPHT (**2**), dicarboxylic acid (**3**), mono (**4**)- and di-acetoxy (**5**) derivatives.

CHAPTER 4 – CONCLUSIONS

This chapter summarizes the main conclusions concerning this dissertation.

CHAPTER 5 – MATERIAL AND METHODS

In this chapter, the general methods including the material used, reagents and also the structure characterization methods are described, as well as, the experimental procedures and conditions used for the synthesis of NAPHT (**2**), dicarboxilic acid (**3**), and mono (**4**)- and di-acetoxy (**5**) derivatives of MTX (**1**).

CHAPTER 6 – REFERENCES

In this chapter, the references cited throughout the dissertation are presented. The main bibliographic research motors were Scopus, PubMed and Google Scholar.

CHAPTER 1

Introduction

CHAPTER 1 – INTRODUCTION

1.1. Importance of the study of metabolism

During the drug development process, a selected drug candidate is thoroughly evaluated regarding the information of its metabolic pathway and pharmacokinetics. This information is required by regulatory agencies to better assess the safety of a drug candidate before it can be approved[1]. Many regulatory agencies have chosen over the years to incorporate metabolites on their safety evaluation guidelines[2] mainly because of putative active/toxic metabolites formation. In other words, if metabolites are suspected to contain a reactive functional group, it is important to assess the potential toxicity of reactive metabolites. In fact, many drugs can give rise to one or more metabolites with biological activity[1]. It should be noted that for the pharmaceutical researchers and regulatory agencies, the patient's safety is of paramount concern, especially if metabolites are suspected to be reactive and toxic[3].

Concerning toxicity, the early information on human metabolism of a new drug is essential to foresee the potential clinical drug–drug interactions and to select the appropriate animal species where those drugs are to be tested in pre-clinical studies. Regulatory agencies require human risk assessment to show that the systemic exposure to an unchanged drug and its major metabolites do not exceed the safety margin. Ideally, the metabolite profile of a drug obtained *in vitro* should generally mimic the *in vivo* metabolite pattern; however, *in vitro* models have limitations. Therefore, the comparison between animal and human metabolism should be performed in the early stage of the drug development process[1].

Different enzymes catalyse different steps of the metabolic pathways and these enzymes catalyse the biotransformation of xenobiotics, including drugs used in the clinical practice. Drug metabolism is usually divided in two phases: phase I or functionalization reactions and phase II or conjugation reactions. Phase I metabolism includes oxidation, reduction, hydrolysis, and hydration reactions. The cytochrome (CYP) P450 system has a major role in phase I reactions. The functionalization step usually transforms a drug into a more soluble and easier drug to eliminate. The phase II reactions or conjugation reactions include glucuronidation, sulfation, amino acid conjugation, acetylation, methylation or glutathione conjugation and they usually facilitate elimination[4].

As stated, the drug metabolism/biotransformation can lead to pharmacological activation or inactivation (Scheme 1). When metabolism results in the pharmacological activation with formation of pharmacologically active metabolites, a

process of bioactivation occurs. Fura *et al*. defined an active metabolite, as "a pharmacologically active metabolic product with activity against the same pharmacological target as the parent molecule". This concept of active metabolite differs from the definition of reactive metabolites that correspond to chemically reactive intermediates formed during metabolism. These reactive intermediates, when bound to biomolecules via covalent bonds, may elicit toxicity. Parameters, such as the contribution to the total pharmacological activity of a given dose of the parent compound, its intrinsic activity, and the relative concentration at the action site, measure the importance of a particular active metabolite[5]. Regarding the pharmacokinetic data, the mechanisms of distribution and clearance of active metabolites often differ from the parent drug. Therefore, to predict the therapeutic outcome and explain the toxicity of specific drugs, it is important to understand the kinetics of the formation of an active or reactive metabolite[1].

Another biotransformation process important in the drug discovery process is associated with the prodrug design. A prodrug can be defined as a pharmacologically inactive drug that turns into a pharmacologically active form, after *in vivo* administration. This transformation can occur either by metabolism or by spontaneous chemical breakdown[6]. Targeted prodrug approach is one of the new trends in the treatment of cancer. An ideal prodrug is one that increases the bioavailability and eliminates undesirable side effects of a drug. Prodrugs of antitumour agents are usually designed to be organ-specific and tumour-specific targeting. An alternative strategy used to reach the activation site in the field of prodrugs is the use of enzyme immunoconjugates towards antigens expressed on tumours cells and that, therefore, can target the tumour site[7].

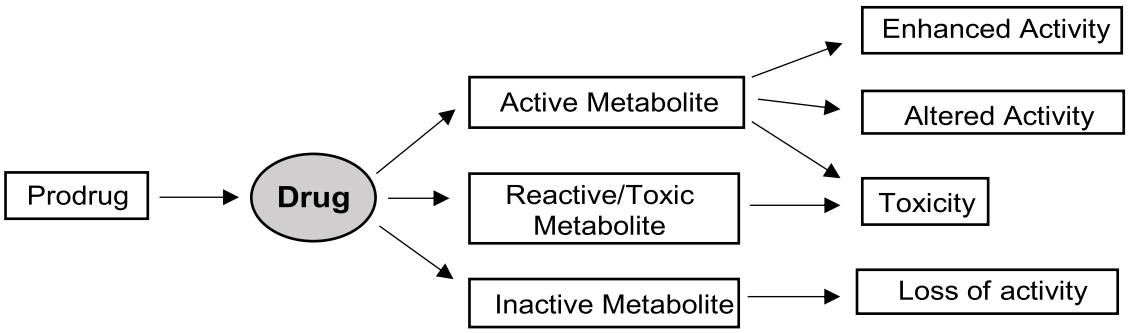

Scheme 1 – Biotransformation of drugs and its consequences. Adapted from[8].

1.2. *In vitro* and *in vivo* methods to study metabolism

In vitro and *in vivo* studies are performed in the pre-clinical stage to assess the toxicity of a drug and the metabolite profile before the drug goes into human clinical trials. This thorough evaluation is done in order to avoid failures and serious toxicity later on the drug development process[8]. Early *in vivo* investigations should assess the main metabolic routes[9] and the pharmacokinetic parameters of the most prominent compounds selected from *in vitro* studies[8].

In vitro studies are suited to determine the potential drug–drug interactions in clinical trials. Food and Drug Administration (FDA) guidelines suggest first the use of *in vitro* models to assess the effect of the drug on the metabolic pathways. If the results indicate possible drug–drug interactions, *in vivo* assays will follow. The main goal of the pre-clinical studies is to predict the *in vivo* outcome in humans. However, despite of the improvement of *in vitro* assays, the general consensus is that *in vitro* models are too simplistic to completely replace *in vivo* studies[8]. One can usually assume that potential clinical risks of the parent drug and its metabolites have been adequately investigated during nonclinical studies when the metabolite profiling of a parent drug is similar qualitatively and quantitatively across species, based on the data obtained from *in vitro* and *in vivo* metabolism studies[10].

1.2.1. *In vitro* studies

The *in vitro* studies during pre-clinical screening are based on low-throughput systems. It is presently possible to better predict the potential drug-drug interactions before clinical trials since there is a greater availability of human tissues and recombinant enzymes. *In vitro* studies have two major goals: identify the major metabolic pathways of the drug and its metabolites, and explore the effect of the test drug on the metabolism of other drugs. In addition, these studies may help to determine that a particular drug is not a substrate for certain metabolic pathways. The data obtained allows reducing or eliminating the need to study the possible inhibitory effects of that drug on other drugs metabolized by the same pathway. Usually, the first *in vitro* metabolic systems used in drug metabolism studies involve hepatic enzymes or tissue preparations[8] because liver is the main organ where biotransformation of foreign compounds takes place. Even so, other organs may also be involved in drug biotransformation[11], but they will not be addressed here for systematic purposes. The metabolites generated in the liver can, through distribution

on the blood, reach most of the organs, namely the heart. *In vitro* studies can give information about metabolite stability, metabolite profile, metabolite identification, allow interspecies comparisons, toxicology species selection, CYP induction/inhibition and drug/drug interaction studies, CYP isoform identifications and phase II enzyme studies[8]. Several *in vitro* human liver models have been developed, including: supersomes, cytosol, cell lines, transgenic cell lines, microsomes, isolated hepatocytes, tissue slices, S9 fractions, and isolated perfused liver. All these models except primary hepatocytes, cell lines, liver slices, and isolated perfused liver require exogenous cofactors to achieve the complete enzymatic activity[11].

1.2.2. *In vivo* studies

As part of the drug development process, pharmaceutical companies are required by regulatory agencies to study the metabolism of a given drug candidate. It is a part of the pre-clinical absorption-distribution-metabolism-excretion-transport (ADMET) studies, which are usually performed *in vivo* using animal models like rat, dog, or monkey[12]. The pharmacokinetic evaluation after multiple dosing can also be evaluated to identify potential auto induction. However, the fact that two drugs share a common metabolic pathway does not guarantee that they will have a clinically significant pharmacokinetic interaction when coadministered to a patient. Whether the two coadministered drugs will interact in humans depends on various factors, including the relative affinities of each drug for the binding site on the metabolizing enzyme, as well as, the effective free drug concentration available locally for binding. However, a small pharmacokinetic interaction can result in significant pharmacodynamic adverse effects for drugs with narrow therapeutic index[13].

In vivo drug metabolism studies include metabolite profiling in blood, selected tissues, urine, and bile to assess distribution and disposition of potentially important metabolites, such as the major metabolites and human unique metabolites. In many cases, metabolites can be easily found in excreta instead of blood. Since metabolites of a drug are present in the excreta, one can assume that systemic exposure to the drug has occurred[10]. FDA guidance defines major metabolites primarily as those identified in human plasma that account for higher than 10% of drug related material (administered dose or systemic exposure, whichever is lower)[14].

Appropriate qualitative and quantitative methods should be used to evaluate urine, faeces, and expired air (if certain amount of the drug and its metabolites is expected to be exhaled into air) from treated animals. In metabolites detected in

humans, as well as in animals, adequacy of systemic exposure should be assessed by measuring the concentration of the test drug in serum or plasma *versus* time curve (area under the curve, AUC). The AUC includes both the plasma concentration of the drug candidate and the residence time *in vivo*[10].

Pharmacovigilance studies in the later phase of the clinical drug development are valuable as a complement to test efficacy/safety. Some differences in the safety and efficacy of drugs are caused by genetic polymorphisms of metabolizing enzymes. Other factors may compromise efficacy/safety, namely transporters and drug receptors genetic polymorphisms. It is known that five CYP P450 enzymes - CYP1A2, 2C9, 2C19, 2D6, and 3A4 - are responsible for metabolizing most of the drugs commercially available. The CYP3A4 enzyme accounts for the biotransformation of 50% of these drugs. CYP2C9, CYP2C19, and CYP2D6 enzymes account for approximately another 40% of drug metabolism by CYP P450s and they exhibit high polymorphic rates[13].

Although the liver is the most important metabolizing organ, the gut is also a very important organ regarding metabolization. The anatomical location of enzymes in the gut wall provides an important and highly sensitive site of metabolically based interactions in orally administered drugs. The main intestinal biotransformation enzymes responsible for phase I reactions include CYP, esterases, epoxide hydrolase and alcohol dehydrogenase, and for phase II reactions glucosyltransferases, sulfotransferases (ST), *N*-acetyl transferases (NAT), and glutathione S-transferases (GST)[10].

1.3. Mitoxantrone

Chemotherapy-induced cardiotoxicity is a major drawback to the effective use of several anticancer drugs. Both conventional chemotherapy and targeted therapy agents cause cardiotoxicity[15-16].

Mitoxantrone (MTX, **1**), a synthetic anthraquinone, has a toxicity profile similar to the anthracyclines[17]. It is an antineoplastic agent with antiviral, antibacterial, and antitumour properties with a large spectrum of antitumour activity found in the late 1970s. Since then, MTX (**1**) has been used to treat breast cancer, acute leukaemia's, acute lymphomas, prostate cancer, and multiple sclerosis in adults[18].

1.3.1. Reasons that led to mitoxantrone synthesis

MTX (**1**) belongs to the class of anthracenediones. This is an important group of naturally occurring quinones found in plants and animals with a relative lack of any antitumour activity. However, the anthracyclines, doxorubicin and daunorubicin, exhibit outstanding antitumour activity and contain the anthracenedione ring framework in the tetracyclic chromophore portion of their ring structures (Figure 2)[19-20]. Nevertheless, the serious toxicity, especially causing irreversible damage to the heart muscle after extended therapy, and the difficulties in their chemical synthesis, namely the stereochemistry involved with the nonplanar, unaromatised ring moiety of tetracyclic aglycone, brought the need to further research. That research resulted in the production of a number of *bis*-substituted aminoanthracenedione derivatives[19]. Of those derivatives, the most active was MTX (**1**) (Figure 2)[20-22]. These derivatives arose from structural modifications of ametantrone (1,4-bis-[(2-[(2-hydroxyethyl) amino]ethyl)amino]-9,10-anthraquinone) (Figure 2), originally developed to be used as a ballpoint pen ink, and have shown to possess significant antineoplastic activity[19-20]. Thus, the analogues were synthesized and screened after the structural modification of doxorubicin and daunorubicin, based on the proposed N-O-O triangle theory (Figure 3)[20]. It consists of three electronegative atoms, each containing at least one lone pair of electrons (one nitrogen and two oxygen atoms) to form a triangular pattern and they are separated from one another at appropriate interatomic distances. The nitrogen component of the proposed triangular pattern for doxorubicin is located in the amino sugar daunosamine, whereas the two oxygen units are found in the aglycone portion of these molecules. This hypothesis was developed based on the interaction of aminoalkylaminoanthraquinones with deoxyribonucleic acid (DNA)[20]. Based in this N-O-O triangle theory, it was proposed to remove the daunosamine from these molecules and replace the amino function with a pertinent nitrogen atom as to complete the triangulation feature at a proper spatial distance from the oxygen atoms on the aglycone moiety. Another reason for the proposed removal of the amino sugar was that it was associated to the unwanted cardiac actions of anthracyclines[23].

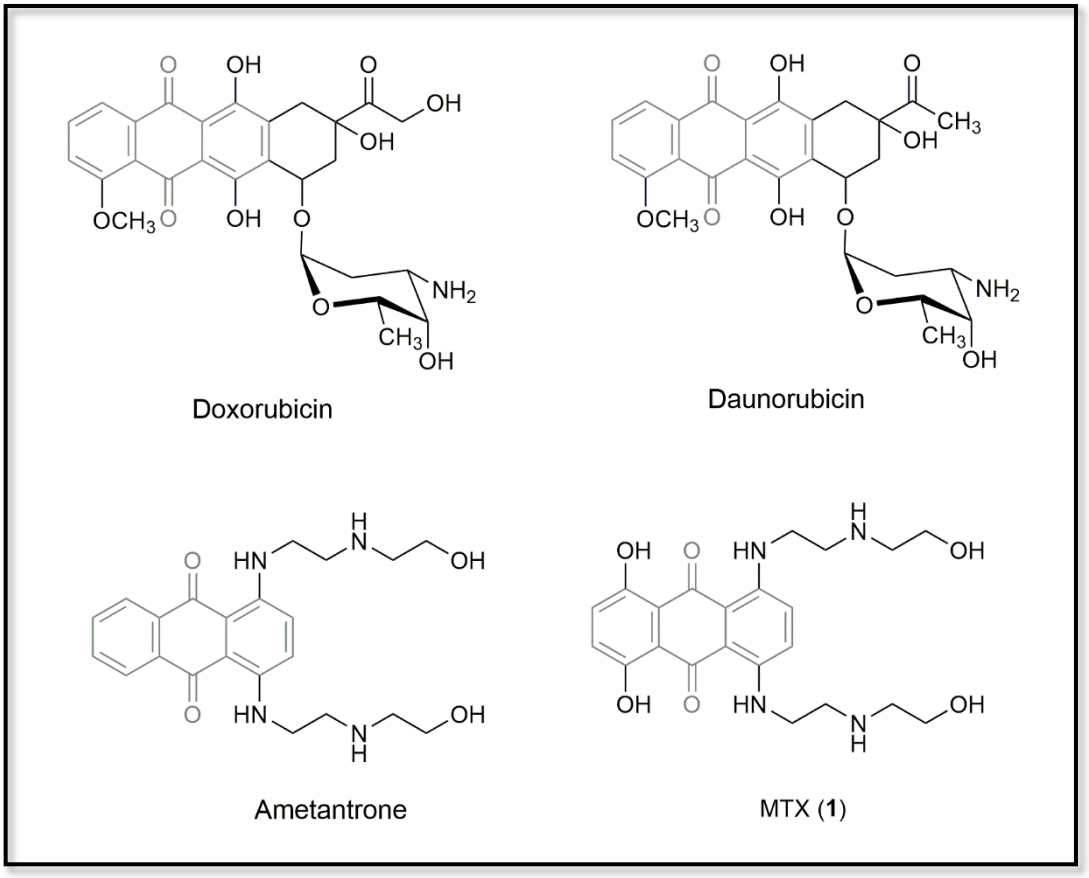

Figure 2 – Chemical structure of doxorubicin, daunorubicin, ametantrone, and MTX (**1**).

The aminoalkylaminoethanol side chain of ametantrone is quite unique in the sense that minor structural modifications resulted in compounds with diminished antineoplastic activity. Substitution or replacement of the nitrogen atom in the centre of this side chain by other atoms, such as sulphur or carbon, resulted in total loss of antineoplastic activity. Therefore, nitrogen atom in the centre of the side chain is very important for antineoplastic activity[20, 22]. The structural and spatial relationship of this nitrogen atom to two oxygen atoms on the dihydroxyanthracenedione ring of ametantrone has been correlated with that of the amino atom of daunosamine to the two oxygen functions on the aglycones of doxorubicin and daunorubicin (Figure 3)[20].

A comparative study between the structures of doxorubicin and of the ametantrone using molecular models revealed that, when the anthraquinone ring of ametantrone is placed directly over the planar portion of the aglycone of doxorubicin, the aminoethylaminoethanol side chain of ametantrone can be turned along its axis in such a way that the nitrogen atom in the centre of this chain and the nitrogen atom of the aminosugar daunosamine of doxorubicin are superimposable. When lacking

the nitrogen linkage, the derivative formed is totally devoid of antineoplastic activity[20]. The relevancy of this nitrogen atom to the originally proposed N-O-O triangulation pharmacophore was also confirmed by other authors that developed MTX (**1**)[22]. More, for good antineoplastic activity, the other oxygen atom required in ametantrone should be located on the neighbouring phenyl ring at the position *peri* to the quinone oxygen. Thus, an outstanding antineoplastic agent 1,4-dihydroxy-5,8- bis{[2-(2-hydroxyethyl)amino]ethyl} amino-9,10-anthracenedione, MTX (**1**) was prepared accordingly[20-21].

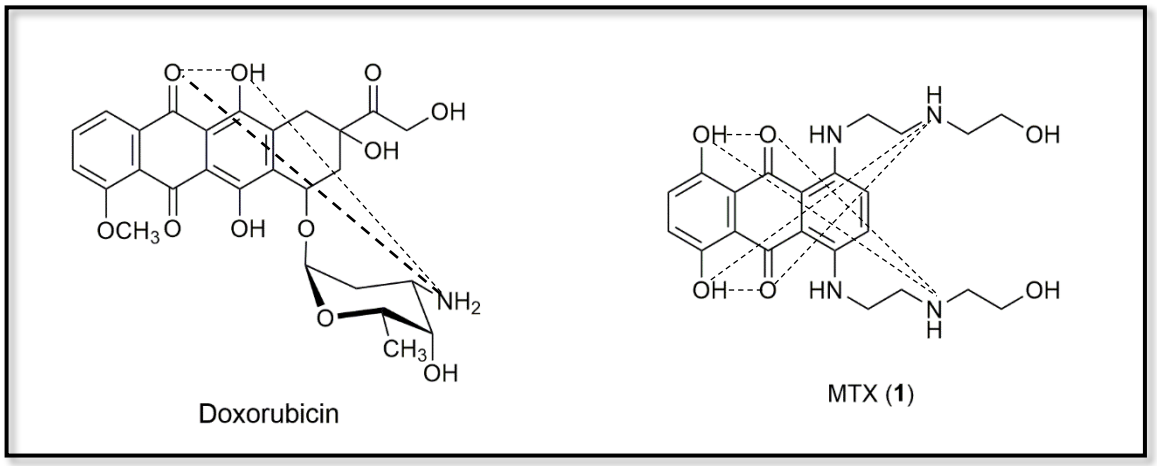

Figure 3 – N-O-O triangle theory.

1.3.1.1. Synthesis of mitoxantrone

The synthesis of MTX (**1**) hydrochloride involves the reaction between leuco-1,4,5,8-tetrahydroxyanthraquinone (**6**) and 2-[(2-aminoethyl)amino]ethanol to form 1,4-dihydroxy-6,7-dihydro-5,8-bis[{2-[(2-hydroxyethyl)amino]ethyl}amino]-9,10-anthranedione (Scheme 2). This product is aromatized with chloranil as the oxidant, and it is converted into MTX (**1**) hydrochloride by treatment with hydrogen chloride in ethanol. The crude product can be recrystallized from water-ethanol mixture[21, 24].

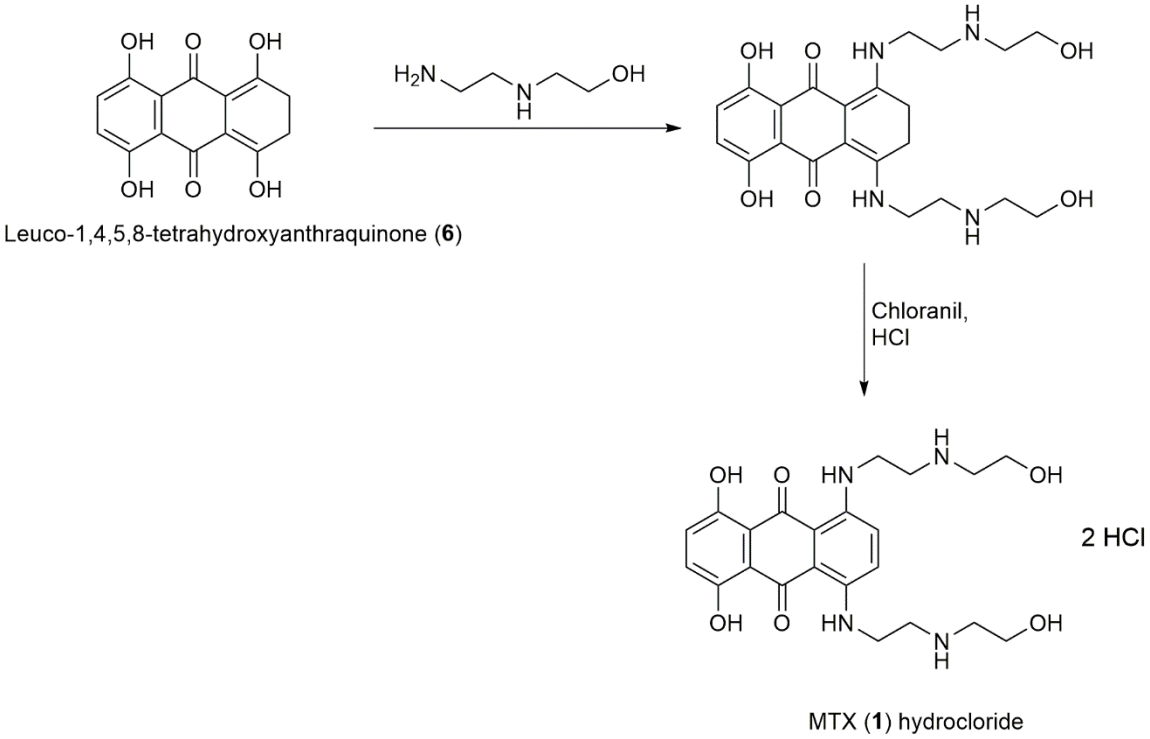

Scheme 2 – Chemical synthesis of MTX (**1**) hydrochloride[21].

An approach to synthetize MTX (**1**) hydrochloride was performed by Chang *et al*. via five reaction steps and started from chrysazin (**7**) with a yield of 32% (Scheme 3). The purification procedures during this synthesis were avoided because all intermediates had the same solubility problems. In this case, the aromatization was executed using dry air and the MTX (**1**) was obtained also by treatment with hydrogen chloride in ethanol[25].

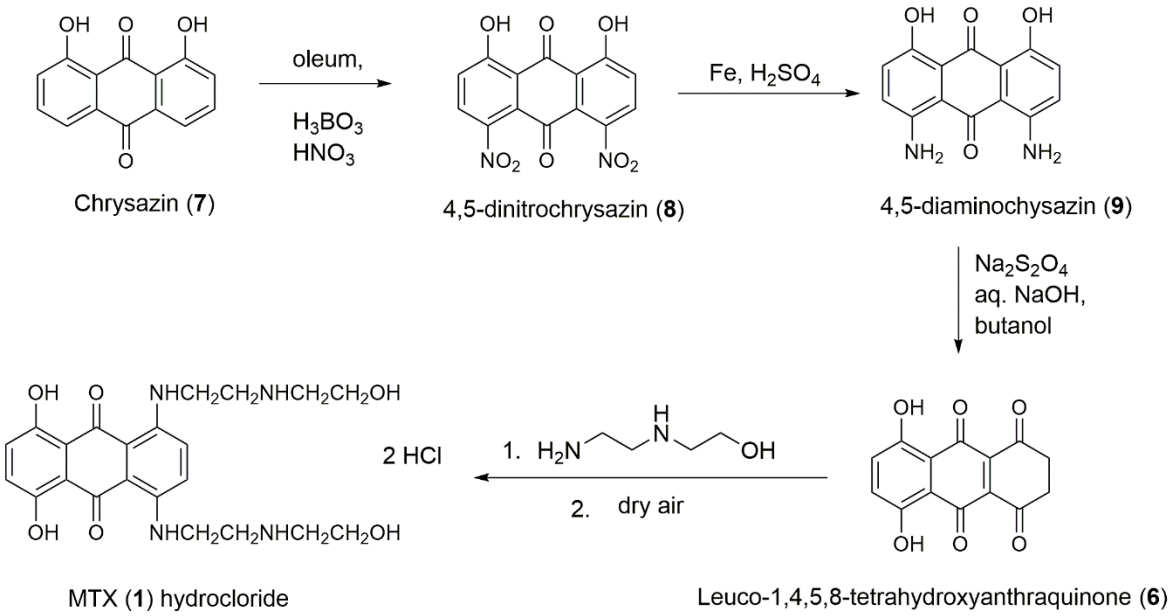

Scheme 3 – Preparation of MTX (**1**) hydrochloride[25]. aq – aqueous.

An alternative synthesis was developed by Krapcho *et al*. in which the starting material was 1,4-difluoro-5,8-dihydroxyanthracene-9,10-dione. The preparation of this product was accomplished using 2,5-difluorobenzoyl chloride and 2,5-dimethoxybenzaldehyde (Scheme 4)[26]. The overall strategy relied on initial ring-forming reactions to build the anthraquinone framework. The amino alcohol side chain is installed at the very last stage by nucleophilic displacement of a fluoride leaving group[26-27].

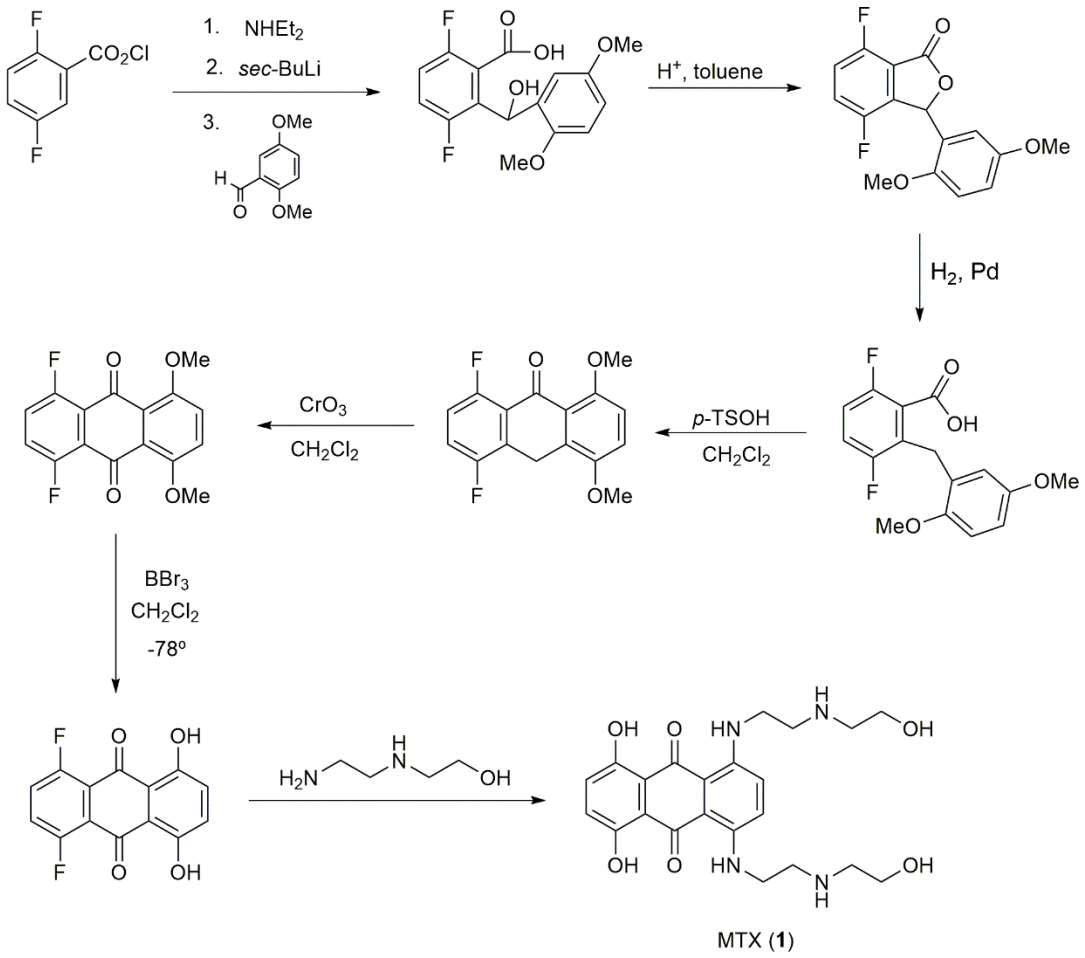

Scheme 4 – Alternative synthesis of MTX (**1**)[26]. $NHEt_2$ – diethylamine; *sec*-BuLi – *sec*-butyllithium; *p*-TSOH – *p*-toluenesulfonic acid.

MTX (**1**) and MTX (**1**) hydrochloride were manufactured and/or formulated in seven and 31 countries, respectively[28].

1.3.2. Anticancer mechanisms of mitoxantrone

The exact mechanisms by which MTX (**1**) exerts anticancer proprieties have not been thoroughly elucidated yet. Different mechanisms of action have been suggested due to the structural characteristics of MTX (**1**) like its planar electron-rich chromophore and to the electrostatic interactions of its basic side chains with the anionic exterior of the DNA chain[19]. Like anthracyclines, namely doxorubicin, MTX (**1**) also intercalates the DNA helix leading to an inhibition of ribonucleic acid (RNA)

and DNA synthesis, induces single strand and double strand breaks in DNA, and causes chromosomal scattering. These drugs cause DNA breakage by stabilisation of a complex formed between DNA and topoisomerase II, an enzyme responsible for uncoiling and repairing damaged DNA[29-30]. Also, doxorubicin is a more potent inhibitor of RNA synthesis, and to a lesser extent of protein synthesis when compared with MTX (**1**)[31]. MTX (**1**) also causes inhibition of prostaglandin biosynthesis and calcium release[19, 32]. MTX (**1**) lacks of cell cycle phase specificity due a cytocidal effect on both proliferating and non-proliferating cultured human cells[33].

1.3.3. Pharmacokinetics

MTX (**1**) has a low absorption rate when administered orally and for this reason MTX (**1**) is administered via intravenous injection[34]. MTX (**1**) presents a large volume of distribution that suggests that much of the drug is sequestered in the tissues[19]. Steady-state volume of distribution exceeds 1.000 L/m^2. The concentrations of MTX (**1**) in tissue appear to exceed those in the blood during the terminal elimination phase. In the concentration range of 26-455 ng/mL, 78% of MTX (**1**) is bound to plasma proteins[33-34]. During a phase II clinical trial, MTX (**1**) (12 mg/sq m) and ^{14}C-labeled MTX (**1**) (8.85 iCi/mg) were administered to eight patients who had advanced soft tissue cancers[35]. Alberts *et al*.[35], concluded that MTX (**1**) appears to distribute into a deep tissue compartment from which it is slowly released. These data provided a pharmacological rationale for the use of MTX (**1**) on an intermittent dosing schedule. MTX (**1**) has relatively low urinary excretion, with only 6.5% of the total MTX (**1**) dose administered excreted in the urine as unchanged drug over the next 5 days. The mean recovery of radioactivity in faeces was 18.3% over 5 days indicating that biliary detoxification is the major excretory pathway in humans. One of the patients died of progressive kidney cancer thirty-five days after MTX (**1**) administration and 15% of MTX (**1**) was found in seven major organs: liver, bone marrow, heart, lungs, spleen, kidney, and thyroid glands[35]. Two major polar metabolites of MTX (**1**) have been isolated and purified from the urine of patients, the mono (**10**)- and di-carboxylic (**3**) acids (Scheme 5), (section 1.3.4)[36].

A long terminal half-life of MTX (**1**) was reported in patients with advanced breast cancer that were treated with MTX (**1**) 14 mg/m^2 as an intravenous infusion over 30 min on day one and cyclophosphamide 600 mg/m^2 intravenous on day two[37]. Those patients had normal renal and liver function and were not previously treated with any chemotherapy agent. The mean alpha half-life of MTX (**1**) is 6 to 12 minutes,

the mean beta half-life is 1.1 to 3.1 hours (h) and the mean gamma (terminal or elimination) half-life is median approximately 75 h (23 to 215 h)[33].

In a study of 1983, a single intravenous dose 12 mg/m^2 of ^{14}C-labelled MTX (**1**) was administrated to eight patients with disseminated solid tumours and the plasma clearance rate of MTX (**1**) was 0.6 L/min/m^2 and the renal clearance rate was 70 mL/min[38].

MTX (**1**) is excreted in urine and faeces, as either unchanged drug or as metabolites [mono (**10**)-, di (**3**)-carboxylic acid derivatives, and their glucuronide conjugates (**11**)][17, 33]. Biliary excretion is an important excretory pathway for MTX (**1**) and its metabolites. In a study of 2010, biliary excretion in rats of the intact drug accounted for 5.69 ± 0.59% of the dose following a 2 mg/kg intravenous dose or 0.5 mg/kg of MTX (**1**). Biliary excretion of the parent drug occurred very rapidly, in the first hour after dosing, and more than 90% of MTX (**1**) is excreted in bile. Breast cancer resistance protein (BCRP) or P-glycoprotein (P-gp), or both, play an important role in the biliary elimination of MTX (**1**) since inhibition by GF-120918, a potent inhibitor of BCRP and P-gp, changed its excretion[39]. The metabolites of MTX (**1**) will be further discussed below.

1.3.4. Metabolites of mitoxantrone: *in vitro* and *in vivo* studies

The main MTX (**1**) metabolites (Scheme 5) were identified as being the monocarboxylic acid (**10**) and dicarboxylic acid (**3**) resulting from the oxidation of the terminal hydroxyl (OH) groups of the side chains. These two metabolites, isolated from patients' urine, are more polar than MTX (**1**)[36, 40]. The patients received intravenous dose of 12 mg/m^2 of MTX (**1**) in both studies[36, 40]. Both the metabolites (**10** and **3**) have been tested for antineoplastic activity but neither has shown any *in vitro* activity. They were also tested against P388 leukaemia in mice and were both inactive. For this reason, mono **10**- and dicarboxylic **3** metabolites are regarded as metabolic detoxification products[36].

There are studies confirming that the glucuronide **11** is also an urinary metabolite of MTX (**1**) in humans[34], whereas the MTX glutathione **12** metabolite (Scheme 5) was only detected in *in vitro* models so far[41-42].

The metabolic profile of MTX (**1**) has been also studied *in vitro*, in several models such as primary cultures of hepatocytes isolated from rats, rabbits, and humans[43-44], microsomes[45], perfused liver[37], cell lines (H9c2 and HepG2), and hepatic rat S9 fractions[42].

In a study with isolated perfused rat liver model, it was demonstrated that MTX (**1**) was extensively and rapidly metabolized and the mono- **10** and dicarboxylic **3** acid derivatives represented a very low percentage of the metabolites excreted in bile[46]. In another study, Wolf *et al.*, identified the glutathione **12**- and glucurono **11**-conjugates of MTX (**1**) as the main MTX (**1**) metabolites in rat liver microsomal fractions and in hepatocyte homogenates[45]. In the case of the cyclic naphtoquinoxaline (NAPHT, **2**) metabolite, it has been stated that it may have anticancer properties[47] but in *in vitro* models (e.g. neonatal cardiomyocytes of the rat and in H9c2 differentiated cells), it seems a more cardio-safe metabolite when compared with MTX (**1**)[48-49]. Moreover, the other metabolites described above were not studied yet regarding their cardiotoxicity.

In a recent study, Rossato *et al.* studied the metabolic profile of MTX (**1**) after incubation of 100 µM of MTX (**1**) at 37 ºC, for 4 h using phenobarbital-induced hepatic S9 fraction from adult rats and five metabolites were identified by liquid chromatography-diode array detection/electrospray ionization-mass spectrometer (LC-DAD/ESI–MS) after 4 h. Those metabolites were the NAPHT **2** metabolite, acetoxy ester metabolite **13**, glutathione metabolites **14, 15** and the monocarboxylic acid derivative **16** (Scheme 5). In the same study, the cytotoxic effects of MTX (**1**) and MTX (**1**) metabolites mixture was assessed in non-differentiated H9c2 cells by the reduction of 3-(4,5-dimethylthiazol-2-yl)-2,5-diphenyltetrazolium bromide (MTT). Even with a reduction of 35 % of the MTX (**1**) content in the mixture obtained after S9 fractions, the mixture of MTX (**1**) and metabolites was more cytotoxic than MTX (**1**) at higher levels. It was also shown, in a cardiomyoblast model, that prevention of MTX (**1**)-induced cytotoxic effects was accomplished by co-incubation with CYP450 metabolism inhibitors, namely by a CYP2E1 inhibitor[42].

NAPHT (**2**), a product of biotransformation of MTX (**1**) *in vivo* in humans, pigs, and rats[40, 42], is a product of metabolism of CYP P450 enzymes or peroxidases[50]. This transformation to a metabolite **2** containing an additional ring proves the existence of a redox system involving MTX (**1**) and its oxidized form is responsible for the generation of a free radical intermediate [51]. MTX (**1**) was administered at a dose of 12 mg/m^2 to patients with breast cancer and cyclophosphamide was administered at a dose of 600 mg at the same day. In case of rats, 9.7 mg/kg of radioactive MTX (**1**) was given and, in pigs, 6.5 mg/kg of ^{13}C-labeled was injected[40]. In both studies, the presence of the metabolite NAPHT **2** in the urine was detected, thus proving the existence of intracellular enzymes capable of oxidizing MTX (**1**) *in vivo.* Moreover, Rossato *et al*, evaluated the metabolic profile *in vivo* in rats that received 7.5 mg/kg of MTX (**1**) 24 h before. In the liver of the MTX (**1**)-treated animals

four metabolites were identified: NAPHT **2**, acetoxy ester metabolite **13**, glutathione metabolite **14**, and monocarboxylic acid derivative of MTX **16**, whereas, in the heart the NAPHT **2** was the only metabolite detected[42].

In another study that aimed to explore the biotransformation of MTX (**1**), it was incubated with rat, rabbit, and human hepatocytes. When MTX (**1**) was incubated with rat hepatocytes (between 10 and 100 µM), it was rapidly taken up by the cells as observed by the cellular distribution of the blue drug. Two metabolites were produced in rabbit and human hepatocytes but not in rat hepatocytes, the mono- **10** and dicarboxylic **3** acids. Moreover, the glutathione **14**, cysteinylglycine **17** and, cysteine derivatives of MTX **18**, and a thioether conjugate of MTX (**19**) (Scheme 5) were also identified[41]. In the same study, human HepG2 hepatoma cells were incubated with MTX (**1**) for 24 h and in the cell lysates of HepG2 cells, 2-(L-cysteine-5-yl)-MTX (**18**) was identified, while the glutathione metabolite **14** and cysteinylglycine **17** metabolite were not detected. Moreover, the cytotoxic effect of MTX (**1**) on HepG2 cells revealed that these cells were less sensitive to the parental compound than to its metabolites: only at concentrations above 200 µM of MTX (**1**) a significant cytotoxic effect was observed, leading to about 20% cell death, during a 9 h incubation period, while in rat hepatocytes 400 µM of MTX (**1**) killed approximately 50% of the hepatocytes. An increasing number of hepatocytes were affected after 9 h of incubation, and 20% of hepatocytes were killed at 25 µM of MTX (**1**), according to the leakage of lactate dehydrogenase assay. However, no MTX (**1**)-induced cytotoxicity occurred in HepG2 cells and rat hepatocytes (up to 200 to 400 µM) after inhibition of CYP P450 with metyrapone[41]. Previously, it was demonstrated that the cytotoxicity of this quinone could be enhanced by inhibiting epoxide hydrolase[31]. The authors claimed that the cytotoxicity of MTX (**1**) is dependent upon metabolism by CYP P450 isoenzymes and of the formation of the thioether conjugates **19**[41]. Moreover, the metabolites **14** and **15** were previously found after incubation of MTX (**1**) with horseradish peroxidase (HRP) and glutathione[40].

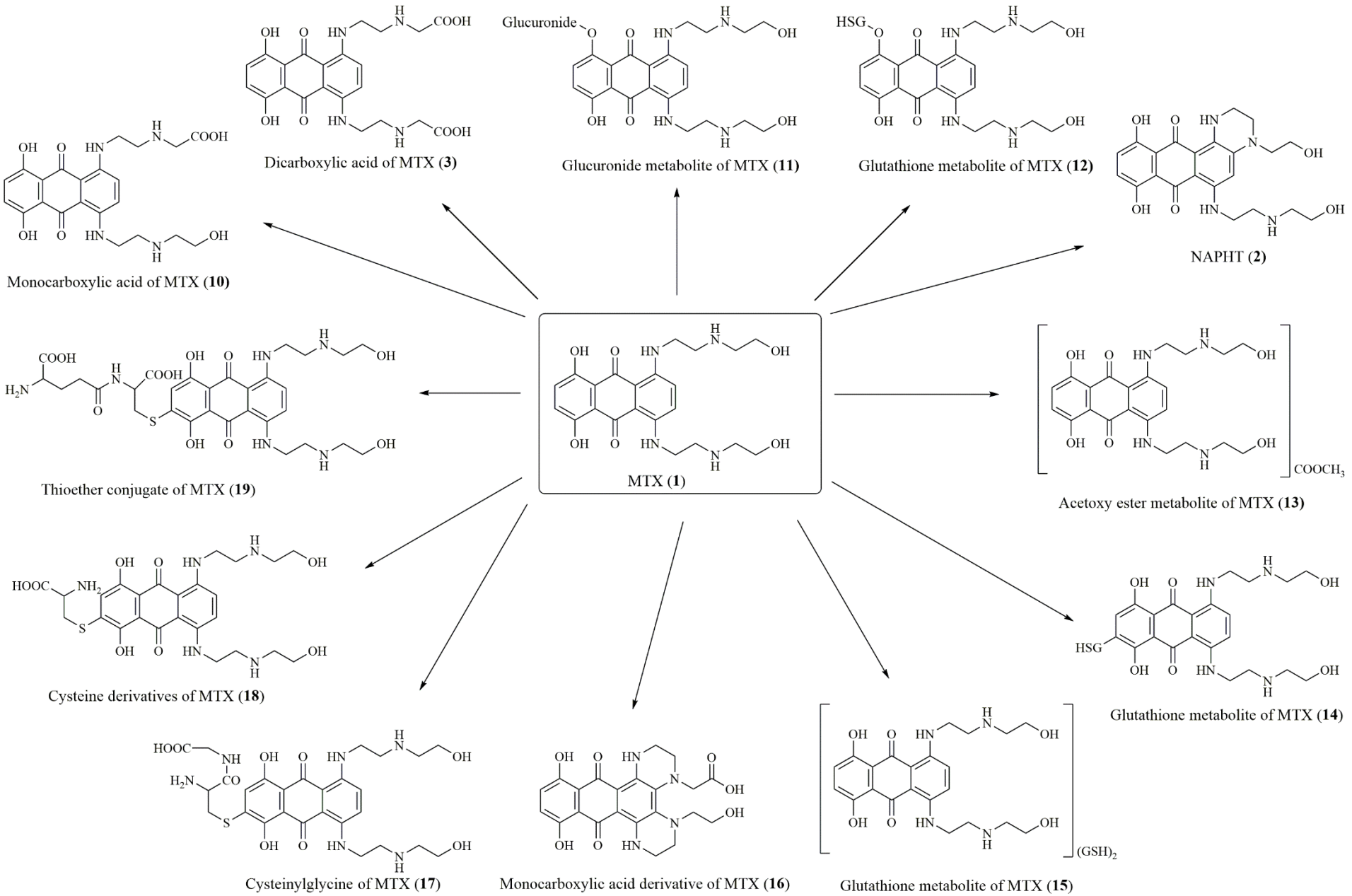

Scheme 5 - Metabolites resulting from MTX (**1**)[41-42, 52].

1.3.4.1. Chemical synthesis of metabolites

The metabolites can be identified from biological fluids such as plasma, urine, or faeces or using *in vitro* models. However, the metabolites are often present at low concentrations in biological fluids and chemical synthesis emerges in this scenario as a valuable approach since high amounts of metabolites are often necessary to research their activity/toxicity[53]. The synthesis of metabolites may be done by classical synthesis using total or semi-synthesis and/or enzymes. The use of the enzymatic methods in the synthesis of drug metabolites has the advantage of enabling in one step, by a biomimetic synthesis, to obtain the drug metabolites using the same biotransformation reactions that occur *in vivo*. Nevertheless, this biomimetic method for obtaining metabolites is not always accurate; it is very specific for each metabolite and can be also very time consuming. The synthetic procedures used to obtain MTX (**1**) metabolites will be highlighted in the next section.

1.3.4.1.1. Synthesis of mitoxantrone metabolites

In most studies, the metabolites are chemically obtained and then isolated using diverse purification procedures[40]. Nevertheless, in some cases, the crude product was used in biological studies without further purification[36, 54]. Most of the syntheses involved chemical reagents, but in conjugations reactions, enzymes are more frequently applied[55]. Regarding MTX (**1**), very few studies were done using the metabolites[48-49] in cellular models, while others made identification of the metabolites in biological matrixes[40-42]. Moreover, very few works were done regarding their synthesis and reported yields were low.

The mono **10**- and dicarboxylic **3** metabolites were synthesized from the same starting material, 2,3-dihydro-1,4,5,8-tetrahydroxy-9,10-anthracenedione as for the synthesis of MTX (**1**). In the case of the dicarboxylic acid **3**, this was prepared with *tert*-butyl 2-aminoethylaminoacetate, followed by oxidation with chloranil and acid hydrolysis. The monocarboxylic acid **10** metabolite was prepared with 2-(2-aminoethylamino)ethanol and *tert*-butyl 2-aminoethylaminoacetate, followed also by oxidation and hydrolysis[36]. Nevertheless, details concerning the experimental procedure for their synthesis or their structure elucidation were not provided.

The synthesis of NAPHT (**2**) metabolite was also already described and began by dissolution of MTX (**1**) in ammonium acetate buffer (pH 5) containing hydrogen peroxide (H_2O_2) (3%) with dry HRP. This reaction was completed by addition of ascorbic acid[40]. A more recent synthesis of NAPHT (**2**) metabolite, performed by Reis-Mendes *et al*., in 2017 presented a similar procedure. The synthesis began with solution of MTX (**1**) in sodium acetate buffer (pH 6), HRP with perhydrol. In this case, the crude product was purified by preparative column chromatography with silica C18[49].

Finally, the synthesis of glutathione conjugate **12** of MTX (**1**) followed the same conditions as described in the synthetic procedure for NAPHT (**2**) metabolite but with addition of solid glutathione before the HRP addition had to be performed[40].

1.3.5. Adverse effects of mitoxantrone

MTX (**1**) has long been used as a first-line single agent in patients with solid tumours[56]. In 1979, the first phase I trials using MTX (**1**) were begun. All patients had received prior treatment with multiple chemotherapeutic agents and 45% had received prior radiotherapy to the primary tumour or metastases. Twenty-five patients received a single intravenous injection in a total of 41 courses of the drug in a dose range of 1.2 to 14 mg/sq m (based on dosages used in dog toxicity studies). Dosage was increased if no toxicity was seen 3 weeks after the therapy at the previous level. The results indicated that MTX (**1**) has tolerable toxicity and can be given safely as a single dose every 28 days. Only leukopenia and thrombocytopenia were dose limiting side effects but those effects were of short duration and rapidly reversible[57]. In another study, twenty-six patients with relapsed acute leukaemia were treated with MTX (**1**). All patients, with one exception, had been treated previously with anthracyclines. The drug was given as a rapid intravenous infusion in higher dosages ranging from 8 to 20 mg/m^2 for 5 days. Mucositis oral was the dose-limiting toxicity[58].

Like other anthracyclines, the main side effect of MTX (**1**) is cardiotoxicity and this acute toxicity has been reported[59-60]. MTX (**1**) is a chemotherapeutic agent used in the treatment of some cancers and aggressive multiple sclerosis that causes a progressive heart failure and, consequently, can result in cardiac death[18]. The short and long term toxicity of MTX (**1**) was first considered lower compared with doxorubicin[19]. However, at the same clinically equivalent dose, MTX (**1**) causes equivalent

cardiotoxicity compared with doxorubicin[30, 52]. In large phase II studies, summarized by Smith *et al*. of 505 patients treated MTX (**1**) at the standard dose of 12–14 mg/m^2, 5% experienced very severe leukopenia and 0.8% experienced very severe thrombocytopenia. Also after treatment with MTX (**1**), eight out of 543 patients experienced unspecified cardiotoxicity and seven others congestive cardiac failure or pulmonary oedema. Total incidence of cardiotoxicity was approximately 3%[60]. Some risk factors, like previous anthracycline therapy, mediastinal radiotherapy and a history of cardiovascular disease may be predictive of the cardiotoxicity of this drug[59]. Myelosuppression is the principal dose limiting toxicity of MTX (**1**) and is predominantly due to granulocytopenia. Other toxic effects seen with standard 12–14 mg/m^2 doses of MTX (**1**) include nausea and vomiting in 50% of patients, diarrhoea in 15%, stomatitis and mucositis in 20% and alopecia in 50% of patients. These secondary effects are usually mild and transient[59]. As the drug is an intense blue colour, it often occurs discolouration of urine and skin. MTX (**1**) also induces onycholysis when administrated intravenously 15 mg (10 mg/m^2)[61]. With higher doses like 90 mg/m^2, the toxic effects are more severe[62]. Hepatotoxicity also has been reported[63].

1.3.5.1. Cardiotoxicity of mitoxantrone

At a chemical level, the main alteration of MTX (**1**) when compared to anthracyclines is the replacement of the amino sugar on the anthracyclines for an aminoalkylalcohol chain[64]. This compound was structurally designed to have little or no cardiotoxicity when compared to its analogue, doxorubicin. Batra *et al*., tried to demonstrate the lower short and long term MTX (**1**) toxicity when compared to doxorubicin [34] in animal models; however in other animal studies[65-66] the data first gathered was not corroborated. The cardiotoxicity of MTX (**1**) was verified in animal models and in clinical settings. In animals, MTX (**1**) caused changes in the cardiac structure and increases in the % of relative heart mass per body weight[65]. In mature adult animals, MTX (**1**) caused several cardiac insults, while juvenile animals seem more resilient to cardiac damage provoked by MTX (**1**)[66]. In a phase II clinical study, important side effects following administration of MTX (**1**) to patients with malignant solid tumours were sometimes reversible; however, fatal congestive heart failure has been also detected[64]. The number of cardiotoxic events increases with cumulative doses of MTX

(**1**). Henderson *et al*. reported in eight of 132 patients treated with cumulative doses >100 mg/m^2 of MTX (**1**), moderate to severe decreases in left-ventricular ejection fraction[67]. MTX (**1**) also is associated with the deterioration of cardiac function[67].

In patients with prior anthracycline therapy, MTX (**1**) has been associated with cardiac toxic events in a few patients, ranging from transient electrocardiographic changes to congestive heart failure, being that haematological effects are dose-limiting[59]. In a phase II trial done to evaluate left ventricular function in seven patients with no prior doxorubicin exposure that received up to 204 mg/m^2 of MTX (**1**), none of these patients showed evidence of clinically significant myocardial damage but one had a decline in left ventricular ejection fraction from 70% to 50% at a maximum dose of 108 mg/m^2 [68]. Patients treated with MTX (**1**) for childhood malignancies are at risk of developing cardiotoxicity, those odds being between 0 and 6.7% for clinical heart failure and between 0 and 80% for asymptomatic cardiac dysfunction[69].

More recently, MTX (**1**) has been established efficacious for treatment of multiple sclerosis, yet its usage is limited by serious toxicities, such as cardiotoxicity and myelosuppression[70-73]. MTX (**1**) induced a profound reduction in immune response by inhibiting T-cell, B-cell, and macrophage proliferation. This reduces neurologic disability and relapse frequency in patients with secondary progressive multiple sclerosis[74]. MTX (**1**)-treated multiple sclerosis patients are at higher risk of developing cardiotoxicity. Because of this risk of cardiotoxicity, the cumulative lifetime dose of MTX (**1**) in patients with multiple sclerosis must be limited to 100 mg/m^2, or 2 to 3 years of therapy at the approved dosage of 12 mg/m^2 [33]. There are reports where 25 % of patients with multiple sclerosis have subclinical ventricular dysfunction and decreased ventricular ejection fraction[74]. In 2005, 73 patients (25 with primary progressive, 47 with secondary progressive and one with relapsing-remitting multiple sclerosis) received at least four courses of MTX (**1**) (114.0 ± 33.8 mg/m^2). The mean age of the patients was 48 ±12 years and ranged from 20-75 years. In this study, MTX (**1**) did not cause signs of congestive heart failure in any of the patients[70]. In another study, four of 18 patients (without history of cardiac disease, cardiovascular risk factors or pretreatment with cardiotoxic substances) with secondary progressive multiple sclerosis reported a temporary and considerable decrease in left ventricular ejection fraction, and with additional echocardiographic findings of diastolic dysfunction after only one or two doses of MTX (**1**)[71]. A total of 41 patients with secondary progressive multiple sclerosis were treated with 12 mg/m^2 of MTX (**1**) every 3 months and 16% of patients showed

asymptomatic cardiotoxicity. Still, in a patients' re-evaluation off-study, none maintained a left-ventricular ejection fraction lower than 50%. This suggests that, although cardiotoxicity is a concern, it may not be permanent[72]. Class III and IV studies report frequency and severity of MTX (**1**)-related cardiotoxicity: asymptomatic decreased systolic function in 12% of patients with multiple sclerosis, while congestive heart failure occurs in 0.4%, and leukaemia occurs in 0.8%[73].

Some pathways associated with cardiac toxicity of anthracyclines and MTX (**1**) correspond to generation of reactive oxygen species (ROS), iron accumulation, and mitochondrial dysfunction[30]. It is believe that the production of semiquinone radical metabolites after one-electron reductive activation during drug metabolism by nitric oxide synthases and nicotinamide adenine dinucleotide phosphate (NADPH) oxidase is the main pathway of doxorubicin cardiotoxicity, since it induces superoxide anion radical ($O_2^{\bullet -}$) formation in the ubiquinone-binding sites in complexes I and III of the mitochondrial membrane and the flavin prosthetic group in complex I. $O_2^{\bullet -}$ can generate other ROS, such as H_2O_2 and the hydroxyl radical ($^{\bullet}OH$) by reacting with iron. Thus, doxorubicin-increased ROS generation results in the oxidation of lipids, proteins, and signalling molecules and leads to oxidative stress[75]. MTX (**1**) contains a quinone functional group in its structure and it undergoes activation by phase I metabolic enzymes, like doxorubicin[30]. It was demonstrated, in HepG2 and MCF-7 cells, that MTX (**1**) is oxidized by a CYP P450-mediated reaction producing quinone or quinonediimine intermediates through a two electron reduction[31, 76] and it is also oxidized by human myeloperoxidase (MPO) at a high H_2O_2 concentrations to metabolites that bind covalently to DNA (Scheme 6)[77]. However, unlike doxorubicin, MTX (**1**) has a weaker capacity to enter in futile redox cycling[18], which means that it is not able to cause an early and abrupt oxidative stress like aglycones and semiquinones of doxorubicin[52]. In non-differentiated H9c2 cells, a mild late (96 h) oxidative stress was observed[42]. The authors claimed, however, that the ROS increase is secondary to the energy imbalance observed and not a process that directly involved the drug. This happened because MTX (**1**) largely accumulates in the heart impairing cardiac adenosine triphosphate (ATP) homeostasis[78]. In another study, after several MTX (**1**) intraperitoneal administration to Wistar rats, the activities of electron transport chain complexes were affected at the 22-and 48-day time points, which led to a decrease in ATP generation in heart mitochondria[65].

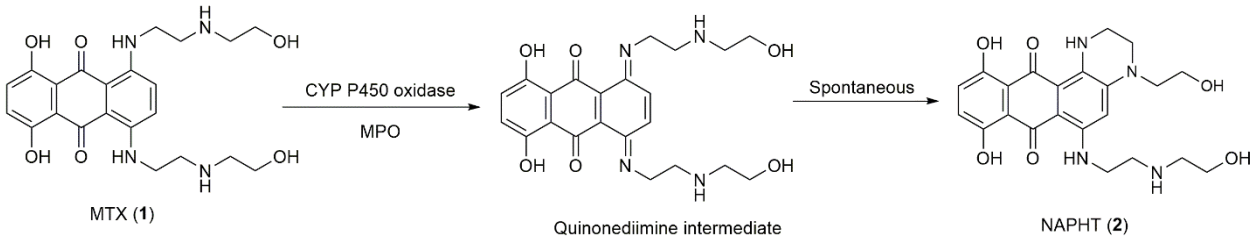

Scheme 6 – MTX (**1**) is oxidized through a CYP P450 and by human myeloperoxidase (MPO) at a high H_2O_2 concentration reaction generating quinone or quinonediimine intermediates with intracellular nucleophilic components.

Other potential mechanism of myocardial oxidative damage caused by anthracyclines is the formation of complexes with iron in heart cell mitochondria, producing ROS via a redox cycle[79]. Doxorubicin binds to iron in the presence of oxygen and forms a doxorubicin-Fe^{3+} complex that can be reduced in the presence of NADPH cytochrome P450 reductase to the doxorubicin-Fe^{2+} complex and leads to semiquinone free radical and formation of oxidative stress[80]. It has been demonstrated that MTX (**1**) has a high affinity for Fe^{3+} and the mitochondrial alterations induced by this drug in rats were much more severe than those induced by doxorubicin[81].

Doxorubicin and MTX (**1**) induce late cardiomyopathy[30]. Doxorubicin causes an a redox cycle and both interact with iron to generate ROS[52]. MTX (**1**) induces energy imbalance while doxorubicin is a more redox-interfering drug[30]. Moreover, both inhibit topoisomerase IIβ activity, impair mitochondrial biogenesis, and lead to oxidative stress. Zhang *et al*. showed that cardiomyocyte-specific deletion of topoisomerase IIβ protects mice from doxorubicin-induced progressive heart failure[82]. The genetic variant of retinoic acid receptor gamma (RARG) has been associated in humans with increased cardiotoxicity after anthracycline regiments in children subjected to anthracycline treatments. RARG was found to repress topoisomerase IIβ expression[83], thus further corroborating topoisomerase IIβ involvement in the cardiotoxicity promoted by anthracyclines. No data regarding MTX (**1**) is yet available.

The underlying mechanisms of MTX (**1**)-induced cardiotoxicity are poorly known. The biologic activity of MTX (**1**) metabolites and their putative responsibility on its cardiotoxicity are scarcely studied so far.

CHAPTER 2

Aims

CHAPTER 2 – AIMS

MTX (**1**) is an antineoplastic agent used to treat several types of cancers and on multiple sclerosis but it has a high incidence of cardiotoxicity. Still, the underlying mechanisms of MTX (**1**) cardiotoxicity are poorly understood and the potential toxicity of its metabolites scarcely investigated. Therefore, previously, in our group, the metabolite NAPHT (**2**) was synthesized in limited quantities and its cytotoxicity was investigated in differentiated H9c2 cells. It is was discovered that NAPHT (**2**) is less cardiotoxic than MTX (**1**)[49]. In relation to the other metabolites, the mono (**10**)- and di (**3**)-carboxylic acids, no cardiotoxicity studies are known so far.

Thus, the main objectives of the present dissertation were to:

1) synthetize the metabolite NAPHT (**2**) with improve yield and purity to continue toxicological tests;

2) synthetize the dicarboxylic acid (**3**) by total synthesis from a commercial available anthraquinone based in the synthesis already described of MTX (**1**);

3) synthetize the dicarboxylic acid (**3**) in one step from commercially available MTX (**1**);

4) to obtain acetoxy derivatives since an acetylated metabolite has already been described.

It is also intended to perform the structural characterization of the synthesized derivatives by spectroscopic techniques, such as infrared (IR), ^{1}H nuclear magnetic resonance (NMR) and high-resolution mass spectrometry (HRMS).

CHAPTER 3

Results and discussion

CHAPTER 3 – RESULTS AND DISCUSSION

3.1. Synthesis of the mitoxantrone naphtoquinoxaline derivative

MTX (**1**) and related structures are more resistant to reductive enzymatic activation than anthracyclines, namely doxorubicin. MTX (**1**) and related structures are easy targets for oxidative enzymatic action since these drugs contain within their structure functional groups known to be susceptible to enzymatic oxidation. Since 1988, the enzymatically transformation of MTX (**1**) to a metabolite containing an additional ring has been reported. This transformation was detected by spectroscopic techniques and accompanied by the generation of a free radical intermediate[40, 50-51, 54]. Rezka and co-workers indicated that NAPHT (**2**) is a central metabolite in the oxidation cascade[50]. The metabolite, NAPHT (**2**) has an additional ring formed in the 6 position of the chromophore and it is a substituted hexahydronaphtho [2,3-f]quinoxaline-7,12-dione[51]. Due to the formation of highly reactive species from MTX (**1**), it was previously considered that the oxidative biotransformation of MTX (**1**) was an activation of the drug within cells containing high peroxidase activity. Those high peroxidase cells were considered to be main targets of the drug[40].

The synthesis and structure elucidation of 8,11-dihydroxy-4-(2-hydroxyethyl)-6[[2-[(2-hydroxyethyl)amino]ethyl]-amino]-1,2,3,4,7,12-hexahydronaphto -[2,3-f]quinoxaline-7,12-dione (NAPHT, **2**) was already accomplished within our group[49]. In order to obtain more NAPHT (**2**) to perform further toxicological studies, the same conditions were used in the synthesis by using HRP-catalysed H_2O_2, as depicted in Scheme 7 but with the addition of ascorbic acid. This type of reaction with peroxidase implies formation of substrate-derived free radicals as intermediates in the oxidation, like ascorbate[50]. Ascorbic acid acts as a reducing agent that is easily oxidized and is an excellent source of electrons. In this reaction, ascorbic acid presents a protective effect attributed to competitive reaction with the HRP/H_2O_2 system. Moreover, it prevents the oxidative degradation of the NAPHT (**2**)[40, 51].

HRP is easily obtained and is similar to physiologically relevant systems. HRP-catalysed oxidation of MTX (**1**) results firstly into radical species, which then disproportionate, leading to internal cyclisation of a single amino-alkyl side-chain and formation of the redox-active NAPHT (**2**) using H_2O_2 as the primary oxidant[54-55].

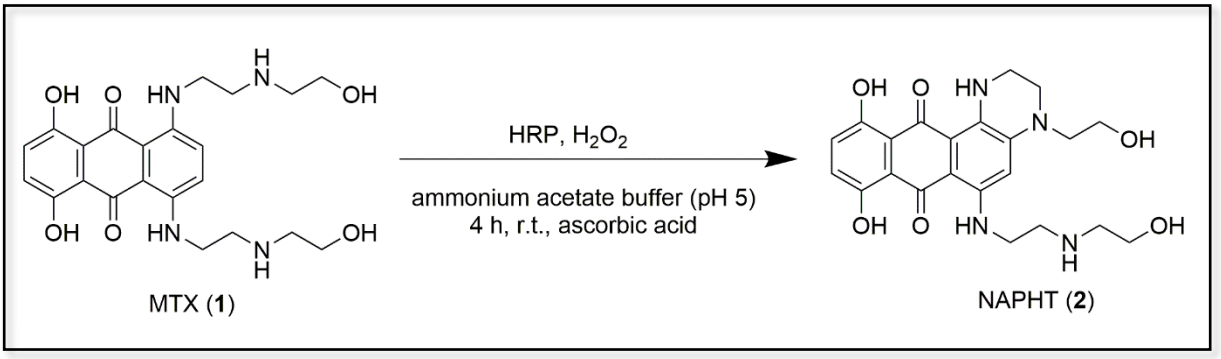

Scheme 7 – The synthesis of NAPHT (**2**) from MTX (**1**) with HRP. HRP - horseradish peroxidase; r.t. – room temperature.

The formation mechanism of NAPHT (**2**) (Scheme 8) requires electrochemical oxidation of two electrons of the phenylenediamine substructure (**A**) to form a highly reactive quinone-diimine (**B**). The structure **B** is protonated at the basic amino groups of the side chains, which protects the oxidation product **B** from rapid intramolecular 1,4-addition of one amino group of the side chain with the reactive double bond on the quinone-diimine moiety. The basic amino group of the side chain of the nonprotonated form of the equilibrium (**D**) reacts by an intramolecular attack with the electrophilic centre at carbon-6 of MTX (**1**) radical cation. Subsequent oxidation of the cyclized radical (**E**) with ascorbic acid leads to the formation of the desired product, NAPHT (**2**) (Scheme 8).

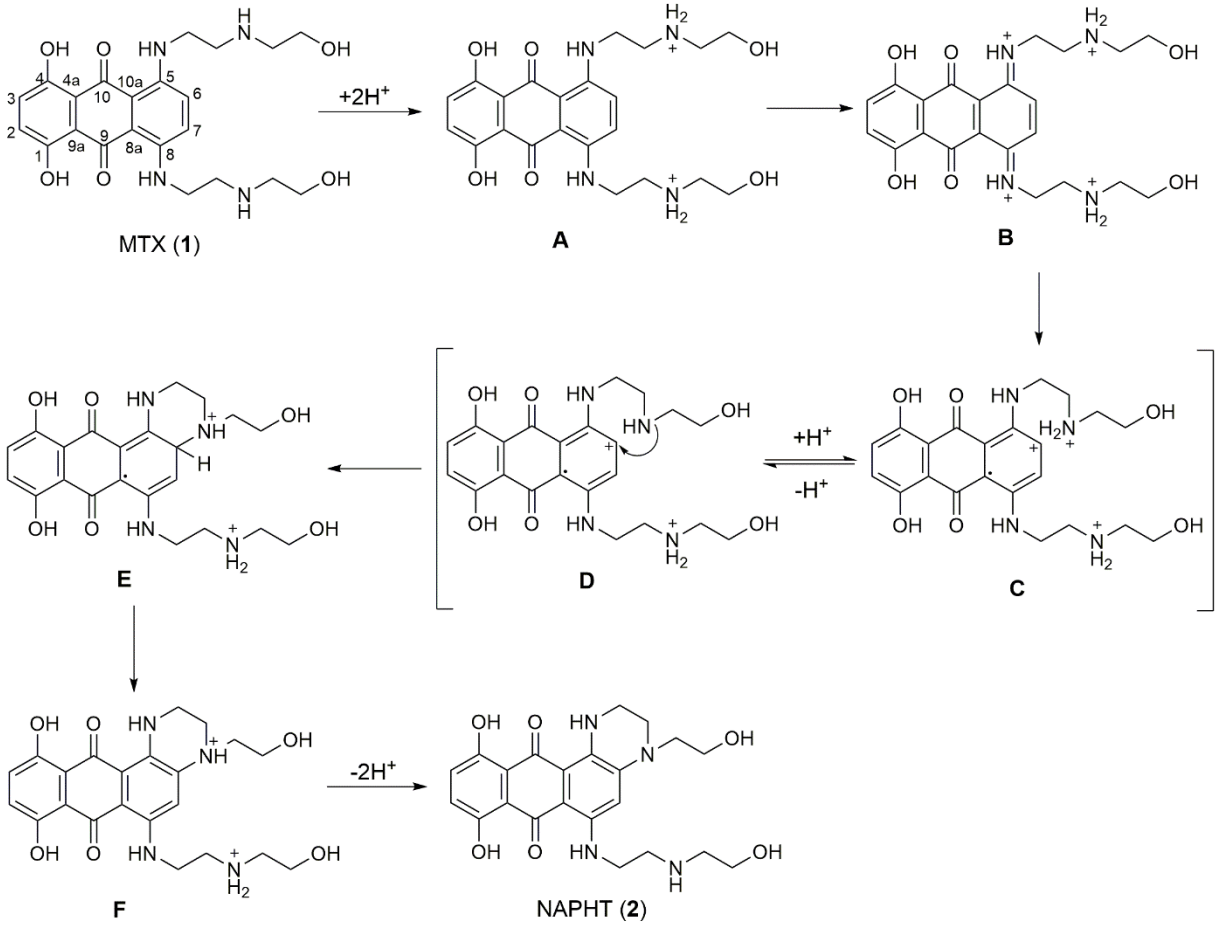

Scheme 8 – Oxidative mechanism of MTX (**1**) to form NAPHT (**2**).

Several alternative sites in the MTX (**1**) chromophore, such as amino groups at the 5,8-position or OH groups at the 1,4-position, may be considered as possible sites of enzymatic oxidation but, with the applied conditions, only NAPHT **2** was isolated. In this reaction, the initial oxidative attack takes place at the aromatic nitrogen and not in the OH functions; this occurs because amines are good substrates for enzymatic oxidation[50-51]. The 1,4-OH groups of MTX (**1**) are probably responsible for the stability of the free radical cation formed**.** Also, the presence of a free amine in the side-chain for cyclization of one of the side-chain amines is necessary.

The reaction in aqueous solution is difficult since those compounds can exist in various stages of protonation, depending on the pH of the medium. The low pH creates stabilizing conditions and consequently, pH $\geq$ 5 seems to result in high reactivity of the

neutral radicals and consequent dimerization. H_2O_2 is also consumed in the oxidation reaction and it is used as an oxidizer[50].

In the oxidation reaction of MTX (**1**) previous performed by Reis-Mendes *et al*., the formation of other minority product was observed and attributed to 3-((2-((4-(2-carboxyethyl)-8,11-dihydroxy-7,12-dioxo-1,2,3,4,7,12-hexahydronaphto-[2,3,*f*]-quinoxalin-6-yl)amino)ethyl)amino)propanoic acid formation; however, with the modified conditions, namely the addition of ascorbic acid, only one product was isolated and identified as 8,11-dihydroxy-4-(2-hydroxyethyl)-6[[2-[(2-hydroxyethyl)amino]ethyl]-amino]-1,2,3,4,7,12-hexahydronaphto-[2,3-f]quinoxaline-7,12-dione (**2**).

In the present dissertation, the crude product was purified in semi-preparative C18 column due to its the great versatility and capability for retaining and separating a wide variety of charged polar compounds, like NAPHT (**2**) and MTX (**1**). NAPHT (**2**) was identified by HPLC comparing with a standard previously obtained in the group. The purity was determined by diode-array analysis performed in a HPLC-DAD. A chromatographic peak was obtained and corresponded to the desired product with 95% of purity (Figure 4) and 42% yield. The purity of commercial available MTX (**1**) was also determined and corresponded to 98%. HPLC analysis indicated that NAPHT (**2**) presented a retention time of 10.98 minutes and MTX (**1**) of 7.09 minutes. To obtain these chromatograms, an isocratic system 3:7 of the eluent B was used [eluent A corresponding to 0.1% aqueous solution of CH_3COOH and the eluent B corresponds to methanol (MeOH)]. The selected mobile phase allowed a better quality of separation of the bands with suitable retention times when compared to previously investigated conditions[49].

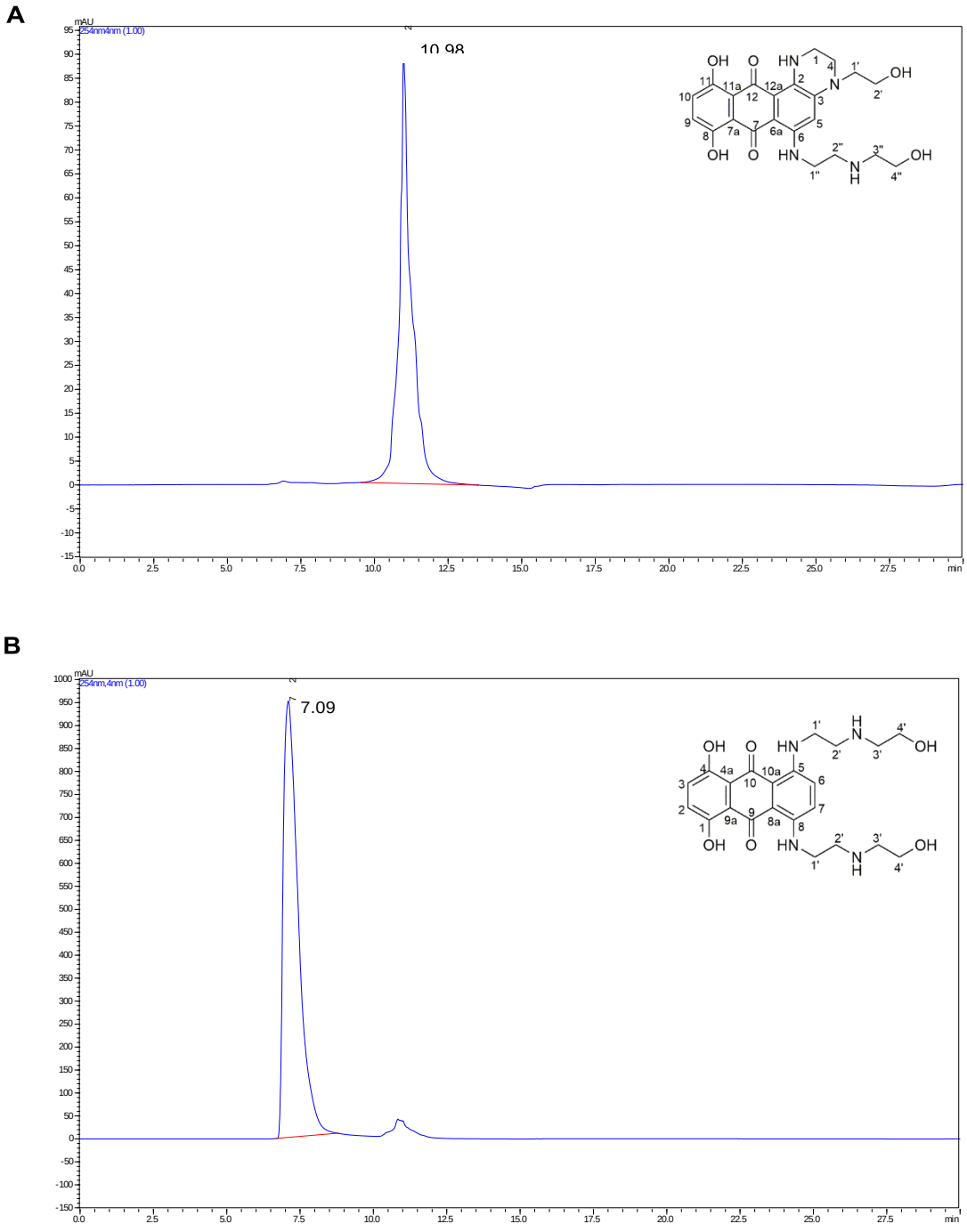

Figure 4 - Representative HPLC chromatograms. A – NAPHT (**2**); B – MTX (**1**). [λ= 254 nm, C18, isocratic system 3:7 of eluent B within 30 min (eluent A: 0.1% aqueous solution of CH_3COOH; eluent B: MeOH)].

NAPHT (**2**) was analysed by UV-Vis spectrophotometry at a wavelength of 254 nm and UV-Vis spectra were registered between 230 and 800 nm (Figure 5). The UV-Vis spectrum of NAPHT (**2**) presented similar spectral features, maximum absorption at around 241 and 276 nm, in the ultraviolet range and different features in the visible range comparing to MTX (**1**) spectrum. This is indicative that a new chromophore was formed. Absorbance maxima of MTX (**1**) are located at 610 nm and 660 nm due to the transition of electron from substituent OH and amino group on the anthraquinone ring, respectively[55, 84] , while NAPHT (**2**) showed reduced absorbance maxima between 584 and 631 nm. This absorbance in the visible is also due to the blue colour of the two compounds. Also, when comparing the two spectra, A and B (Figure 5), one can verify that a wavelength shift occurred in MTX (**1**) spectrum (Figure 5B) to lower values for NAPHT (**2**) (Figure 5A), due to a hypsochromic effect. The UV-Vis spectra obtained was also superimposable to the UV-Vis spectrum of the standard product previously obtained in our group[49].

The HRMS of NAPHT (**2**) exhibited the molecular ion at m/z 443.19313 with the molecular formula of $C_{22}H_{27}N_4O_6$, with decresement of two protons compared with MTX (**1**).

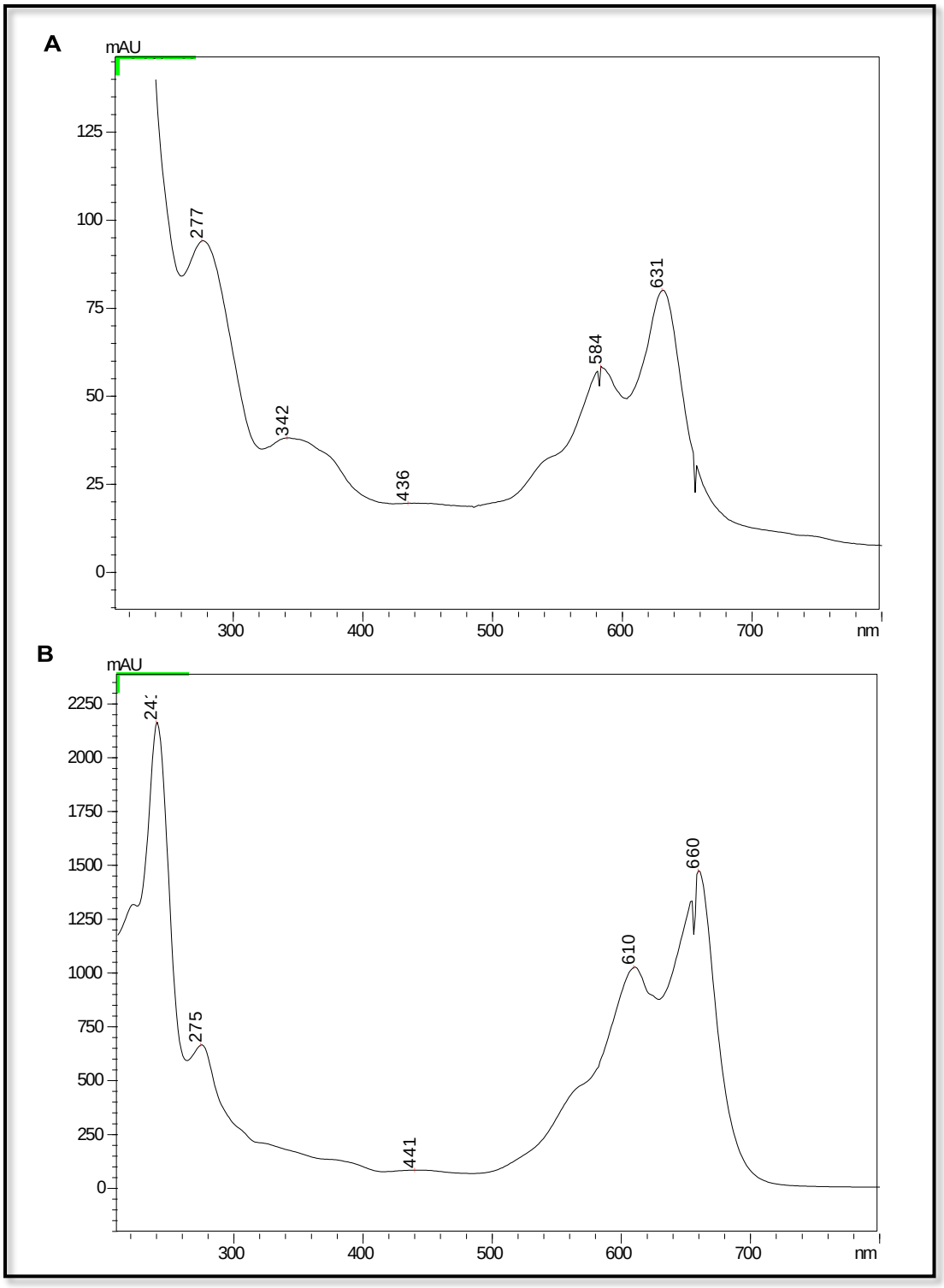

Figure 5 – A – UV-Vis spectra of isolated product NAPHT (**2**); B – UV-Vis spectra of MTX (**1**).

The NAPHT (**2**) derivative was further characterized by IR technique and the presence of several characteristic bands in the IR confirmed that it is the desired compound. The stretching vibration of the O-H group appears at around 3432 cm^{-1} and stretch band of aromatics C-H bonds occur at 2920 cm^{-1}. The band corresponding to the N-H bond of an aliphatic secondary amine aroused at 1701 cm^{-1}. The vibration band of the C=O bond appears at 1628 cm^{-1} and the band corresponding to the aromatics C=C bonds at 1556 cm^{-1}. The vibrations of the single bond C-H and C-N, C-O appear at 1397 and 1319 cm^{-1}, respectively. In Table 1, the IR data of NAPHT (**2**) and MTX (**1**) are summarized. Moreover, NAPHT (**2**) derivative was compared with the standard product previously obtained by our group, confirming that it was the desired compound.

Table 1 – IR data of MTX (**1**) and NAPHT (**2**) derivative.

Compound	**Group**	**υ(cm^{-1})**
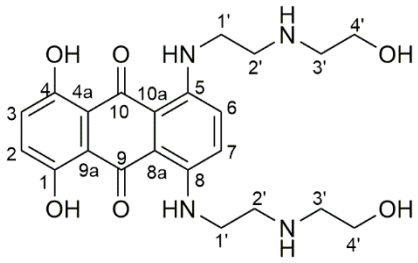 MTX (**1**)	O-H	3404
	N-H attached to aromatic ring	3052
	C-H aromatic	2962, 2774
	N-H aliphatic	1611
	C=O ketone	1571
	C=C aromatic	1514
	C-H aliphatic	1489-1365
	C-N, C-O	1209
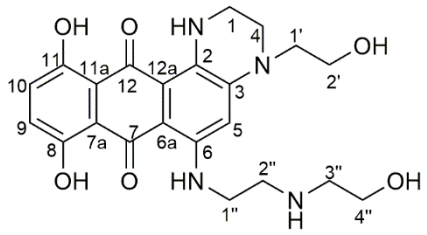 NAPHT (**2**)	O-H	3432
	C-H aromatic	2920
	N-H aliphatic	1701
	C=O ketone	1628
	C=C aromatic	1556
	C-H aliphatic	1397
	C-N, C-O	1319

υ - wavenumber.

The synthesis and the study of this metabolite are important since this oxidative transformation of MTX (**1**) also occurs in patients subjected to MTX (**1**) therapy and this

oxidation may be relevant to the mode of action of this agent. In fact, it has been demonstrated that NAPHT (**2**) may contribute in cellular systems to the cytotoxic activity of MTX (**1**)[31, 41].

3.2. Synthesis of dicarboxylic acid of mitoxantrone

The MTX (**1**) was first synthesized in 1978 but total synthesis of its metabolites is sparse. The total synthesis of dicarboxylic acid derivative (**3**) was adapted following the synthesis of MTX (**1**) performed by Cheng *et al*.[20] in 1981 (Scheme 3). The main difference between the synthesis of dicarboxylic acid (**3**) and MTX (**1**) relies in the side chain.

To synthetize dicarboxylic acid (**3**), initially, a synthetic route with five steps was proposed, in which the starting reagent was chrysazin (**7**) (Scheme 9)[85]. The first step consists in the preparation of 4,5-dinitrochrysazin (**8**), key intermediary for the synthesis of this metabolite. The formation of this nitroanthraquinone occurs by the direct nitration of the chrysazin (**7**) in the presence of sodium nitrite ($NaNO_2$) in trifluoroacetic acid (TFA). Following the reaction scheme, the 4,5-dinitrochrysazin intermediate (**8**) is subjected to a reduction reaction with stannous dichloride in ethanol to give 4,5-diaminochrysazin (**9**). This product, in turn, is treated with sodium hydrosulfite ($Na_2S_2O_4$) in an alkaline solution, to be converted into leuco-1,4,5,8-tetrahydroxyanthraquinone (**6**). This step comprises two stages of reduction and hydrolysis[85]. Finally, the fourth step is a condensation reaction of leuco-1,4,5,8-tetrahydroxyanthraquinone (**6**) with an *N*-(2-aminoetil)glycine in pyridine (Py), to obtain a Schiff base, which is subsequently converted by oxidation to dicarboxylic acid (**3**) with oxygen gas and absolute ethanol at 55-60 °C (Scheme 9)[25, 27, 86].

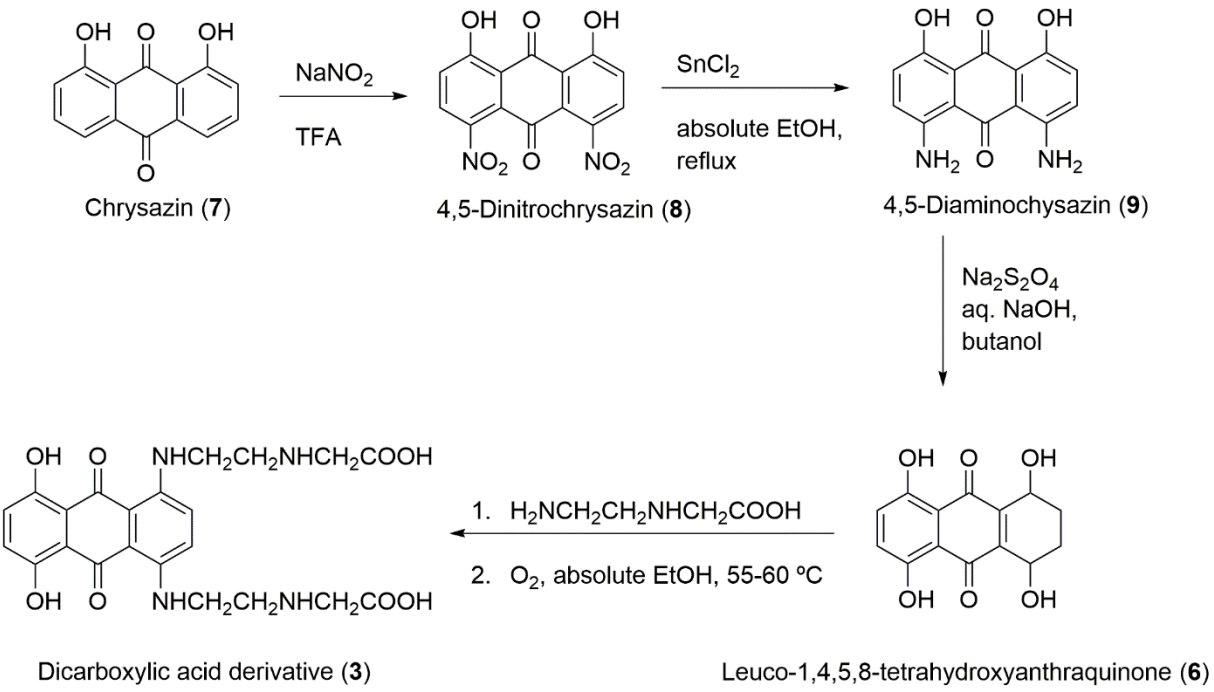

Scheme 9 - General scheme of the proposed synthesis for dicarboxylic acid (**3**) derivative.

3.2.1. Synthesis of 4,5-dinitrochrysazin (8)

To synthetize 4,5-dinitrochrysazin (**8**), chrysazin (**7**) was used as starting material, $NaNO_2$ as nitration reagent, and TFA as solvent (Scheme 10). The use of $NaNO_2$/TFA to assure nitration conditions instead of oleum, nitric acid (HNO_3), and boric acid (H_3BO_3) (hazardous) was based on previously results obtained for other aromatic scaffolds, in which these conditions proved to successfully nitrate similar derivatives[87]. This reaction is classified as an aromatic electrophilic substitution, wherein substitution of a hydrogen atom attached to the aromatic ring by a nitro group occurs.

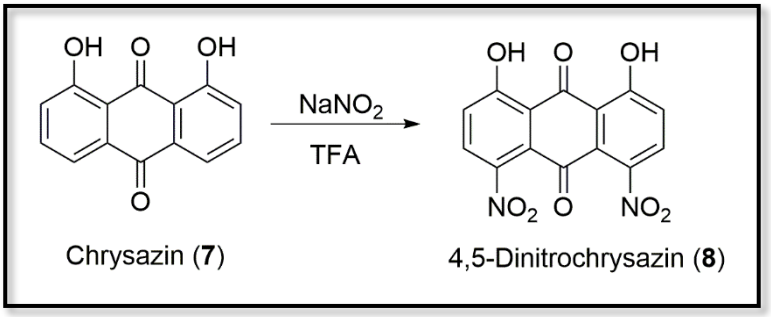

Scheme 10 – Synthesis of 4,5-dinitrochrysazin (**8**). TFA – trifluoroacetic acid.

In this reaction, the aromatic ring behaves like a nucleophile and for the reaction to occur, it is necessary, initially, to form a highly electrophilic species, the nitronium ion (NO_2^+). This highly reactive cation is formed in an acidic environment, in presence of TFA. TFA has high acidity and is a good solvent for many aromatic compounds. Unlike the nitronium ion, the aromatic ring has very low reactivity and only reacts with electrophiles. Thus, the nitronium ion accepts a pair of electrons from the aromatic ring to give a resonance stabilized carbocation or Wheland intermediate. Finally, the last step, usually fast, corresponds to the regeneration of aromaticity giving the 4-nitrochysazin (**20**) compound (Scheme 11). To form the desired product, 4,5-dinitrochrysazin (**8**), a second nitration in the ring in 5 position by the same mechanisms is necessary.

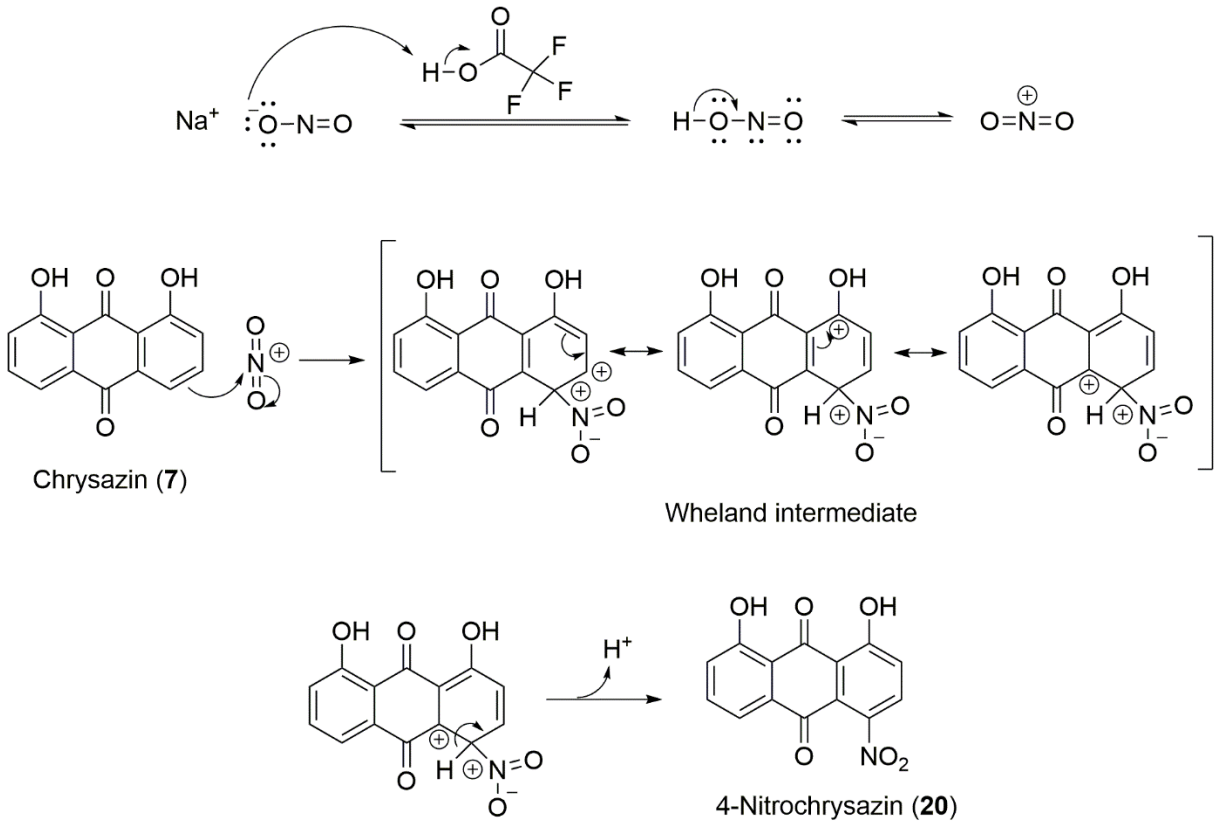

Scheme 11 – Mechanism of the nitration reaction of chrysazin (**7**).

Initially, the reaction was investigated with 10 equivalents of $NaNO_2$ and after ^1H NMR analysis of the major product, it was shown to correspond to the 4-nitrochrysazin (**20**). The reaction was repeated again using 20 equivalents of $NaNO_2$ reagent that allowed the formation of 4,5-dinitrochrysazin (**8**) as the major product. Despite the mixture of compounds, it was possible to identify the major compound by its ^1H NMR spectrum. Thus, in this procedure, the reaction mixture of chrysazin (**7**), TFA and 20 equivalents $NaNO_2$ was stirred at room temperature (r.t.) for 54 h. The yellow precipitate formed after neutralization of the reaction was isolated by filtration and the product washed with water. Then, the product was dried to furnish a yellow solid containing mainly 4,5-dinitrochrysazin (**8**), with a corresponding yield of 47%.

The formation of the mixture of compounds can be explained by the presence of the OH group (electron donor) that activated the ring, increases the electron density, and increases the speed of the reaction. The resonance effect caused by this group on the aromatic ring indicates that the substitution of the nitro group will occur preferably in

the *ortho* and/or *para* position relative to the OH group (Scheme 12). The *para* substitution regarding the OH group is also favoured by the resonance caused by the presence of the carbonyl group (Scheme 13).

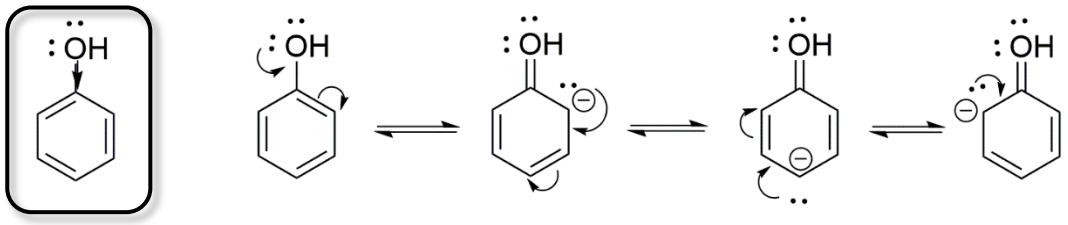

Scheme 12 – Resonance effect of OH group.

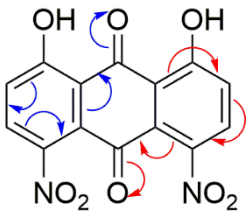

Scheme 13 - Carbonyl group in resonance with the aromatic ring.

The purification procedures like chromatography column, crystallization, and solid phase extraction (SPE) were applied for this reaction step but revealed to be unsuccessful due to the polarity and solubility of these compounds. However, in order to verify that the crude product had the desired compound, 4,5-dinitrochrysazin (**8**), a small amount was purified by preparative thin-layer chromatography (TLC) with *n*-hexane:ethyl acetate, 6:4 as an eluent followed by preparative TLC with chloroform/acetone [$(CH_3)_2CO$], 9:1. The structure elucidation of 4,5-dinitrochrysazin (**8**) will be presented in the next section (3.3.2).

To overcome the solubility problems and to prevent the formation of minor products, an attempt was made to methylate the chrisazin (**7**) (presented in the following subsection). The methyl bulky group would increase the steric hindrance and, consequently, increase the regioselectivity of the nitration. Also, the protection of the OH groups would facilitate the purification of the product by chromatographic techniques.

3.2.1.1. Synthesis of 1,8-dimethoxychrysazin (21)

The synthesis of 1,8-dimethoxychrysazin (**21**) occured based on the previously described synthesis of 1,8-diethoxyanthraquinone by Kumar *et al*.[88] The reaction mixture of chrysazin (**7**) in *N*,*N*-dimethylformamide (DMF), potassium carbonate (K_2CO_3), and dimethyl sulfate (DMS) was heated to 100 ºC over a 3-days period (Scheme 14).

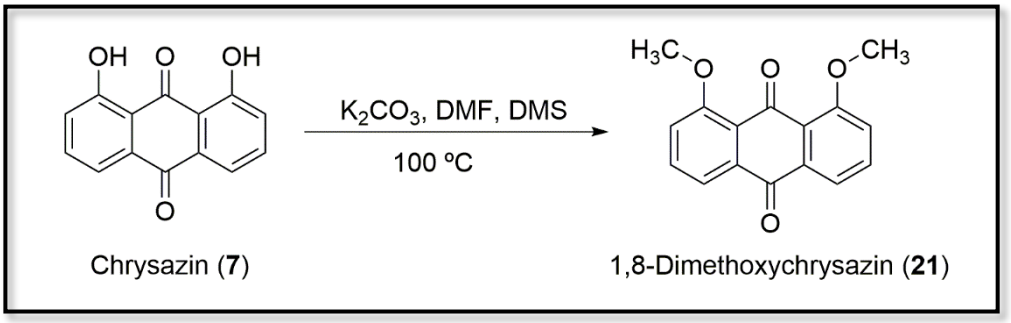

Scheme 14 – Synthesis of 1,8-dimethoxychrysazin (**21**). DMF - *N*,*N*-dimethylformamide, DMS - dimethyl sulfate.

In this step, the OH groups were protected as methyl ethers. K_2CO_3 is added in order to deprotonate both OH groups of the chrysazin (**7**) and DMS transfers its methyl group to the deprotonated OH group at the benzene ring. This organic reaction, Williamson reaction, occurs via an S_N2 reaction (Scheme 15).

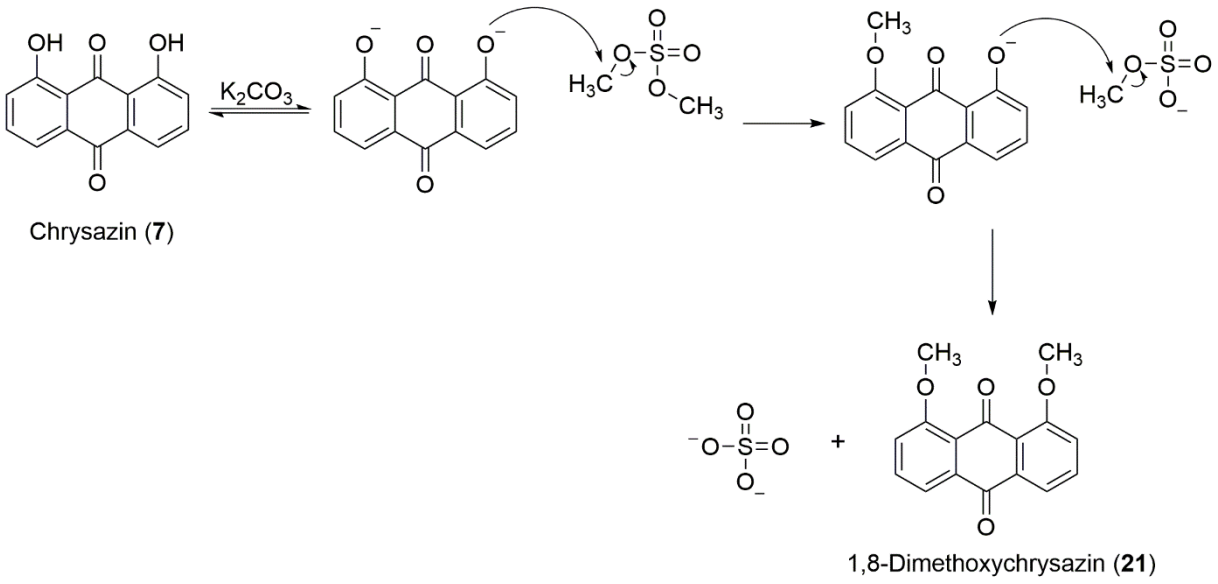

Scheme 15 – Mechanism of methylation reaction of chrysazin (**7**).

After 3 days, the reaction was not completely finished but it was stopped and the crude product was precipitated and filtrated. The solid was washed with water and dried. Purification by flash column chromatography with *n*-hexane/ethyl acetate 8:2 afforded 1,8-dimethoxychrysazin (**21**) as a yellow solid with 0.17% yield. Unfortunately, this process led to a very low yield after purification. Hence, the crude extract obtained in the previous reaction (3.2.1) was used without further purification to accomplish the following reaction. The structure elucidation of 1,8-dimethoxychrysazin (**21**) will be shown in the next section (3.3.1).

3.2.2. Synthesis of 4,5-diaminochrysazin (9)

The 4,5-dinitrochrysazin (**8**) was submitted to a reduction with stannous chloride and absolute ethanol at 70 ºC under nitrogen in a non acidic and non aqueous medium (Scheme 16)[27].

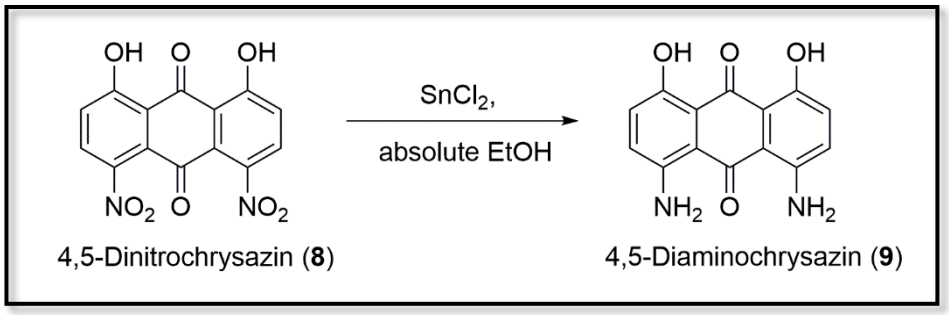

Scheme 16 – Synthesis of 4,5-diaminochrysazin (**9**).

The process results from the electron transfer from the metal (Sn), the source of electrons, to the nitro group, electron acceptor (Scheme 17). The same mechanism is applied for the reduction of the second nitro group.

The work-up of the reaction consisted in pouring the solution into ice slightly basified (pH 8) by the addition of 5% of aqueous sodium bicarbonate ($NaHCO_3$) and the resulting basic mixture was kept 1 h under stirring in order to allow the tin salts to hydrolyse. Then, the aqueous mixture was extracted with ethyl acetate, the organic phase was washed with brine to promote salting out, treated with charcoal and dried over anhydrous sodium sulphate (Na_2SO_4) to remove undesirable impurities and water, respectively. Thus, a purple solid product was obtained with 8.4% yield.

Attempts to purify the major product from the crude extract by preparative TLC were unsuccessful. For that reason, the entire crude product, as 4,5-diaminochrysazin (**9**), was used without purification for the next reaction due to the similar chromatographic behaviour of the impurities. Nevertheless, spraying with ninhydrin and ^1H RMN analysis of the crude extract demonstrated the desirable transformation depicted in Scheme 16.

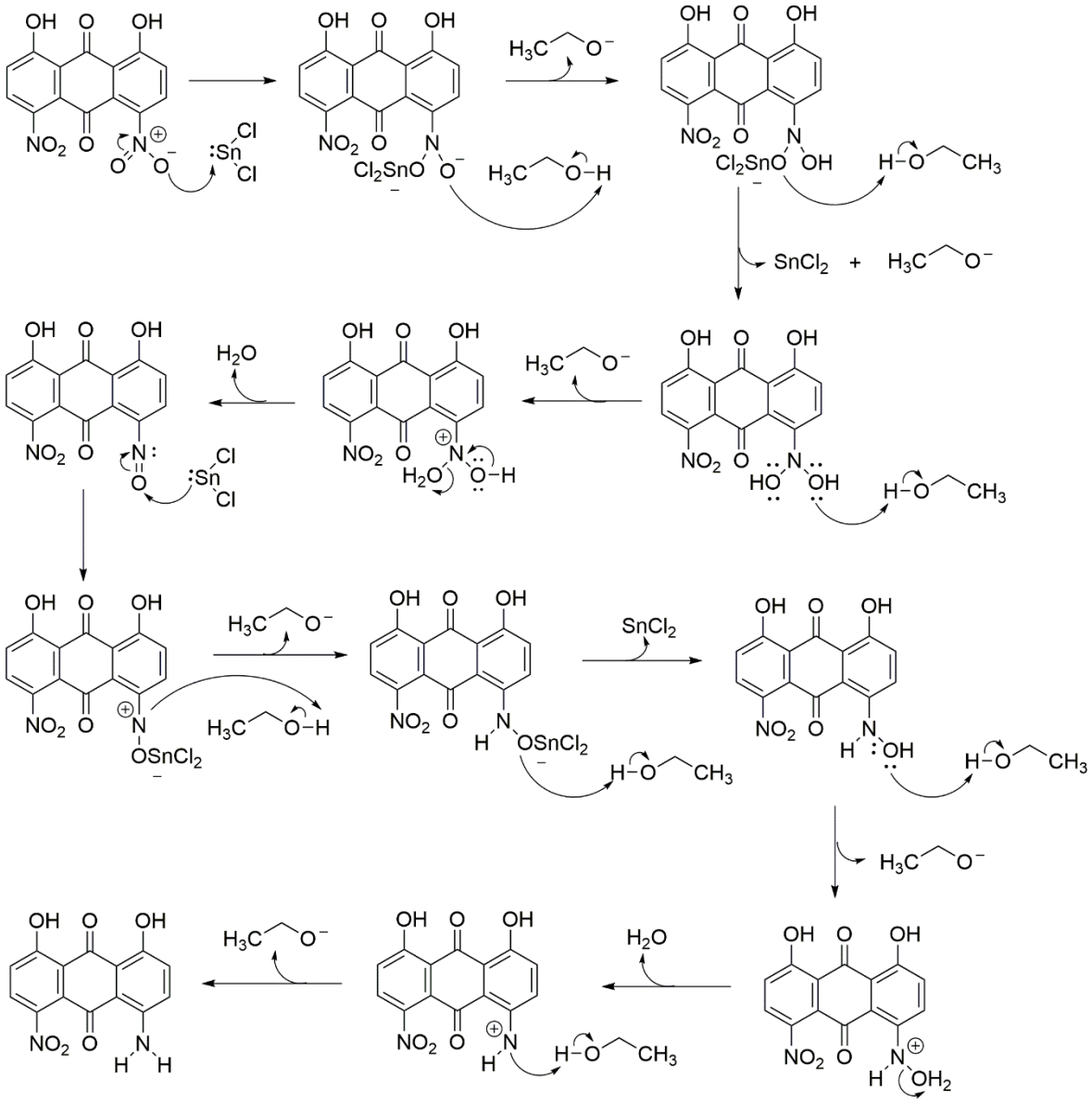

Scheme 17 – Mechanism of the reduction reaction of nitro group.

3.2.3. Synthesis of leuco-1,4,5,8-tetrahydroxyanthraquinone (6)

The conversion of 4,5-diaminochrysazin (**9**) into leuco-1,4,5,8-tetrahydroxy-anthraquinone (**6**) corresponds to a reductive hydrolysis[85].

The reaction mixture of 4,5-diaminochrysazin (**9**) and sodium hydrosulfite ($Na_2S_2O_4$) in 10% sodium hydroxide (NaOH) aqueous solution containing *n*-butanol was heated at 60 ºC for 48 h (Scheme 18).

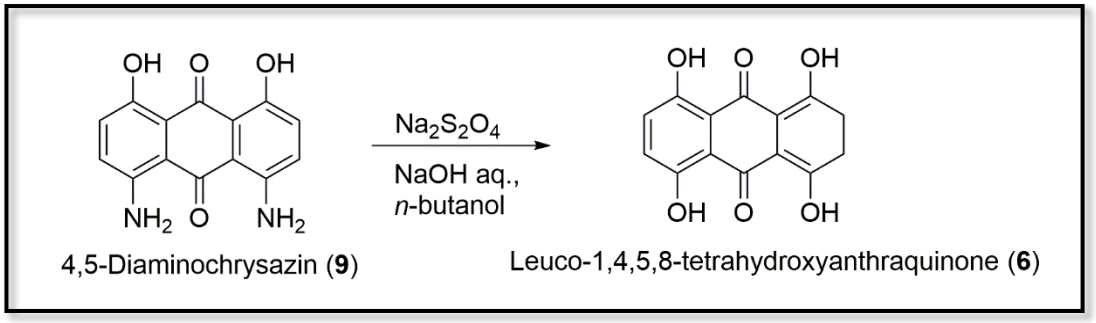

Scheme 18 – Synthesis of leuco-1,4,5,8-tetrahydroxyanthraquinone (**6**). aq – aqueous.

In this step, the $Na_2S_2O_4$ was used as the reducing agent; the aqueous solution of NaOH 10% promotes the hydrolysis and prevents the rapid decomposition of $Na_2S_2O_4$.

After 48 h, the reaction was finished and it was cooled to r.t.. Then, the reaction mixture was subjected to neutralization with HCl (1M) and the resulting precipitate was collected by filtration, washed with water and dried in vacuum at 50 ºC. The purple solid was obtained with 78% yield.

Several products were observed by TLC analysis and to separate the major product three several procedures, namely anionic SPE column, preparative TLC and flash column chromatography, were tested without success due the similar behaviour of all compounds. Again, the crude product was used for the next reaction without further purification procedures.

3.2.4. Synthesis of dicarboxylic acid (3) derivative

The reaction involves two steps: condensation of the leuco-1,4,5,8,-tetrahydroxyanthraquinone (**6**) intermediate with an amino acid *N*-(2-aminoethyl)-

glycine (**22**) in Py to form a Schiff base and, oxidation of Schiff base to the final product, dicarboxylic acid (**3**), with the use of dry air (Scheme 19)[25].

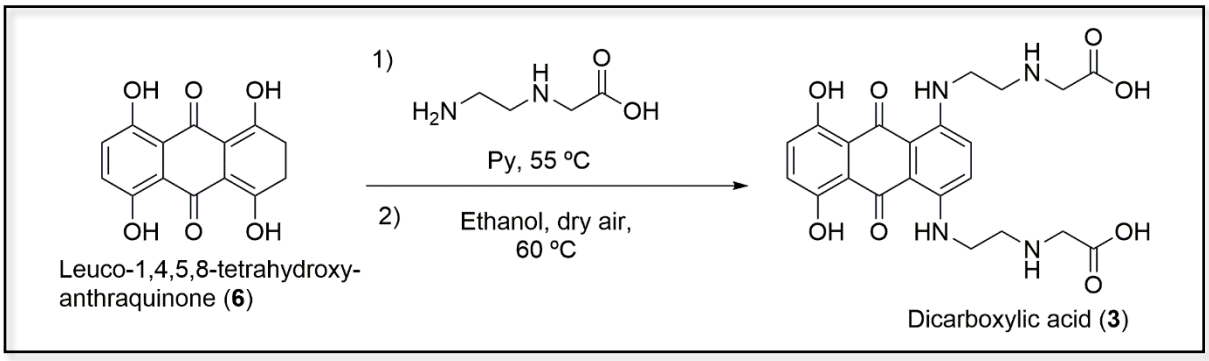

Scheme 19 – Synthesis of dicarboxylic acid (**3**) derivative. Py – pyridine.

This reaction of condensation may be accompanied by a subsequent cyclization of the side chain favoured by elevated temperatures. For this reason, in the condensation procedure, a low temperature (55 ºC) was used to avoid such cyclization. After 7 h, the Py was evaporated and the solid was immediately used in the next step without further purification. The second step, the oxidation reaction, aims to recover the aromaticity. By TLC analysis, although the consumption of the amino acid was observed after spraying with ninhydrin, no changes were observed comparatively to the starting material **6**. For this reason, the next strategy was to protect the amino alcohol to avoid the degradation of the amino acid in these conditions.

3.2.4.1. Protection reaction of *N*-(2-aminoethyl)glycine (22)

Fisher esterification is a commonly used reaction to protect functional groups, like carboxylic acids with alcohols to give esters. To obtain the protective derivative, three conditions were attempted (Table 2).

Table 2 – Tested conditions for protection of compound **22**.

N-(2-aminoethyl)glycine (**22**) — *Tert*-butyl *N*-(2-aminoethyl)glycinate (**23**)

Entry	Conditions	Results
1	*tert*-butanol, H_2SO_4, reflux	Several products were obtained in low yields.

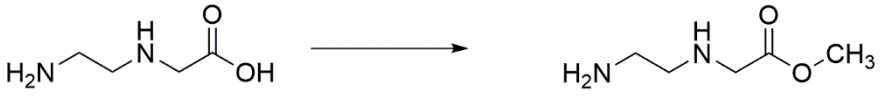

N-(2-aminoethyl)glycine (**22**) — Methyl *N*-(2-aminoethyl)glycinate (**24**)

Entry	Conditions	Results
2	MeOH, H_2SO_4, reflux	Several products were obtained in low yields.
3	TMSCl, MeOH, stirring at r.t.	Several product were obtained in low yields.

TMSCl - chlorotrimethylsilane

In this process, nucleophilic attack of the alcohol (*tert*-butanol or MeOH) gives a tetrahedral intermediate in which there are two equivalent OH groups. One of these OH groups is eliminated after a proton shift (tautomerism) to give water and the ester (Scheme 20).

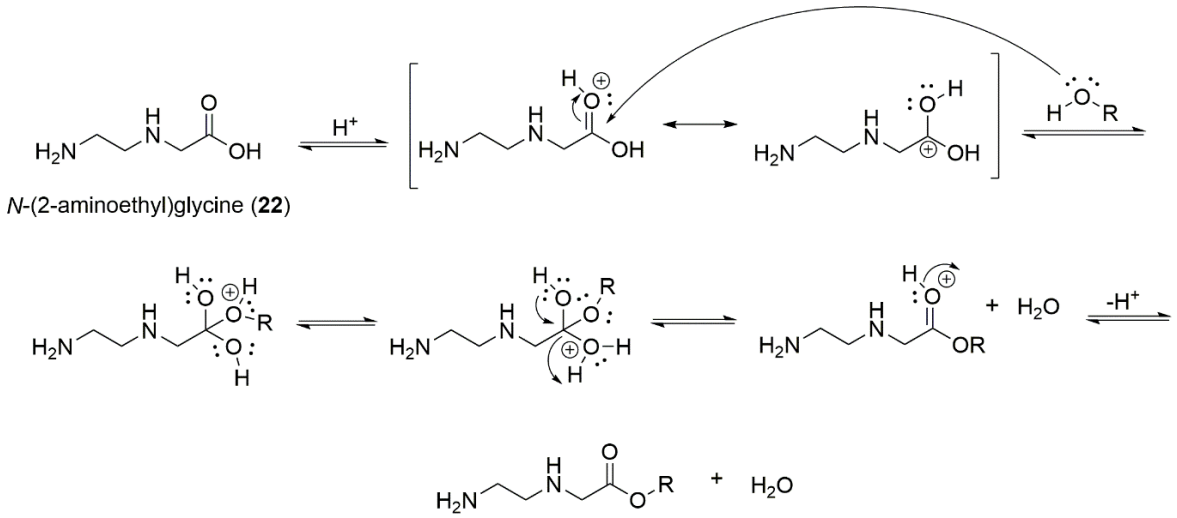

N-(2-aminoethyl)glycine (**22**)

Scheme 20 - General mechanism of Fischer esterification.

After several attempts with H_2SO_4 as a catalyst, (Table 2, entries 1 and 2) several products were obtained, as observed by TLC analysis and in low yields.

In order to reduce the formation of by-products and improve yields, a new method for obtaining the methyl acid ester was tested (Table 2, entry 3). MeOH/trimethylchlorosilane (TMSCl) has been shown to be a convenient system for the preparation of methyl esters of various carboxylic acids. This method relying in MeOH/TMSCl was found to be more advantageous due to the following features: easy operation, mild reaction conditions, simple workup and good to excellent yields[89]. This reaction was repeated several times but, many products were formed and, when using IR analysis and comparing with the IR library, the product was attributed to be a cyclized amide derivative.

Because of these poor results and low yields, the commercial available compound **23** was acquired to perform the condensation and oxidation reactions (3.2.4).

3.2.4.2. Synthesis of dicarboxylic acid (3) from compound 23.

In this reaction, to synthetize dicarboxylic acid (**3**) derivative from leuco 1,4,5,8-tetrahydroxyanthraquinone (**6**) and compound **23** three steps are involved: condensation and oxidation reactions previously described to form intermediate **25** and deprotection reaction to form the desired product (Scheme 21).

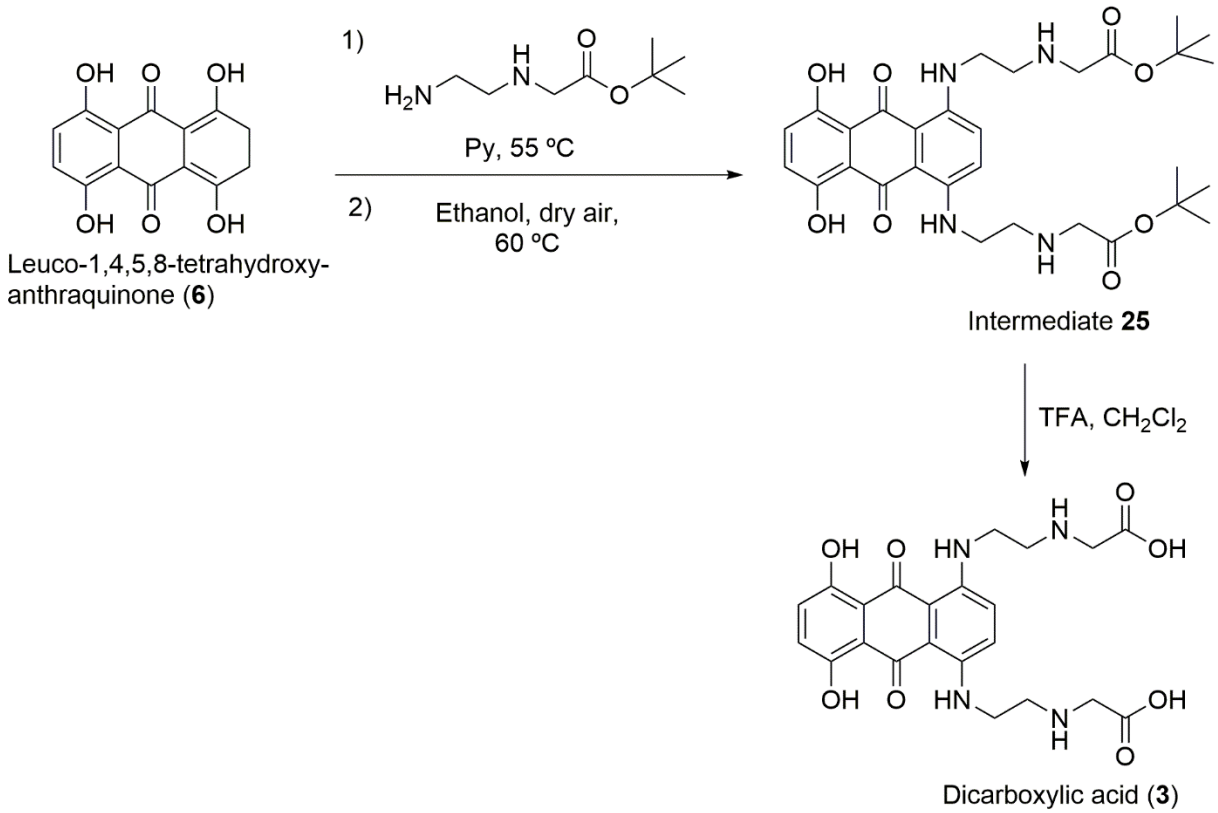

Scheme 21 – Synthesis of intermediate **25** and dicarboxylic acid (**3**) derivative. Py – pyridine; TFA – trifluoroacetic acid.

After 7 h, the reaction of condensation was finished. The Py was evaporated and the solid was used immediately in the next step without further purification. The second step, oxidation reaction, lasted for about 48 h. In this step, a colour change from purple to dark blue was evident. After completion of the reaction, the blue crude product was purified using three different methods: crystallization, anionic SPE, and flash column chromatography (Table 3).

Table 3 – Conditions and results of the purification methods.

Method	Conditions	Results
Crystallization	Ethanol/water	No crystals formed.
Anionic SPE	Elution with dichloromethane	No separation of the compounds.
Flash column chromatography	Gradient elution with *n*-hexane/ethyl acetate (6:4) – 100% ethyl acetate; ethyl acetate/MeOH (1:9) – 100% MeOH	The dark blue solid, intermediate **25**, was obtained as a major compound with ethyl acetate:MeOH, 7:3 with 82% yield.

MeOH - methanol

The structure elucidation of the di-*tert*-butyl-1,4-dihydroxy-5,8- bis{[2-(2-hydroxyethyl)amino]ethyl} amino-9,10-anthracene dione-diacetate (**25**) will be presented in the next section (3.3.3).

To obtain the dicarboxylic acid (**3**), the next step consisted in a deprotection reaction of the intermediate **25**.

3.2.5. Deprotection reaction of intermediate 25

The deprotection reaction represented in Scheme 22 catalysed by acid is standard for the removal of the *tert*-butyl ester. The reaction mixture of intermediate **25** in CH_2Cl_2 and TFA was cooled at 0 ºC for 5 h (Scheme 22). The reaction mixture changed from dark blue to dark red.

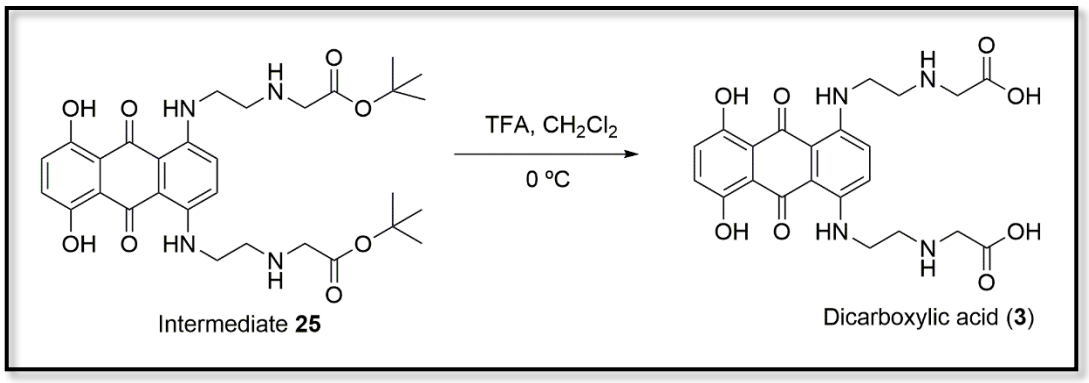

Scheme 22 – Deprotection reaction of intermediate **25.**

The TFA-mediated removal of *tert*-butyl groups leads to the formation of *tert*-butyl trifluoroacetate[90], since *tert*-butyl carbonium ions are formed during deprotection. To form the desired product, dicarboxylic acid (**3**), a second deprotection in the *tert*-butyl group through the same mechanism (Scheme 23) is necessary.

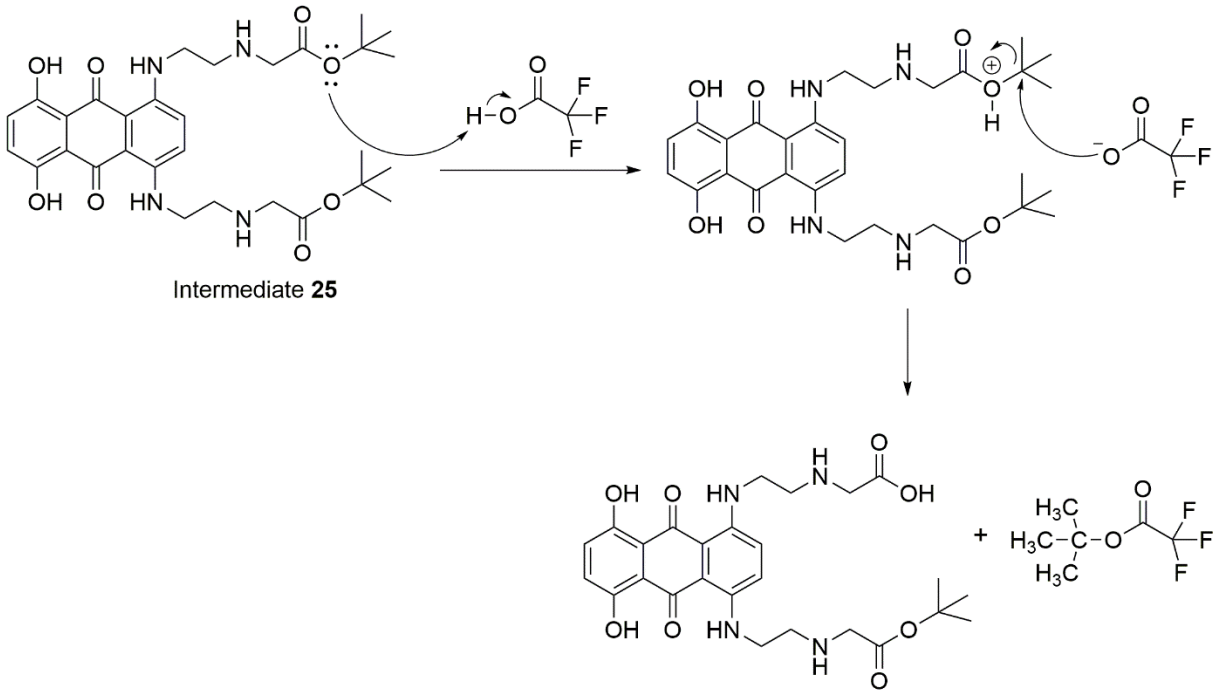

Scheme 23 – Mechanism of the deprotection reaction of intermediate **25**.

After 5 h, the reaction was finished and the TFA was evaporated and co-evaporated with CH_2Cl_2 under nitrogen at 40 ºC. The crude product obtained was purified by column chromatography using sephadex LH-20 with CH_2Cl_2/MeOH 9:1 as eluent to give 1,4-dihydroxy-5,8- bis{[2-(2-hydroxyethyl)amino]ethyl} amino-9,10-anthracene dione-diacetic acid (**3**). Further, the resulting product was filtered with nitrocellulose and hydrophilic VDF filters with 0.8 and 0.22 µm pore size, respectively in 1.7% yield. The structure elucidation of this compound will be presented in the next section (3.3.4).

The purity of dicarboxylic acid (**3**) was determined by diode-array analysis performed in a HPLC-DAD and was found to be of 83%. To proceed with toxicological tests, it will be necessary, in the future, to further purify this derivative **3** by reversed-phase HPLC.

3.3. Structure Elucidation

3.3.1. 1,8-Dimethoxychrysazin (21)

The structure elucidation of 1,8-dimetoxychrysazin (**21**) was established by IR and ^{1}H NMR techniques. IR spectrum showed one strong band at 1212 cm^{-1} typical of C-O ether stretching vibration and the absence of the O-H band, which suggested the presence of methoxy groups (Table 4).

Table 4 – IR data of 1,8-dimethoxychrysazin (**21**).

Compound	Group	υ(cm^{-1})
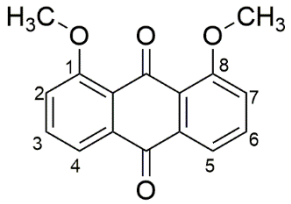	C-H aliphatic	2984
	C=O ketone	1674
	C=C aromatic	1600
	C-C aromatic	1467
	C-O ether	1212
1,8-Dimethoxychrysazin (21)		

υ – wavenumber

The ^{1}H NMR spectrum shows the presence of four signals corresponding to the 12 protons presented in the compound.

Characteristic signals of the aromatic protons H-3 and H-6, H-4 and H-5, and H-2 and H-7 appeared as a triplet, a double doublet and, a double doublet at δ_H 7.76, 7.69, and 7.54 ppm, respectively. The protons H-4 and H-5 were attributed to signals appearing in low fields, and are more deprotected, relative to protons H-2 and H-7 because of the magnetic anisotropic effect. One signal characteristic of aliphatic protons as singlet was observed at δ_H 3.92 ppm that corresponds to the 6 protons in the compound. Assignments of the proton signals of the 1,8-dimethoxychrysazin (**21**) are presented in Figure 6.

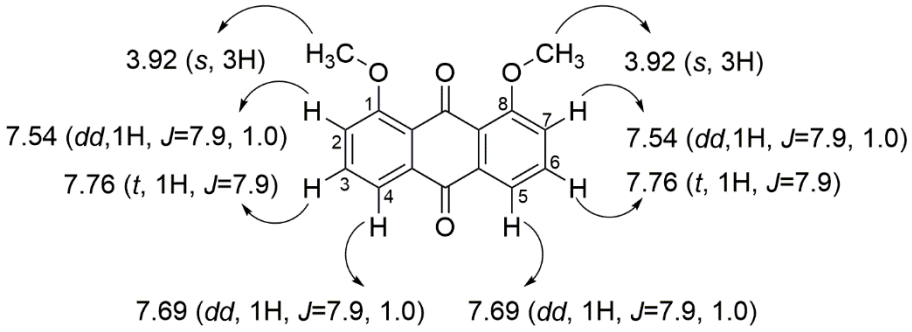

Figure 6 – Assignments of the proton signals in the 1,8-dimethoxychrysazin (**21**) molecule. Chemical deviation values, δ_H, in ppm relative to tetramethylsilane (TMS – internal reference); *s* – singlet; *dd* – double doublet; *t* – triplet.

3.3.2. 4,5-Dinitrochrysazin (8)

The structure elucidation of 4,5-dinitrochrysazin (**8**) was established by IR and ^{1}H NMR.

IR spectrum showed strong band at 3447 cm^{-1} typical of O-H stretching vibration and two bands at 1526 and 1354 cm^{-1} typical of N-O asymmetric and symmetric vibrations, respectively (Table 5).

Table 5 – IR data of 4,5-dinitrochrysazin (**8**).

Compound	Group	υ(cm^{-1})
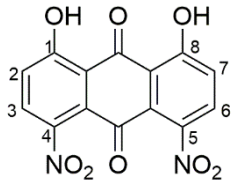 **4,5-Dinitrochrysazin (8)**	O-H	3447
	C-H aromatic	3080
	C=O ketone	1676
	C=C aromatic	1604
	N-O nitro	1526
	N-O nitro	1354
	C-O hydroxyl	1256

υ – wavenumber

The ^{1}H NMR spectrum shows the presence of three signals corresponding to six protons presented in the compound. Typical signals of the aromatic protons H-2 and H-7 and H-3 and H-6 appeared as duplets at δ_H 8.13 and 7.52 ppm, respectively. Signals corresponding to the OH protons do not appear in the ^{1}H RMN and that can be explained by intermolecular exchange of the protons with the solvent containing small traces of water. Assignment of the proton signals of the 4,5-dinitrochrysazin (**8**) are presented in Figure 7.

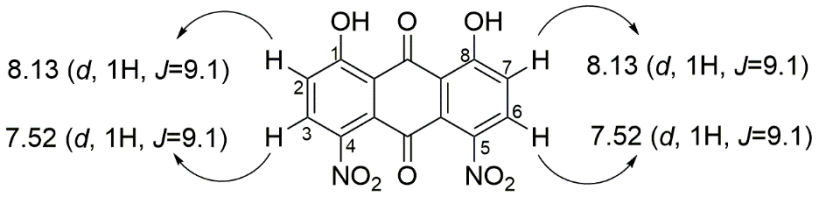

Figure 7 – Assignments of the proton signals in the 4,5-dinitrochrysazin (**8**) molecule. Chemical deviation values, δ_H, in ppm relative to TMS (internal reference); *d* – doublet.

3.3.3. Intermediate 25

The structure elucidation of intermediate **25** was established by IR and ^{1}H NMR. The IR data for intermediate **25** shown in Table 6 indicate the presence of bands corresponding to the important functional groups presented in its structure.

Table 6 – IR data of intermediate **25**.

Compound	Group	υ(cm^{-1})
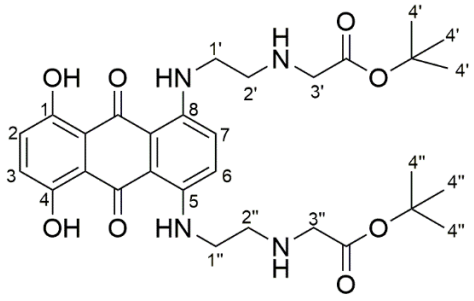 **Intermediate 25**	O-H	3442
	C-H aliphatic	2924
	C=O ester	1685
	C=O ketone	1650
	C=C aromatic	1522
	C-N aliphatic	1206
	C-O ester/ketone	1139

υ – wavenumber

The ^{1}H NMR spectrum shows the presence of 10 signals corresponding to 40 protons presented in the compound. Signals corresponding to the OH phenolic protons appear at δ_H 13.84 ppm as a singlet. Typical signals of the aromatic protons H-2, H-3, H-6, and H-7 appeared at δ_H 7.28, 7.19, 6.84, and 6.77 ppm, respectively. For the aliphatic chain, the first signal appearing at δ_H 3.16 ppm, as a singlet, was attributed to H-3' and H-3'' due to the proximity to an ester. The next signals appear as a multiplet at δ_H 2.51 ppm corresponding to H-1' and H-1'' following by signals of H-2' and H-2'' that appear at δ_H 1.99 ppm. Finally, the last signals corresponding to the *tert* group appear at δ_H 1.75 ppm as a singlet. Assignment of the proton signals of the intermediate **25** are presented in Figure 8.

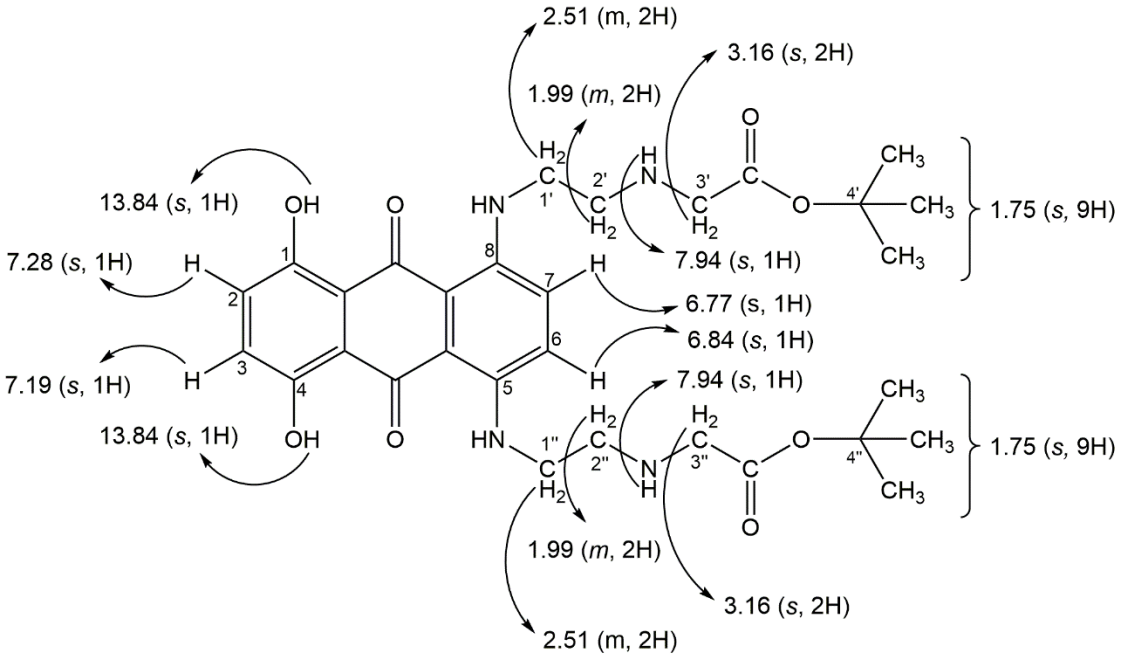

Figure 8 – Assignments of the proton signals in the intermediate **25**. Chemical deviation values, δ_H, in ppm relative to TMS (internal reference); s – singlet; *m* – multiplet.

3.3.4. Dicarboxylic acid (3) derivative

The structure elucidation of dicarboxylic acid (**3**) was established by IR and ^{1}H NMR. The IR data for dicarboxylic acid (**3**) shown in Table 7 indicate the presence of bands corresponding to the important functional groups presented in this structure.

The most characteristic bands of this compound are the bands corresponding to the N-H (amine group), O-H (alcohol and carboxylic acid) and, C=O (ketone and carboxylic acid). The band corresponding to the N-H bonds was observed at 2958 cm^{-1}. The O-H bond was detected at 3443 cm^{-3} and the C=O bond was attributed to the band at 1740 and 1637 cm^{-1} corresponding to the carboxylic acid and ketone, respectively. Other bands were detected for this structure, such as the bands corresponding to C-C bond in the aromatic ring at 1560 cm^{-1}, the bands corresponding to C-N bond at 1282 cm^{-1} and C-O at 1205 cm^{-1}.

Table 7 – IR data of dicarboxylic acid (**3**) derivative.

Compound	Group	υ(cm^{-1})
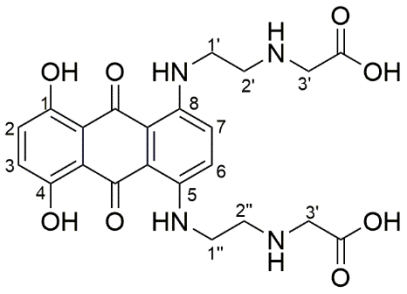	O-H	3443
	N-H amine	2958
	C-H aliphatic	2920
	C=O acid	1740
	C=O ketone	1637
	C-C aromatic	1560
	C-N aromatic	1282
Dicarboxylic acid (3)	C-O acid/ketone	1205

υ – wavenumber

The ^{1}H NMR spectrum (Figure 9) shows the presence of 11 signals corresponding to the 24 proton presented in compound **3**. Figure 9 also has the data of ^{1}H NMR of MTX (**1**). The presence of two signals with the high chemical shifts corresponding to the OH groups of phenol and carboxylic acid at δ_H 14.65 and 14.54 ppm, respectively, were noted. The OH group of the phenol is more deprotected due to the electronegative effect of oxygen, an electron withdrawing atom, and the resonance effect, which makes the protons more acidic, as well as the possibility of intramolecular hydrogen interaction. The next two signals correspond to the amine protons, aromatic and aliphatic, which appear at δ_H 10.48 and 8.50 ppm, respectively, whereas the corresponding signals of these protons appeared at δ_H 10.41 and 8.80-9.05 ppm in MTX (**1**). These protons are more protected from the above signals since the oxygen atom is more electronegative relative to the nitrogen atom. Once again, the aromatic amine shows the greatest chemical shift due to the resonance effect when compared to the aliphatic amine. Four signals corresponding to four aromatic protons namely H-2, H-3, H-6, and H-7 appear as four doublets at δ_H 7.53, 7.30, 7.15, and 6.60 ppm, whereas the corresponding signals of these protons appeared at δ_H 7.65 and 7.19 ppm. For the methylene protons, the first signal appearing at δ_H 3.81 ppm corresponds to H-3' and H-3'' as a singlet due to no neighbouring proton attached to carbon and its proximity to a carboxylic acid, which has an electronegativity effect that can withdraw electronic density to the electrons. The next signals referring to the geminal protons appear as a multiplet at δ_H 3.64 ppm. This chemical shift value is influenced by the electronegativity

of the aromatic amine and by the anisotropic effect produced by the aromatic ring. The last signal corresponding to H-2’ and H-2'' appears at δ_H 3.50 ppm under the water. In the MTX (**1**) molecule, the signals of H-1' and H-1'' as multiplet at δ_H 3.89-3.87 pm first appeared, then signals corresponding to H-4' and H-4'' as multiplet at δ_H 3.69-3.66 ppm, following by signals of H-2’ and H-2'' that appear at δ_H 3.21-3.17 ppm, and finally, the last signals corresponding to H-3’ and H-3'' appear at δ_H 3.07-3.04 ppm.

Assignments of the proton signals of the dicarboxylic acid (**3**) and MTX (**1**) are presented in Figure 9.

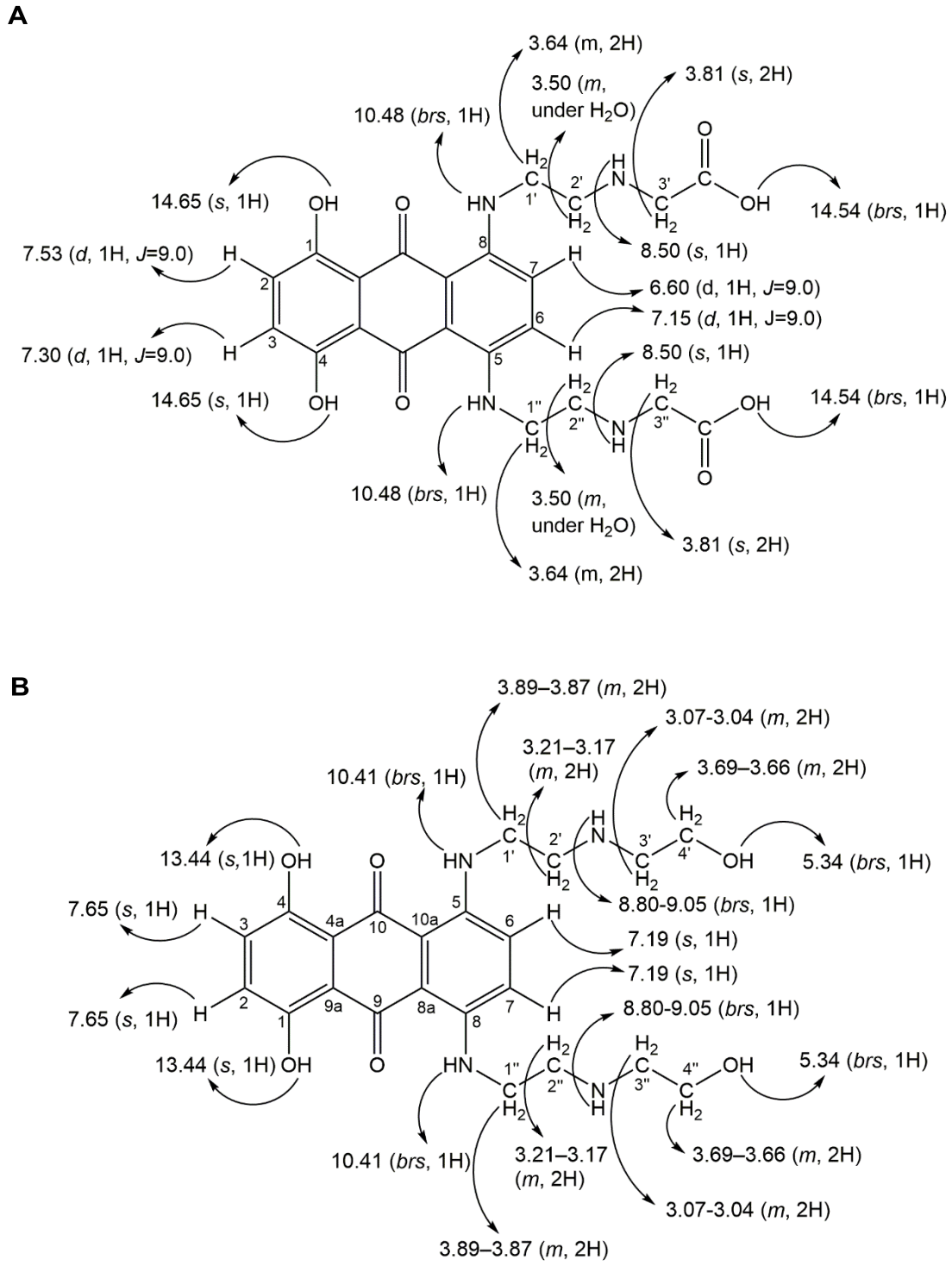

Figure 9 – Assignments of the proton signals (**A**) – in the dicarboxylic acid (**3**) molecule and (**B**) – in the MTX (**1**). Chemical deviation values, δ_H, in ppm relative to TMS (internal reference); *brs* – broad singlet; s – singlet; *d* – doublet; *m* – multiplet.

3.4. Oxidation reactions to obtain dicarboxylic acid (3)

In this section, different oxidation reactions conditions of alcohols were applied to MTX (**1**) (Scheme 24) in order to obtain the dicarboxylic acid (**3**) metabolite in a single step and with better yields than the previous attempts done.

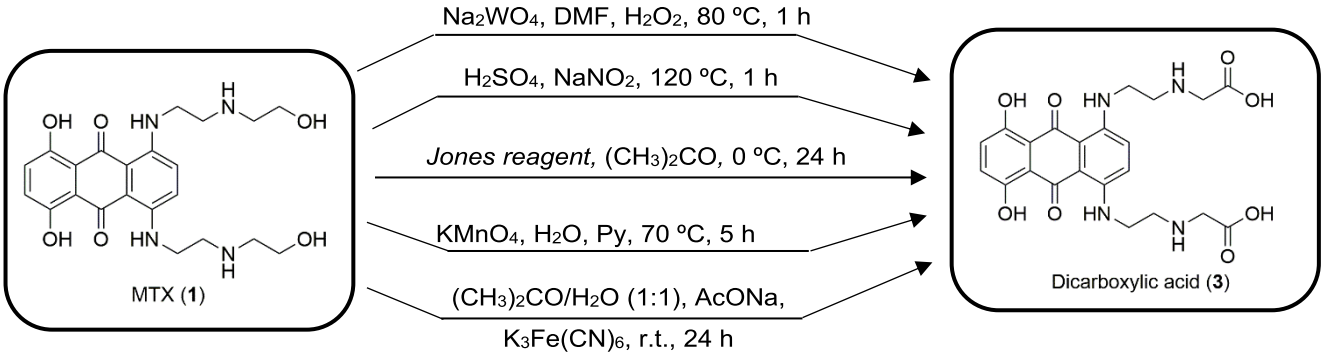

Scheme 24 – Oxidation reactions of alcohols tested for the MTX (**1**) molecule. AcOH – acetic acid; DMF – *N*,*N*-dimethylformamide; Py – pyridine.

3.4.1. Tungstate-catalysed oxidation

This oxidation reaction is catalysed by sodium tungstate (Na_2WO_4). The reaction mixture of MTX (**1**), DMF, Na_2WO_4, and H_2O_2 was heated to 80 ºC for 1 h (Scheme 24).

The oxidation of primary alcohols to carboxylic acids occurs by way of aldehyde intermediates. The Na_2WO_4 is soluble only in the aqueous phase; thus, in an aqueous phase, the catalyst precursor Na_2WO_4 is rapidly oxidized by H_2O_2 resulting into the bisperoxotungstate compound **I**[91]; Compound **I** is in equilibrium with **II** and **III**, according to the representation in Scheme 25.

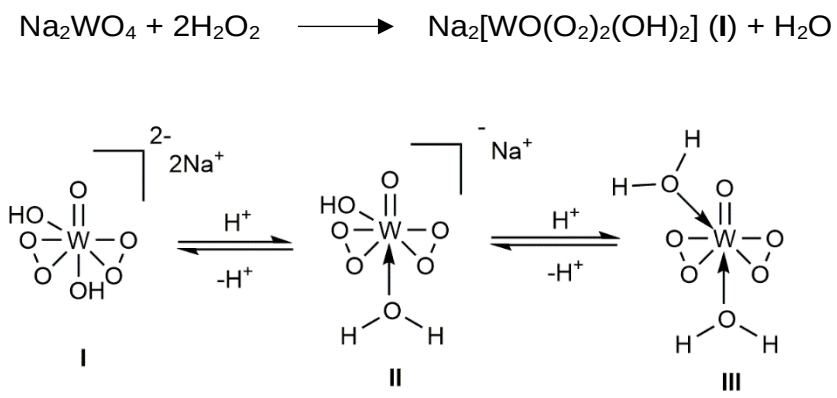

Scheme 25 –Tungstate-catalysed oxidation mechanism in aqueous phase.

The mono- (**II**) and di-protonated (**III**) forms are sufficiently reactive toward alcohols, while the dianion **I** is feebly active. The catalytic activity is highly dependent on the acidity of the reaction medium: in a pH range above 4, the catalytic system that contains largely **I** has only weak oxidative activity while at pH range of 0.4–3, the mono-protonated species **II** is dominant[91]. The sodium tungstate also can catalyse oxidation of secondary amines in a single step with hydrogen peroxide giving the corresponding nitrones[92].

After 1 h, the reaction was complete and the product was extracted by evaporation of DMF under nitrogen at 40 ºC and acidified with 20% HCl until pH 2. The organic phase was dried with Na_2SO_4 and after solvent evaporation, a purple solid was obtained. The solid was redissolved in MeOH and filtered with Syringe Filter, PTFE, with 0.45 µm pore size. The solvent was evaporated to furnish a purple solid with 38% yield. Although by TLC analysis, a single spot was observed in several mobile phases, by HPLC analysis, one major product at 7.43 min and several impurities with similar UV profiles were observed (Figure 10). The HRMS analysis also showed several masses corresponding to various products and the ^{1}H NMR spectrum of this solid was complex concluding that it was a mixture of compounds. One possible structure **26** was attributed to the peak with a m/z value of 441 (Table 8).

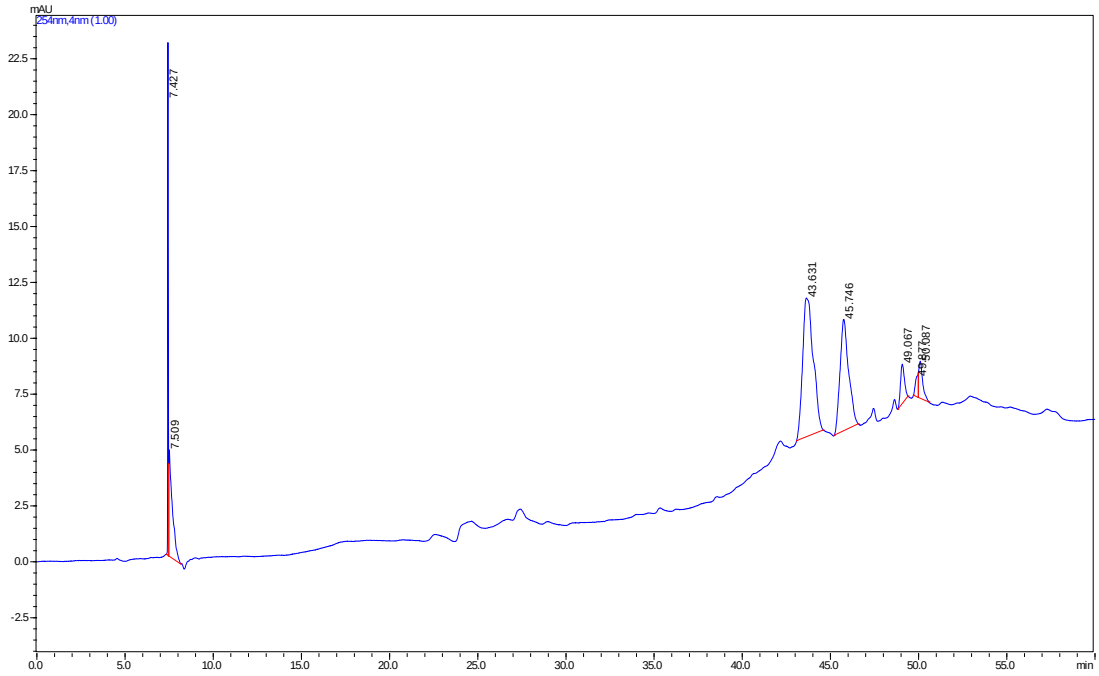

Figure 10 - Representative HPLC chromatogram [λ= 254 nm, C18, linear gradient from 20 to 100% of eluent B within 60 min (eluent A: 0.1% aqueous solution of CH_3COOH; eluent B: MeOH)].

Table 8 – Values of m/z obtained in HRMS spectrum and proposed structure **26**.

	m/z	
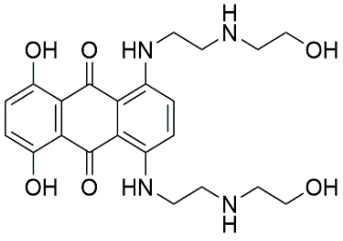 MTX (**1**) **m/z = 445**	441.35606	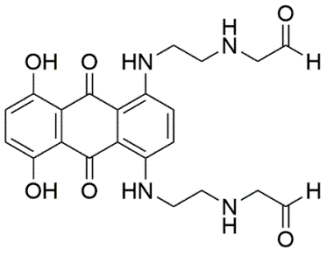 Compound **26** **m/z = 441**
	485.38179	
	529.40793	
	573.43361	
	595.47936	

3.4.2. Oxidation with sodium nitrite

This procedure of oxidation was based in the oxidation of an anthraquinone, aloe-emodin, performed by Gravit and Laddha in 2012[93]. MTX (**1**) was subjected to oxidation reaction with sodium nitrite ($NaNO_2$) in H_2SO_4 (Scheme 24). The solution was heated at 120 ºC over a period of 1 h. After 1 h, the reaction mixture was diluted and extracted with chloroform. The organic solvent was dried with Na_2SO_4 and evaporated to furnish a brown solid. The solid was redissolved in MeOH and filtered with Syringe Filter, PTFE, with 0.45 µm pore size. The solvent was evaporated to furnish a brown solid with 88% yield.

Similarly to the previous results, through TLC analysis it was possible to observe a single spot using several mobile phases, although by HPLC analysis the presence of several impurities with similar UV profile were observed (Figure 11). The HRMS also showed several peaks attributed to various products and the ^1H NMR spectrum of this solid was complex concluding that it was a mixture of compounds. Two possible structures **27** and **28** for m/z = 256 and m/z = 447, respectively were proposed (Table 9).

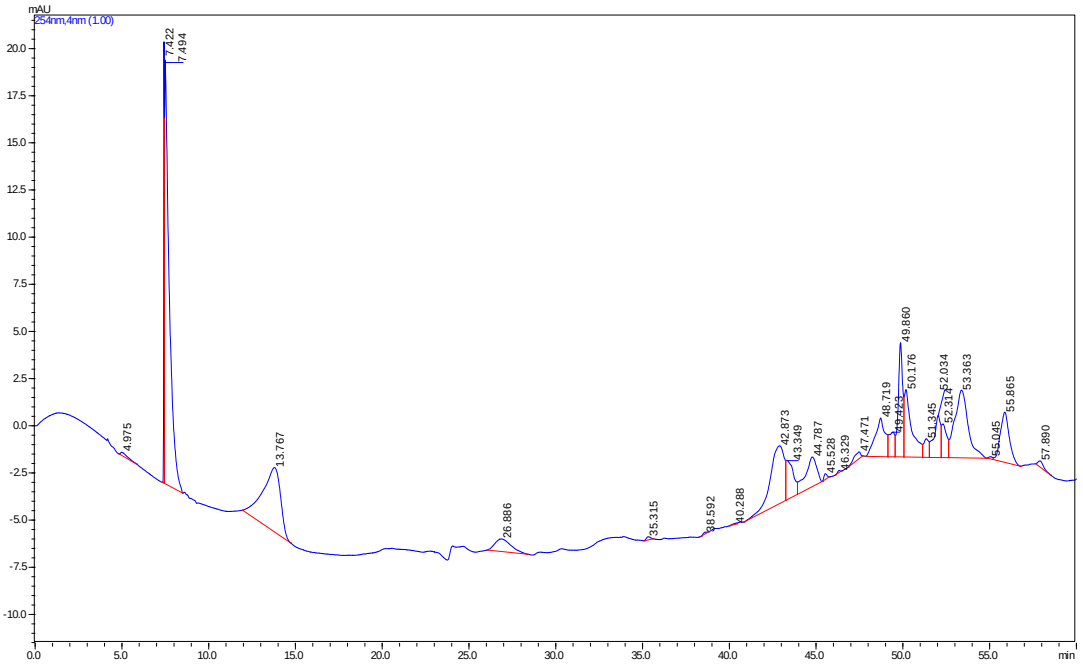

Figure 11 - Representative HPLC chromatogram [λ= 254 nm, C18, linear gradient from 20 to 100% of eluent B within 60 min (eluent A: 0.1% aqueous solution of CH_3COOH; eluent B: MeOH)].

Table 9 – Values of m/z obtained in HRMS spectrum and proposed structures **27** and **28**.

	m/z		
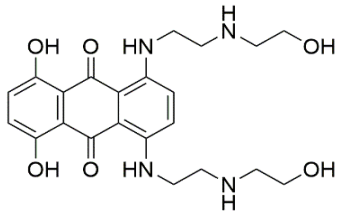 MTX (**1**) **m/z = 445**	256.29976	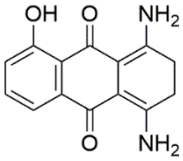 Compound **27** **m/z = 256**	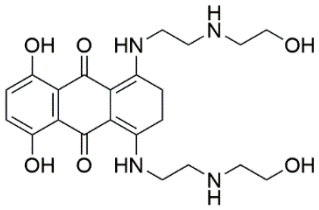 Compound **28** **m/z = 447**
	447.34694		
	529.40586		
	573.43073		

Compound **27** with m/z = 256 value was hypothesized to result from the break of compound **28**. Also, compound **28** with m/z = 447 was hypothesized to result from the reduction of MTX (**1**) molecule.

3.4.3. Chromic acid oxidation

This reaction generally known as the Jones oxidation uses the reagent CrO_3-H_2SO_4-H_2O and is generally carried out in aqueous $(CH_3)_2CO$ (Scheme 24). The alcohol and chromic acid form a chromate ester that either reacts intramolecularly or intermolecularly in the presence of a base (water) to yield the intermediate aldehyde. This aldehyde equilibrates with its hydrate and reacts resulting in the formation of a new chromate ester, which decomposes to a carboxylic acid (Scheme 26). To form the desired product, dicarboxylic acid (**3**), a second oxidation is necessary in the primary alcohol, by the same mechanism.

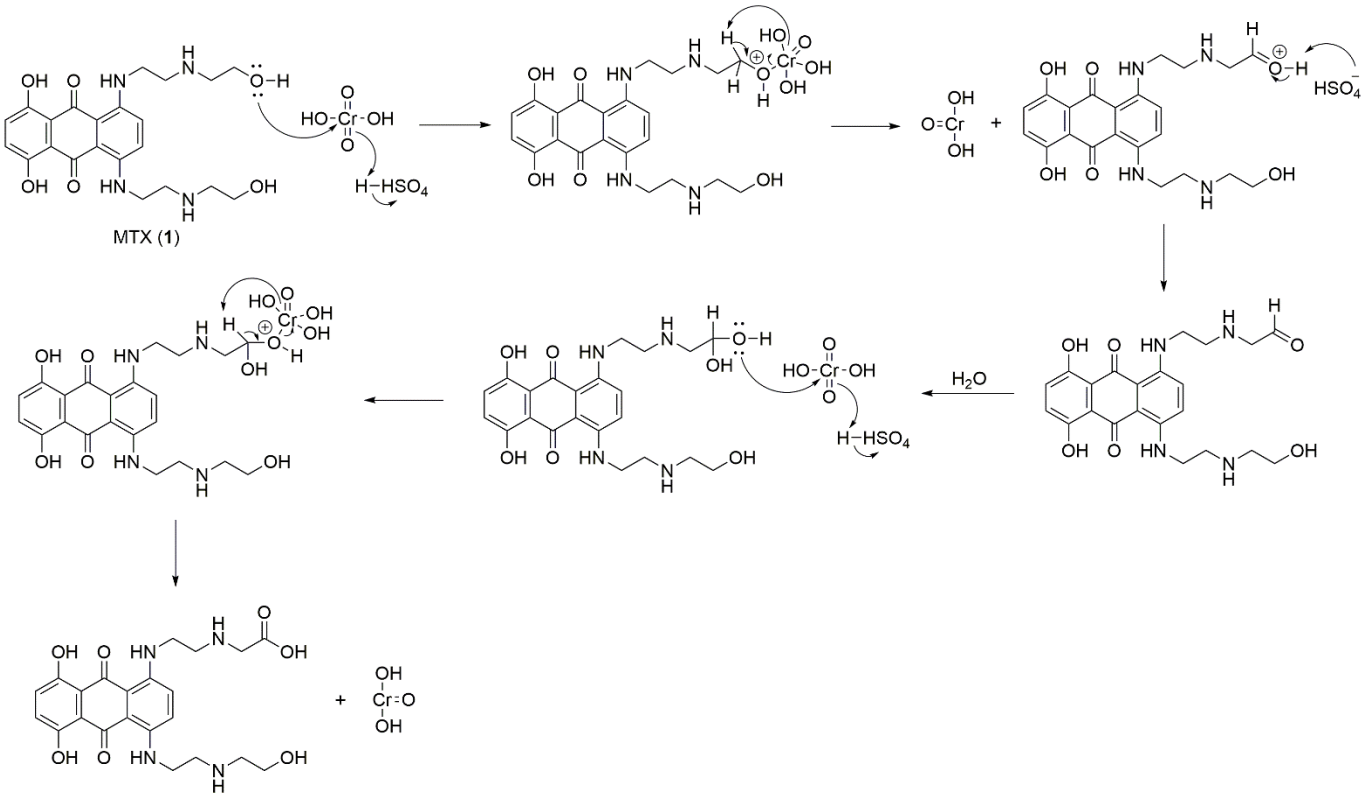

Scheme 26 – Mechanism of the Jones oxidation.

The reaction mixture of MTX (**1**), chromic acid and $(CH_3)_2CO$ was done at 0 ºC for 24 h. After that, the reaction was stopped but it was not completely finished. The excess of oxidant was destroyed by the addition of 2-propanol and the reaction mixture was extracted with chloroform. The organic solvent was dried with Na_2SO_4 and concentrated to furnish a blue solid. The solid was redissolved in MeOH and filtered with with a Syringe Filter, PTFE, with 0.45 µm pore size. The solvent was evaporated and a blue solid with 13% yield was obtained.

Also in this reaction, the TLC analysis showed a single spot detected even when using several mobile phases; however, by HPLC analysis several impurities with similar UV profile were observed (Figure 12). In HRMS spectrum, several peaks corresponding to various products were observed and the ^{1}H NMR spectrum of this blue solid was complex corresponding to a mixture of products (Table 9). As in the previous reaction, this present reaction also forms a compound with m/z = 447 that was proposed to be

the same product, compound **28** (Table 10). A common drawback of this reaction is the formation of dimeric esters, which could explain the presence of peaks with high m/z values.

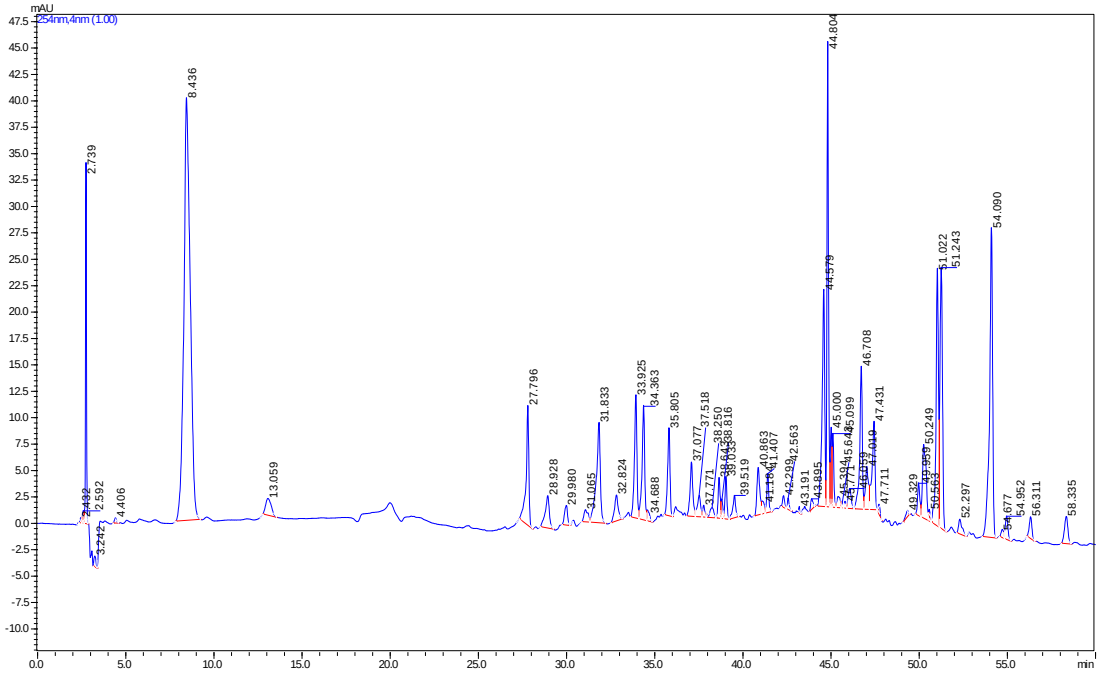

Figure 12 - Representative HPLC chromatogram [λ= 254 nm, C18, linear gradient from 20 to 100% of eluent B within 60 min (eluent A: 0.1% aqueous solution of CH_3COOH; eluent B: MeOH)].

Table 10 – Values of m/z obtained in HRMS spectrum.

	m/z
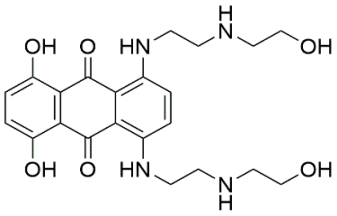 MTX (**1**) **m/z = 445**	283.26350
	447.34702
	507.42614
	551.45310
	595.47865
	663.45535

3.4.4. Oxidation with potassium permanganate

Potassium permanganate ($KMnO_4$) is also a very strong oxidant that converts primary alcohols to carboxylic acids. The reaction mixture of MTX (**1**) in Py, 10% Na_2CO_3 aqueous solution and $KMnO_4$ was heated at 70 ºC for 5 h (Scheme 24)[94]. A hydride is transferred from an alcohol to a permanganate anion MnO_4^- to form an intermediate aldehyde that reacts again with MnO_4^- to obtain the carboxylic acid (Scheme 27).

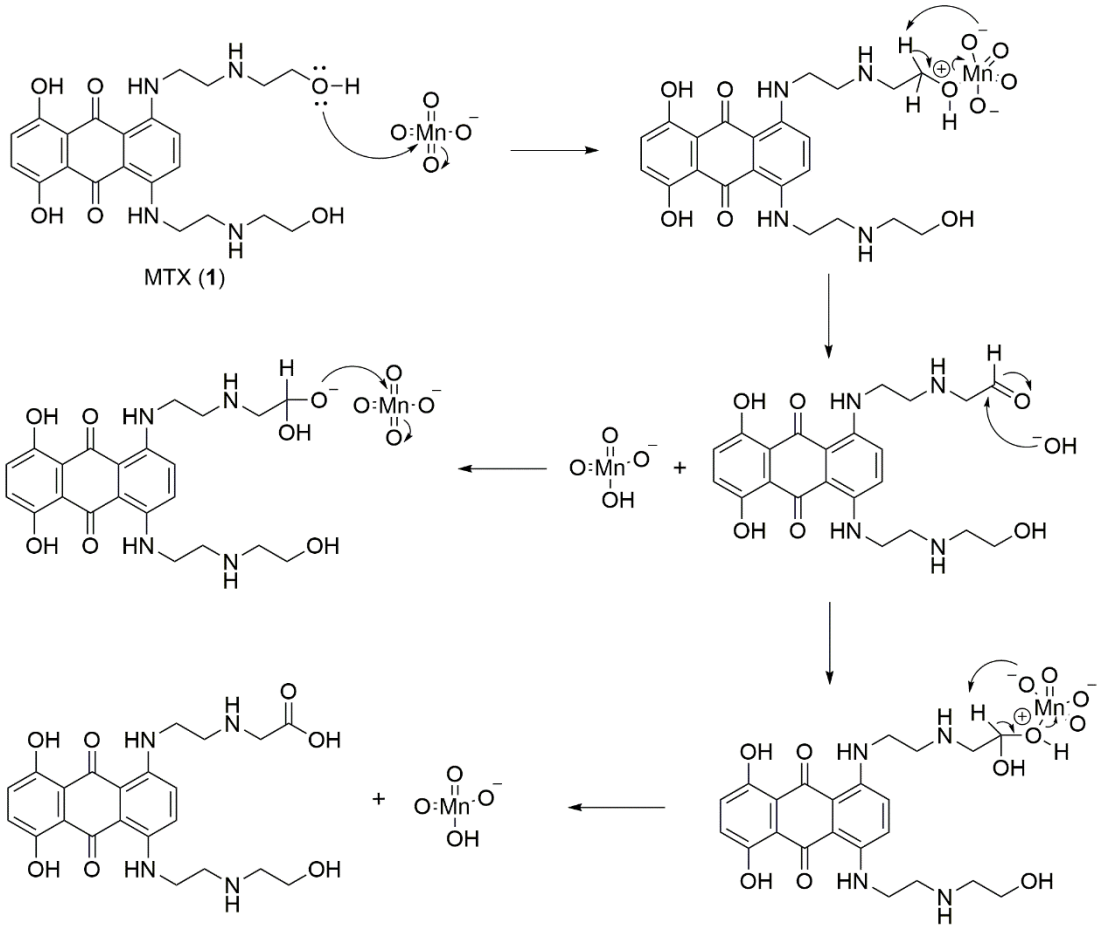

Scheme 27 – Proposed mechanism for the oxidation of alcohols to acids using permanganate.

After 5 h, the reaction was considered to be finished and allowed to cool at r.t.. The reaction mixture was acidified with 10% HCl aqueous solution to remove Py and

extracted with chloroform and ethyl acetate. Nevertheless, in the organic layer, no product could be extracted, as verified by the TLC analysis.

3.4.5. Oxidation with potassium ferrocyanide

Potassium ferrocyanide [$K_3Fe(CN)_6$] is an oxidizing-agent in which the oxidizing species is a complex electron-abstracting ion. In this procedure, MTX (**1**), in $(CH_3)_2CO/H_2O$ (1:1), sodium acetate (AcONa) and [$K_3Fe(CN)_6$], was stirred at r.t. for 24 h (Scheme 24). Since potassium ferrocyanide acts as a "one-electron abstractor," the primary action of this reagent is the formation of a radical.

After 24 h, the reaction was finished and the solid in suspension was filtered. The filtrate was extracted with CH_2Cl_2 and then acidified with 20% HCl aqueous solution. The organic phase was dried with Na_2SO_4 and the solvent concentrated to obtain a blue solid with a yield of 27%. The TLC analysis of the blue solid showed a single spot with several mobile phases but the ^{1}H NMR spectrum and HPLC analysis (Figure 13) of solid was complex and HRMS spectrum shown several products (Table 10), thus concluding that a mixture of compounds was obtained. The HRMS spectrum presented a m/z = 445 value that corresponds to the MTX (**1**) indicating that reaction was not complete. Two possible structures **29** and **30** with m/z values of 282 and 401, respectively, were found and structures proposed (Table 11). The value m/z = 944 corresponds to a dimer of the dicarboxylic acid (**3**), since the m/z of one molecule is 472. The compounds **29** and **30** were hypothesized to be products resulting from the degradation of MTX (**1**).

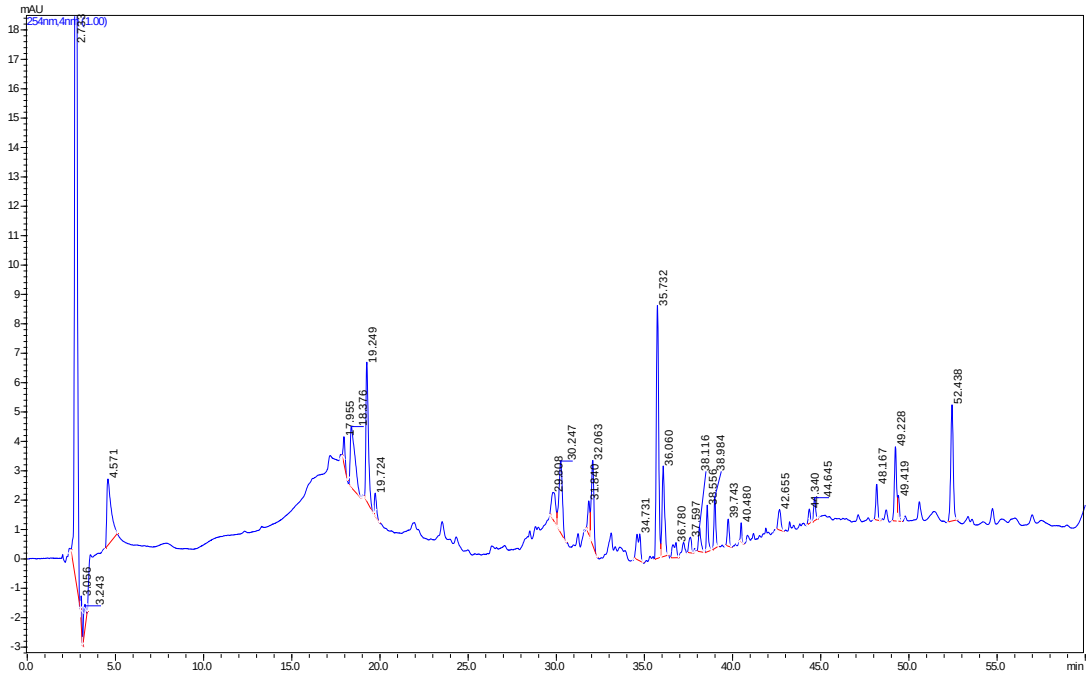

Figure 13 – Representative HPLC chromatogram [λ= 254 nm, C18, linear gradient from 20 to 100% of eluent B within 60 min (eluent A: 0.1% aqueous solution of CH_3COOH; eluent B: MeOH)].

Table 11 – Values of m/z obtained in HRMS spectrum and proposed structures **29** and **30**.

	m/z		
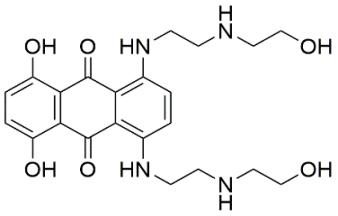 MTX (**1**) **m/z = 445**	282.27921	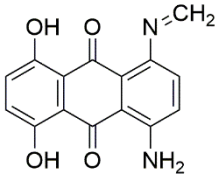 Compound **29** **m/z = 282**	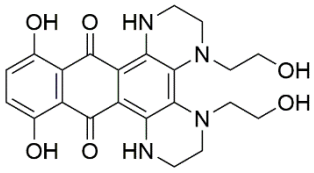 Compound **30** **m/z = 401**
	401.28752		
	445.20839		
	489.33998		
	944.42579		

Of the five oxidation reactions studied, oxidation catalysed by tungstate appears to be most promising to explore in the future, since an aldehyde was formed that could evolve into the carboxylic acid if the oxidizing power increases.

3.5. Synthesis of acetylated derivatives of mitoxantrone

In 2013, Rossato *et al*. described, for the first time, the formation of the acetoxy ester derivative (**13**) of MTX (**1**) in rat hepatic S9 fraction. They suggested that the acetoxy derivative can result from an *N*-oxygenation in the aromatic amine, followed by an acetylation[42]. Due to the few studies done with this metabolite, it was planned to introduce acetyl groups into MTX (**1**) in order to obtain these derivatives for future assays.

The structure of MTX (**1**) contains four OH groups with the following reactivity order: 1,4-OH > 4', 4''-OH. The two phenol groups are more acidic compared to the two primary alcohols, due to the resonance effect, so the reaction will occur first in the phenols and later in the alcohols. To obtain the acetoxy derivatives of MTX (**1**), reaction conditions with acetic anhydride (Ac_2O) and Py were investigated (Scheme 28).

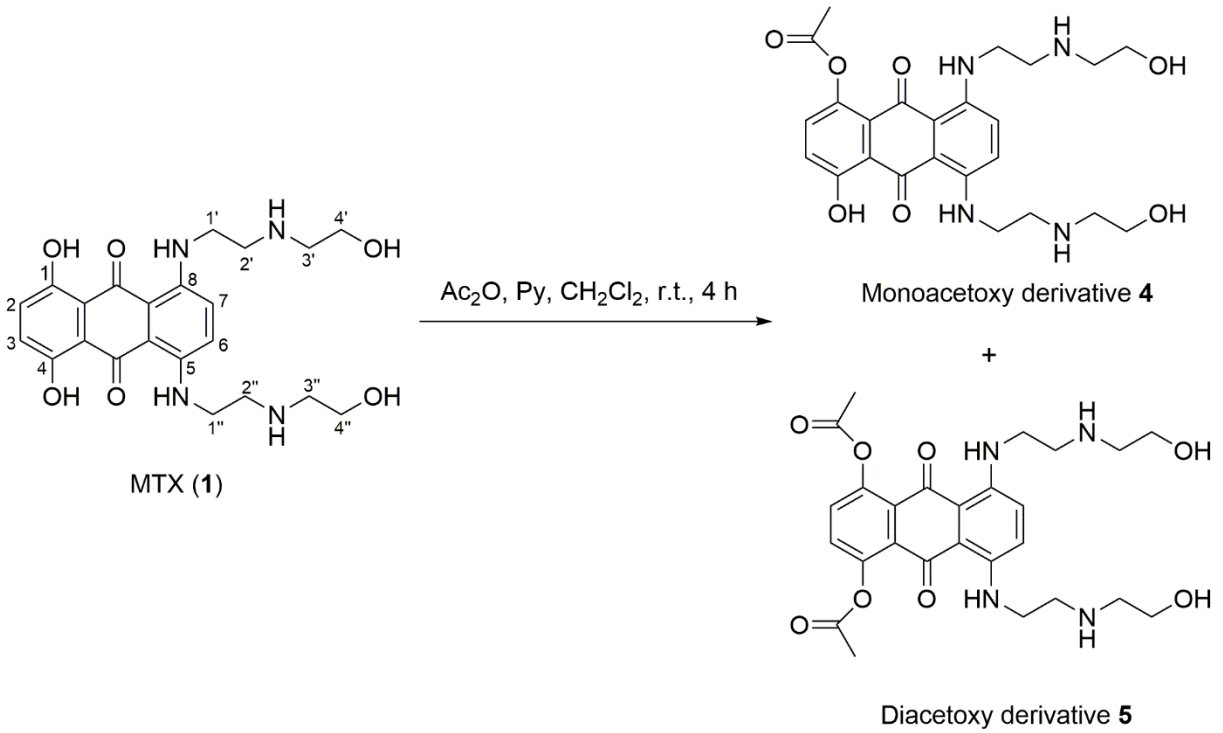

Scheme 28 – Synthesis of mono (**4**)- and di-acetoxy (**5**) derivative from MTX (**1**). Ac_2O – acetic anhydride; Py – pyridine; r.t. – room temperature.

The Ac_2O was chosen due to its wide use in acetylation and Py was the nucleophilic catalyst. The reaction occurs through the nucleophilic attack of the phenolic OH group on the carbon of acetic anhydride (Scheme 29). This type of reaction is classified as a nucleophilic substitution. To obtain the diacetoxy derivative (**5**), a second acetylation in another phenolic group is necessary through the same mechanism.

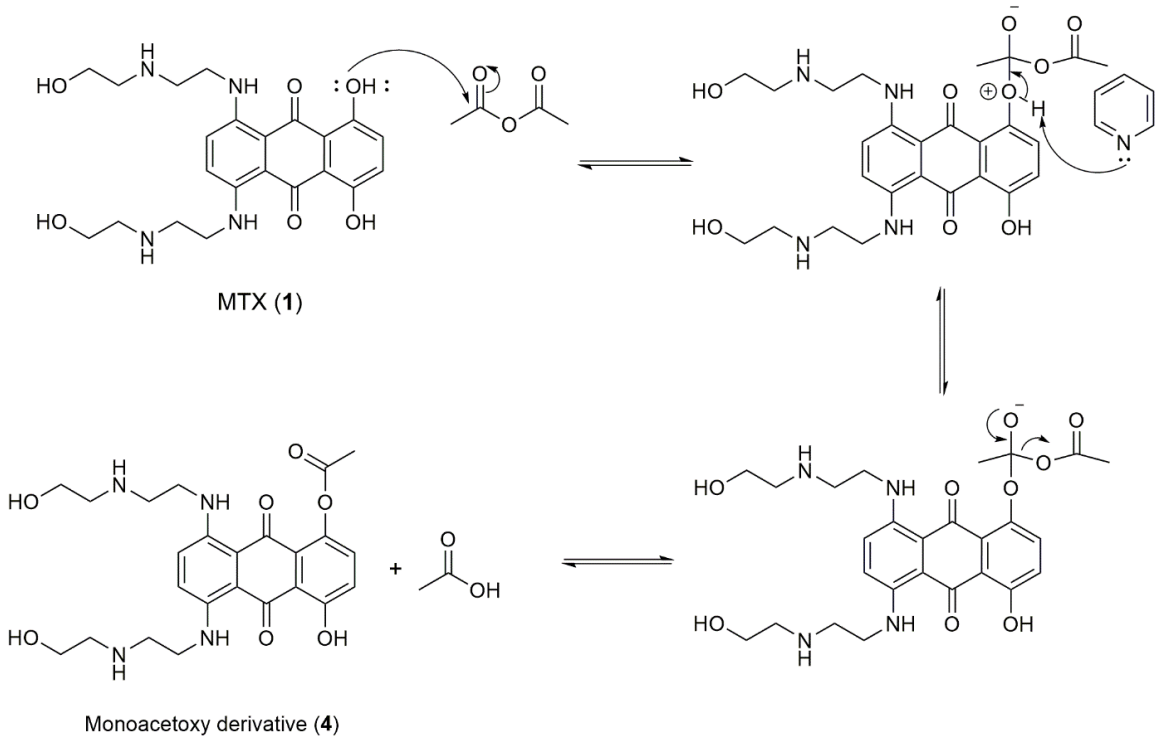

Scheme 29 – Mechanism of acetylation reaction of MTX (**1**).

After 4 h at r. t. the reaction was finished. To remove the Py, 10% HCl aqueous solutions were added sequentially and water was used to wash the organic dichloromethane phase. The organic phase was dried over anhydrous Na_2SO_4 and the solvent was evaporated under reduced pressure. The crude product was purified by preparative TLC. Thus, two products were obtained, 4-hydroxy-5,8- bis{[2-(2-hydroxyethyl)amino]ethyl} amino-9,10-anthracenedion-1-yl acetate **4** and 5,8-bis{[2-(2-hydroxyethyl)amino]ethyl}amino-9,10-anthracenedion-1,4-diyldi-acetate **5** with 38% and 21% yield, respectively.

The purity of the mono- **4** and di-acetoxy **5** derivatives were determined by diode-array analysis performed in a HPLC-DAD and was found to be 77% and 92%, respectively. To improve the purity of these two derivatives (**4** and **5**), in the future, it will be necessary to use semi-preparative C18 column. The UV-Vis spectrum of monoacetoxy **4** and diacetoxy **5** derivative presented similar spectral features to each other in the UV-Vis range.

3.5.1. Structural elucidation of acetylated derivatives

The structure elucidation of monoacetoxy derivative **4** and diacetoxy derivative **5** was established by IR and ^{1}H NMR.

IR spectrum showed strong bands at 1738 cm^{-1} and 1736 cm^{-1} typical of C=O ester stretching vibration, which suggested the presence of acetyl group in monoacetoxy derivative **4** and of acetyl group in diacetoxy derivative **5**, respectively (Table 12).

The ^{1}H NMR data of monoacetoxy derivative **4** and diacetoxy derivative **5** are presented in Figure 14. Characteristic signals of the aromatic protons H-2 and H-3, H-6, and H-7 in the nomoacetylated compound **4** appeared at δ_H 7.71, 7.69, and 7.18-7.16 ppm, and at δ_H 8.52 and 7.14 ppm in the diacetylated compound **5**, whereas the corresponding signals of these protons appeared at δ_H 7.19, and 7.65 ppm in the non-acetylated parent compound. Four signals characteristic of aliphatic protons were observed between δ_H 4.28-3.62 ppm in the monoacetylated derivative **4** and between δ_H 3.62-3.27 ppm in the diacetylated derivative **5**, whereas the corresponding signals of these protons appeared between δ_H 3.89-4.04 ppm in the non-acetylated parent compound, MTX (**1**). Two singlets at δ_H 3.51 and 2.09 ppm, integrating each for three protons, were assigned for -CH_3 protons of acetyl groups in the monoacetylated **4** and diacetylated **5** compounds, respectively, which allowed to establish the structure of derivatives **4** and **5**.

Table 12 – IR data of monoacetoxy derivative (**4**) and diacetoxy derivative (**5**).

Compound	Group	υ(cm^{-1})
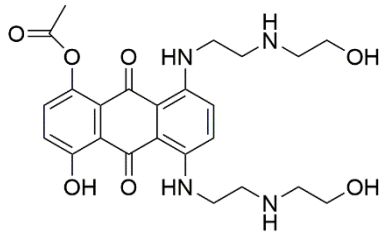 **Monoacetoxy derivative 4**	O-H	3440
	C-H aromatic	2957
	C-H aliphatic	2922, 2851
	C=O ester	1738
	C=C aromatic	1634
	C=O ketone	1563
	C-C aromatic	1464
	C-N aromatic	1260
	C-O ester	1083
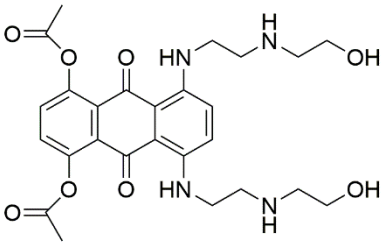 **Diacetoxy derivative 5**	O-H	3439
	C-H aromatic	2921, 2851
	C=O ester	1736
	C=C aromatic	1640
	C=O ketone	1561
	C-C aromatic	1466
	C-O ester	1173

υ – wavenumber.

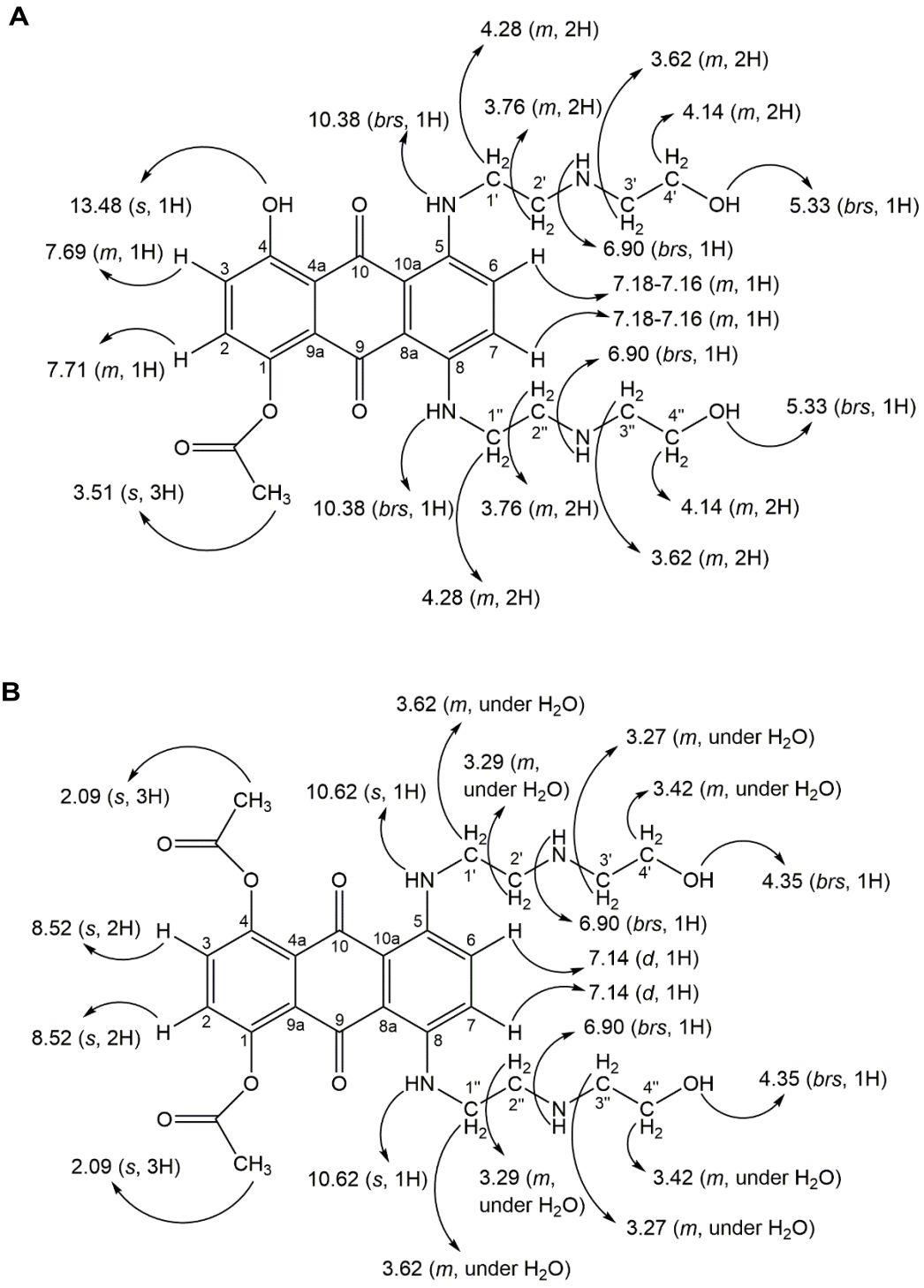

Figure 14 – Assignments of the proton signals (**A**) – in the monocetoxy derivative (**4**); (**B**) – in the diacetoxy derivative (**5**) molecules. Chemical deviation values, δ_H, in ppm relative to TMS (internal reference); *s* – singlet; *brs* – broad singlet; *t* – triplet; *m* – multiplet.

CHAPTER 4

Concluding remarks

CHAPTER 4 – CONCLUDING REMARKS

Cancer is still a disease with poor diagnosis and most of the drugs currently in clinical use have severe side effects. Cardiotoxicity is one of the most relevant side effects on the long-term cancer survivors and there is the possibility that the metabolites of anticancer drugs are possible culprits of their induced-cardiotoxicity.

In this dissertation, the synthesis and structural elucidation of NAPHT (**2**), dicarboxylic acid (**3**) metabolite and mono (**4**)- and di-acetoxy (**5**) metabolites was accomplished along with three intermediates, 4,5-dinitrochrysazin (**8**), 1,8-dimethoxychrysazin (**21**), and di-*tert*-butyl-1,4-dihydroxy-5,8- bis{[2-(2-hydroxyethyl)amino]ethyl} amino-9,10-anthracene dione-diacetate (**25**).

The synthesis of NAPHT (**2**) metabolite was previously synthesized in the group. Unfortunately, we failed to improve yield in this present work but this derivative was obtained by comparison with the standard using another procedure.

Since studies on the human metabolites of MTX (**1**) are sparse, dicarboxylic acid (**3**) has also been synthesized via six steps: nitration of chrysazin (**7**), reduction of 4,5-dinitrochrysazin (**8**), reductive hydrolysis of 4,5-diaminochrysazin (**9**), condensation reaction of leuco 1,4,5,8-tetrahydroxyanthraquinine (**6**) with the protected amino acid and subsequent oxidation, and deprotection reactions. In this synthetic pathway, several problems arose mainly due to the formation of many by-products that made the purification procedures difficult. The yield of the desired compound was very low, 1.7%. Nevertheless, this strategy was successful in furnishing the target molecule, dicarboxylic acid (**3**).

The third part concerns the oxidation studies performed on MTX (**1**) in order to obtain derivative **3** and reduce the number of reaction steps of the previous procedure. Unfortunately, none of the reactions performed resulted in the desirable compound. Several products were obtained and some structures were proposed, which allowed to select oxidation catalysed by tungstate as the most promising conditions that deserves to be further explored.

Finally, the last part of the dissertation corresponds to the synthesis of acetylated metabolites of MTX (**1**). Two derivatives, mono (**4**)- and di-acetoxy (**5**), were obtained by addition the acetoxy group at the MTX (**1**) molecule with Ac_2O in Py. The yield after purification of this compounds was 38 and 21% for mono (**4**)- and di-acetoxy (**5**)

derivatives, respectively. The spectroscopic IR and ^{1}H NMR techniques and HRMS allowed to characterize the synthetized derivatives.

Taking in account the results obtained in this dissertation, the study of the cardiotoxicity of the synthesized derivatives **2-5** would be important to better characterized the influence of MTX (**1**) metabolites in the drugs' cardiotoxicity. Considering the amount of routes addressed and problems solved in the synthesis of these important metabolites, the overall results can pave the way in obtaining other important metabolites.

CHAPTER 5

Experimental section

CHAPTER 5 – EXPERIMENTAL SECTION

5.1 Materials and chemicals

MTX dihydrochloride [MTX (**1**), ≥97% purity], peroxidase from horseradish (Type II), chrysazin (96% purity), sodium nitrite, and ascorbic acid were purchased from Sigma-Aldrich (St. Louis, MO, USA), hydrogen peroxide (H_2O_2) 30%, ammonium acetate, chromium trioxide, sodium bicarbonate, sodium hidrosulfite, sodium hydroxide, sodium nitrite, sodium sulphate, sodium tungstate and charcoal were purchased from Merck (Germany). Tin (II) chloride 2-hydrate was purchase from Panreac Quimica Sau (Barcelona, Spain). Potassium permanganate was acquired from M&B (London). The solvents used were products pro analysis or high performance liquid chromatography (HPLC) grade of the firms Sigma-Aldrich, Chem-Lab NV, Merck, VWR Chemical, and Panreac Quimica Sau. HPLC ultrapure water was generated by a Milli-Q system (Millipore, Bedford, MA, USA). TLC using Merck silica gel 60HF254/kiesel gel 60G plates purchased from Merck (Germany).

Purification of the synthesized compounds was performed by chromatography flash column using Merck silica gel 60 (0.040-0.063 mm), Discovery® DSC-SAX SPE anionic exchange cartridge, 6 mL tubes, lipophilic SEPHADEX LH-20 from Sigma-Aldrich.

Melting points were obtained in a Köfler microscope and are uncorrected. IR spectra were measured in KBr microplate in a Fourier transform infrared spectroscopy spectrometer Nicolet iS10 from Thermo Scientific with Smart OMNI-Transmisson accessory (Software OMNIC 8.3) (cm^{-1}). ^1H NMR spectra were taken in DMSO-d6 at r.t., on Bruker Avance 300 instrument (300.13 MHz for ^1H). Chemical shifts (δ) measures were given in ppm values relative to TMS as an internal reference. Coupling constants (*J*) are reported in hertz (Hz).

The visualization of the TLC chromatograms was made under UV light at 254 and 365 nm or ninhydrin 3 mg/mL in ethanol following heat activation.

HRMS spectra were measured on a APEX III mass spectrometer, recorded as Electrospray ionization mode in Centro de Apoio Científico e Tecnolóxico á Investigation (CACTI, University of Vigo, Spain).

5.2. Synthesis and purification of naphthoquinoxaline mitoxantrone derivative

Thirty milligrams (0.067 mmol) of MTX (**1**) were dissolved in 500 mL ammonium acetate buffer (pH 5) containing 74 µL hydrogen peroxide (3%). After addition of 2 mg dry HRP, the solution was stirred 4 h at r.t.. The reaction was monitored by TLC with methanol (MeOH)/NH_3 25% (10:0.1) and was completed with 2 mL ascorbic acid 57 mM and the enzyme was destroyed by boiling the incubation for 15 min. The solvent was evaporated under a stream of nitrogen and 16.1 mg (54%) of the crude product were obtained. After filtration (0.45 µm, Millipore), the crude was purified by HPLC (42% yield) performed in a system consisted of a Shimadzu LC-20AD pump, equipped with a Shimadzu DGV-20A5 degasser, a Rheodyne 7725i injector fitted with a 500 µL loop, and a SPD-M20A DAD detector (Kyoto, Japan). HPLC was equipped with a DAD ultraviolet (UV) 8000, and using a NUCLEODUR C18 HTec column (5 µm, 250 x 10 mm I.D.) from MACHEREY-NAGEL (Germany). The injected volume was 450 µL and the mobile phase was monitored at 254 nm. Shimadzu LCMS Lab Solution software, version 3.50 SP2. managed chromatographic data. An isocratic elution 3:7 of the eluent B was used [eluent A corresponding to 0.1% aqueous solution of CH_3COOH and the eluent B corresponds to MeOH] was used at a constant flow rate of 1.5 mL/min. All samples were dissolved in MeOH and filtered through a hydrophilic Durapore-GV membrane of 0.45 mm pore size (Millipore) before injection.

8,11-dihydroxy-4-(2-hydroxyethyl)-6[[2-[(2-hydroxyethyl)amino]ethyl]-amino]-1,2,3,4,7,12-hexahydronaphto-[2,3-f]quinoxaline-7,12-dione (**2**): IR (KBr) υmax: 3432, 2920, 1701, 1628, 1556, 1397, 1319. HRMS-ESI m/z calc for $C_{22}H_{27}N_4O_6$ $[M+H]^+$ 443.18859 found was: 443.19313.

5.2.1. High performance liquid chromatography analysis of 8,11-dihydroxy-4-(2-hydroxyethyl)-6[[2-[(2-hydroxyethyl)amino]ethyl]-amino]-1,2,3,4,7,12-hexahydro-naphto-[2,3-f]quinoxaline-7,12-dione (2):

HPLC analysis of the purified product was performed in a system consisted of Shimadzu LC-20AD pump, equipped with a Shimadzu DGV-20A5 degasser, a Rheodyne 7725i injector fitted with a 20 µL loop, and a SPD-M20A DAD detector (Kyoto, Japan). Data acquisition was performed using Shimadzu LCMS Lab Solution software,

version 3.50 SP2. The column used in this study was a C18 (5 µm, 150 mm x 4.6 mm I.D.) from Fortis BIO Technologies (Cheshire, United Kingdom). The mobile phase composition was MeOH:H_2O (30:70 v/v) with 0.1% of CH_3COOH. The flow rate was 0.5 mL/min and the UV detection wavelength was 254 nm. Analyses were performed at r.t. in an isocratic mode. The elution of the derivative was confirmed by the injection of the standard of NAPHT (**2**).

5.3. Synthesis and purification of mitoxantrone dicarboxylic acid derivative (3)

5.3.1. Synthesis of 4,5-dinitrochrysazin (8)

In a round bottom flask, chrysazin (**7**) (10 g, 42 mmol) was dissolved in 335 mL of TFA. To this solution, cooled in an ice bath and under stirring, 20 equivalents (30.1 g) of $NaNO_2$ were added. The reaction flask was removed from the ice bath and allowed to stir for 54 h. The reaction was monitored by TLC (*n*-hexane:ethyl acetate, 6:4). The reaction mixture was poured into ice and the solution neutralized (pH 6-8) with a 20% sodium hydroxide (NaOH) solution. Then, the precipitate was filtered and dried to furnish a yellow solid (6.56 g, 47%) that was used in the following reaction (3.2.2.) without further purification. 20 mg of the crude product were submitted to a preparative plate chromatography [$(CH_3)_2CO$:chloroform, 1:9] furnishing 7 mg of a yellow solid corresponding to 4,5-dinitrochrysazin (**8**).

4,5-Dinitrochrysazin (**8**):

mp >300 ºC; IR (KBr) υmax: 3447, 3080, 1676, 1604, 1526, 1354, 1256; ^{1}H-NMR (DMSO-d6, 300.13 MHz): δ (ppm) = 8.13 (2H, *d*, *J*=9.1, H-2 and H-7); 7.52 (2H, *d*, *J*= 9.1, H-3 and H-6).

5.3.2. Synthesis of 1,8-dimetoxychrysazin (21)

To a stirred solution of chrysazin (**7**) (5.4 g, 22.4 mmol) in DMF (50 mL) K_2CO_3 (25 g, 181 mmol) and DMS (78 mL, 822 mmol) were added and heated to 100 ºC slowly

over a 3-days period. The reaction mixture was then poured into water, filtered, and the solid thus obtained was washed with water and dried to furnish the crude product. The crude product (10.9 g) was purified by flash column chromatography using isocratic system *n*-hexane:ethyl acetate (8:2). The fractions containing the major product were gathered and the solvent evaporated to furnish a yellow solid corresponding to 1,8-dimethoxychrysazin (**21**) in 0.17 % yield.

1,8-Dimethoxychrysazin (**21**):

mp 155-158 ºC; IR (KBr) υmax: 2984, 1674, 1600, 1467,1212; ^{1}H-NMR (DMSO-d6, 300.13 MHz) δ(ppm) = 7.76 (2H, *t*, *J*=7.9, H-3 and H-6), 7.69 (2H, *dd*, *J*=7.9, *J*=1.0 H-4 and H-5), 7.54 (2H, *dd*, *J*=7.9, *J*=1.0, H-2 and H-7), 3.92 (6H, *s*, CH_3-1 and CH_3-2).

5.3.3. Synthesis of 4,5-diaminochrysazin (9)

A mixture of 6.56 g (19.8 mmol) of 4,5-dinitrochrysazin (**8**) and 11.99 g (0.053 mol) of stannous chloride in 75 mL of absolute ethanol was heated at 70 °C under nitrogen. The reaction was monitored by TLC with *n*-hexane:ethyl acetate (6:4). By TLC analysis, after 30 min, the starting material disappeared and the solution was allowed to cool down and then poured into ice. The pH was made slightly basic (pH 8) by addition of 5% aqueous $NaHCO_3$ and the resulting basic mixture was kept 1 h under stirring. The aqueous mixture was extracted with ethyl acetate (3 x 100 mL), the organic phase was washed with brine (2 x 100 mL), treated with charcoal (1 g) and dried over Na_2SO_4. Evaporation of the solvent furnish a purple solid, 4,5-diaminochrysazin (**9**) with 8.4% yield that was used in the following reaction without further purification procedures.

5.3.4. Synthesis of leuco-1,4,5,8-tetrahydroxyanthraquinone (6)

To a NaOH aqueous solution (10%, 140 mL) containing *n*-butanol (6.9 mL), 4,5-diaminochrysazin (**9**) (5.30 g, 19.6 mmol) was added with stirring. The resulting dark-purple suspension was stirred for 15 min, while a stream of N_2 was bubbled through it. $Na_2S_2O_4$ (4.60 g, 2.6 mmol) was gradually added with stirring, while the reaction mixture was heated and maintained at 60 ºC for 48 h. The reaction was monitored by TLC with *n*-hexane:ethyl acetate (6:4). After being cooled to r.t., the reaction mixture was

neutralized with HCl (1M) and allowed to stand. The resulting precipitate was collected by filtration, washed with water and dried in vacuum at 50 ºC to give a dark-purple product that was used in the following reaction without further purification procedures in 78% yield.

5.3.5. Protection of *N*-(2-aminoethyl)glycine (22)

Conditions 1) *N*-(2-aminoethil)glycine **22** (250 mg, 2.12 mmol) was dissolved in *tert*-butanol (3.4 mL) and concentrated H_2SO_4 (0.240 mL) was added. The reaction mixture was heated at reflux with magnetic stirring for 3 h. The reaction was monitored by MeOH:trimethylamine (10:0.1). After no detection of the starting reagent by TLC analysis, the *tert*-butanol excess was evaporated and the solution was poured into water and extracted with diethyl ether (3 x 100 mL). The organic phases were combined, washed successively with $NaHCO_3$ (100 mL) and water (100 mL) and dehydrated with Na_2SO_4. The organic phase was evaporated to furnish a white solid.

Conditions 2) *N*-(2-aminoethil)glycine **22** (250 mg, 2.12 mmol) was dissolved in MeOH (3.4 mL) and concentrated H_2SO_4 (0.240 mL) was added. The reaction mixture was heated at reflux with magnetic stirring for 3 h. The reaction was monitored by MeOH:trimethylamine (10:0.1). After no detection of the starting reagent by TLC analysis, the excess of MeOH was evaporated and the solution was poured into water and extracted with diethyl ether (3 x 100 mL). The organic phases were combined, washed successively with $NaHCO_3$ (100 mL) and water (100 mL) and dehydrated with Na_2SO_4. The organic phase was evaporated to furnish a brown oil.

Conditions 3) *N*-(2-aminoethil)glycine **22** (100 mg, 0.85 mmol) was taken in a round bottom flask. Freshly distilled TMSCl (292 µL, 2.4 mmol) was added slowly with magnetic stirring. Then, MeOH (3 mL) was added and the resulting solution was stirred at r.t.. After the completion of reaction, monitored by TLC with MeOH:trimethylamine (10:0.1), the reaction mixture was concentrated on a rotary evaporator to give a white solid.

5.3.6. Synthesis of intermediate 25

A stirred solution of *tert*-butyl *N*-(2-aminoethyl)glycinate (**23**, 1.5 g) in Py (5 mL) was purged with nitrogen for 30 min. Following, leuco-1,4,5,8-tetrahydroxyanthraquinone (**6**) (0.5 g) was added, and the temperature was maintained at 0-5 ºC for 30 min. Then, the reaction mixture was heated to 55 ºC for 7 h and monitored by TLC (chloroform:MeOH:formic acid, 9:1:0.1). The solvent was evaporated and the solid was immediately mixed with ethanol (30 mL) and a stream of dry air was bubbled through the mixture at 60 ºC for 48 h with stirring. This reaction also was monitored by TLC (chloroform:MeOH:formic acid, 9:1:0.1). The solvent was evaporated to dryness, and the resulting product was purified by flash chromatography column (ethyl acetate:MeOH, 7:3) to furnish a dark blue solid di-*tert*-buthyl-2,2'-(1,4-dihydroxy-5,8- bis{[2-(2-hydroxyethyl)amino]ethyl} amino-9,10-anthracenedione)-diacetate (**25**) 1.3 g (83 %).

Di-*tert*-buthyl-2,2'-(1,4-dihydroxy-5,8- bis{[2-(2-hydroxyethyl)amino]ethyl} amino-9,10-anthracenedione)-diacetate (**25**):

mp 92-96 ºC; IR (KBr) υmax: 3442, 2924, 1685, 1650, 1522, 1206, 1139; ^{1}H-NMR (DMSO-d6, 300.13 MHz) δ(ppm) = 13.48 (2H, *s*, OH-1 e OH-4), 7.94 (2H, *s*, NH-2' and NH-2''), 7.28 (1H, *s*, H-2), 7.19 (1H, *s*, H-3), 6.84 (1H, *s*, H-6), 6.77 (1H, *s*, H-7), 3.16 (4H, *s*, H-3' e H-3''), 2.51 (4H, *m*, H-1' and H-1''), 1.99 (4H, *m*, H-2' and H-2''), 1.75 (18H, *m*, CH_3-4' e CH_3-4'').

5.3.7. Synthesis of dicarboxylic acid (3) of mitoxantrone

To the solid obtained in the previous reaction in CH_2Cl_2 (9 mL) at 0 ºC was added dropwise TFA (5 mL) and the mixture was stirred at 0 ºC for 5 h. The reaction was monitored by TLC with chloroform:MeOH:formic acid (8:2:0.1). The solvent was coevaporated with CH_2Cl_2 (2 x 25 mL) under nitrogen at 40 ºC. The crude product was purified by column chromatography on sephadex LH-20 with CH_2Cl_2:MeOH, 9:1. The fractions containing the desirable product were gathered, the solvent evaporated to furnish a blue solid corresponding to 1,4-dihydroxy-5,8- bis{[2-(2-hydroxyethyl)amino]ethyl} amino-9,10-anthracene dione-diacetic acid (**3**). The resulting

product was filtered with nitrocellulose and hydrophilic VDF filters with 0.8 and 0.22 µm pore size, respectively, in 1.7% yield.

HPLC analysis of the product was performed in the same equipment with isocratic sistem 5:5 of eluent B within 30 min (eluent A: 0.1% aqueous solution of CH_3COOH; eluent B: MeOH), using a KINETEX C18 EVO column (2.6 µm, 150 x 4.6 mm I.D.) from USA. The injected volume was 10 µL and was used at a constant flow rate of 0.5 mL/min.

1,4-Dihydroxy-5,8- bis{[2-(2-hydroxyethyl)amino]ethyl} amino-9,10-anthracene dione-diacetic acid (**3**):

mp 155-159 ºC; IR (KBr) υmax: 3443, 2958, 2920, 1740, 1637, 1560, 1282, 1205; ^{1}H-NMR (DMSO-d6, 300.13 MHz) δ(ppm) = 14.65 (2H, *s*, OH-1 e OH-4), 14.54 (2H, *brs*, OH acidic), 10.48 (2H, *brs*, NH-5 e NH-8), 8.50 (2H, *s*, NH-2' e NH-2''), 7.53 (1H, *d*, *J*=9.0, H-2), 7.30 (1H, *d*, *J*=9.0, H-3), 7.15 (1H, *d*, *J*=9.0, H-6), 6.60 (1H, *d*, *J*=9.0, H-7), 3.81 (4H, *s*, H-3' e H-3''), 3.64 (4H, *m*, H-1' e H-1''), 3.50 (under H_2O, *m*, H-2' e H-2'').

5.4. Oxidative reactions to obtain dicarboxylic acid (3)

5.4.1. Oxidation with sodium tungstate

MTX (**1**) (20 mg, 0.045 mmol) was suspended in DMF (5 mL) and Na_2WO_4 (0.026 mg, 0.088 mmol) was added, and heated to 80 °C. To the reaction solution, 30% H_2O_2 (1.4 mL) was slowly added dropwise. The reaction was monitored by TLC with MeOH:formic acid (10:0.1). After 1 h, the reaction solvent was evaporated with a stream nitrogen to 40 ºC and the solid was acidified with HCl 20% (10 mL), and extracted with chloroform (3 x 15 mL). The organic phases were gathered, dried over Na_2SO_4 and the solvent evaporated. The solid thus obtained was dissolved in MeOH and filtrated with Syringe Filter, PTFE, 0.45 µm to furnish 7.6 mg of a purple solid.

HPLC analysis of the product was performed in the same equipment and column that NAPHT (**2**) with linear gradient from 20 to 100% of eluent B within 60 min (eluent A: 0.1% aqueous solution of CH_3COOH; eluent B: MeOH).

HRMS-ESI m/z calc for $C_{22}H_{24}N_4O_8$ $[M+H]^+$ 472.15941 found were: 441.35606; 485.38179; 529.40793; 573.43361; 595.47936.

5.4.2. Oxidation with sodium nitrite

$NaNO_2$ (26.5 mg, 0.38 mmol) was dissolved in 800 µL of H_2SO_4. The oxidizing medium was heated to 120 °C and then MTX (**1**) (10 mg, 0.022 mmol) was added slowly. The reaction was monitored by TLC with MeOH:formic acid (10:0.1). After completion of the oxidation reaction (1 h), the reaction mixture was poured into 10 mL distilled water and extracted with chloroform (3 x 15 mL) and the organic layer was evaporated. The crude extract was dissolved in MeOH and filtrated with Syringe Filter, PTFE, 0.45 µm to furnish 8.5 mg of a brown solid.

HPLC analysis of the product was performed in the same equipment and column that NAPHT (**2**) with linear gradient from 20 to 100% of eluent B within 60 min (eluent A: 0.1% aqueous solution of CH_3COOH; eluent B: MeOH).

HRMS-ESI m/z calc for $C_{22}H_{24}N_4O_8$ $[M+H]^+$ 472.15941 found were: 256.29976; 447.34694; 529.40586; 573.43073.

5.4.3. Chromic acid oxidation

To a 0.15 M solution of starting MTX (**1**) (20 mg) in $(CH_3)_2CO$, a solution containing Jones reagent (180 µL), prepared by dissolving CrO_3 (23 mg) in a mixture of concentrated H_2SO_4 and water (100:64), was added at 0 ºC. Once the addition was finished, the reaction mixture was left stirring for 24 h until most of the starting compound was consumed. The reaction was monitored by TLC (MeOH:formic acid, 10:0.1). The excess of oxidant was destroyed by the addition of 2-propanol. To the reaction mixture, 10 mL of H_2O were added and extracted with 15 mL of chloroform. The organic phase was dried with Na_2SO_4 and the solvent evaporated to furnish a blue solid, which was dissolved in MeOH and filtered with Syringe Filter, PTFE, 0.45 µm to furnish a 2.4 mg of the final product.

HPLC analysis of the product was performed in the same equipment and column that NAPHT (**2**) with linear gradient from 20 to 100% of eluent B within 60 min (eluent A: 0.1% aqueous solution of CH_3COOH; eluent B: MeOH).

HRMS-ESI m/z calc for $C_{22}H_{24}N_4O_8$ $[M+H]^+$ 472.15941 found were: 283.26350; 447.34702; 507.42614; 551.45310; 595.47865; 663.45535.

5.4.4. Oxidation with potassium permanganate

A suspension of MTX (**1**) (5.8 mg, 0.013 mmol) in Py (1.2 mL) was heated at 70°C until a clear, blue-coloured solution was obtained. Then, a 10 % aqueous Na_2CO_3 solution was added and subsequently $KMnO_4$ (4.1 mg, 0.026 mmol) was added. The reaction was monitored by TLC with MeOH:formic acid (10:0.1). After 5 h, the mixture was acidified with HCl 10% and extracted with chloroform (3 x 15 mL) and ethyl acetate (3 x 15 mL). The organic layers were gathered and dried over Na_2SO_4 and after solvent evaporated, no product could be obtained.

5.4.5. Oxidation with potassium ferrocyanide

To a stirred solution of the MTX (**1**) (15 mg, 0.034 mmol) in $(CH_3)_2CO/H_2O$ 1:1 (20 mL), AcONa (10 mL) and the $K_3[Fe(CN)_6]$ solutions (10 mL) were added at r.t. The reaction was monitored by TLC with MeOH:trimethylamine (10:0.1). After 24 h, the mixture was filtered and the aqueous phase was slightly acidified with 20% HCl and diluted with water. The product was extracted with CH_2Cl_2 (3 x 100 mL); the extract was dried with Na_2SO_4 and the solvent was evaporated to dryness. The product was dissolved in MeOH and filtered through a Minisart membrane of 0.8 mm pore size (Millipore) to give a blue solid (4.4 mg).

HPLC analysis of the product was performed in the same equipment and column that NAPHT (**2**) with linear gradient from 20 to 100% of eluent B within 60 min (eluent A: 0.1% aqueous solution of CH_3COOH; eluent B: MeOH).

HRMS-ESI m/z calc for $C_{22}H_{24}N_4O_8$ $[M+H]^+$ 472.15941 found were: 282.27921; 401.28752; 445. 20839; 489.33998; 944.42579.

5.5. Synthesis of acetylated derivatives of mitoxantrone

MTX (**1**) (20 mg, 0.045 mmol) was dissolved in CH_2Cl_2 (0.4 mL) and Py (0.2 mL). Ac_2O (0.021 mL) was then added dropwise and the mixture was stirred at r. t. for 4 h. The obtained solution was diluted with CH_2Cl_2 (20 mL) and washed with 10 % HCl aqueous solution (3 × 25 mL). The organic layer was then dried over Na_2SO_4, and filtered. The solvent was evaporated under reduced pressure and the residue was

purified by preparative TLC using chloroform:MeOH (9:1) as mobile phase to afford 4-hydroxy-5,8- bis{[2-(2-hydroxyethyl)amino]ethyl} amino-9,10-anthracenedion-1-yl acetate (**4**, 38% yield)- and 5,8- bis{[2-(2-hydroxyethyl)amino]ethyl} amino-9,10-anthracenedion-1,4-diyl diacetate (**5**, 21% yield) as blue solids.

HPLC analysis of these products was performed in the same equipment with isocratic sistem 5:5 of eluent B within 30 min (eluent A: 0.1% aqueous solution of CH_3COOH; eluent B: MeOH), using a KINETEX C18 EVO column (2.6 µm, 150 x 4.6 mm I.D.) from USA. The injected volume was 10 µL and was used at a constant flow rate of 0.5 mL/min.

4-Hydroxy-5,8- bis{[2-(2-hydroxyethyl)amino]ethyl} amino-9,10-anthracenedion-1-yl acetate (**4**):

mp 83-89 ºC (deg.); IR (KBr) υmax: 3440, 2957, 2922, 2851, 1738, 1634, 1563, 1464, 1260,1083; ^{1}H-NMR (DMSO-d6, 300.13 MHz) δ(ppm) = 13.48 (1H, *s*, OH-1), 10.38 (2H, *brs*, NH-5 and NH-8), 7.71 (1H, *m*, H-2), 7.69 (1H, *m*, H-3), 7.18-7.16 (2H, *m*, H-6 and H-7), 6.90 (2H, *brs*, NH-2' and NH-2''), 5.33 (2H, *brs*, OH-4' and OH-4''), 4.28 (2H, *m*, H-1' and H-1''), 4.14 (2H, *m*, H-2' and H-2''), 3.76 (2H, *m* H-4' and H-4''), 3.62 (2H, *m*, H-3' and H-3''), 3.51 (3H, *s*, CH_3-1).

5,8-Bis{[2-(2-hydroxyethyl)amino]ethyl}amino-9,10-anthracenedion-1,4-diyldi-acetate (**5**):

mp >124 ºC (deg.); IR (KBr) υmax: 3434, 2921, 2851, 1736, 1640, 1561, 1466, 1173; ^{1}H-NMR (DMSO-d6, 300.13 MHz) δ(ppm) = 10.62 (2H, *s*, H-5 and H-8), 8.52 (2H, *s*, H-2 and H-3), 7.14 (2H, *d*, H-6 and H-7), 6.90 (2H, *brs*, NH-2' and NH-2''), 4.35 (2H, *brs*, OH-4' and OH-4''), 3.62 (under H_2O, *m*, H-1' and H-1''), 3.42 (under H_2O, *m*, H-4' and H-4''), 3.29 (under H_2O, *m*, H-2' and H-2''), 3.27 (under H_2O, *m*, H-3' and H-3''), 2.09 (6H, *s*, CH_3-1 and CH_3-4).

CHAPTER 6

References

CHAPTER 6 - REFERENCES

1. Lin, J. H.; Lu, A. Y., Role of pharmacokinetics and metabolism in drug discovery and development. *Pharmacol Rev* **1997,** *49* (4), 403-49.

2. Baillie, T. A.; Cayen, M. N.; Fouda, H.; Gerson, R. J.; Green, J. D.; Grossman, S. J.; Klunk, L. J.; LeBlanc, B.; Perkins, D. G.; Shipley, L. A., Drug metabolites in safety testing. *Toxicol Appl Pharmacol* **2002,** *182* (3), 188-196.

3. Luffer-Atlas, D., Unique/Major human metabolites: why, how, and when to test for safety in animals. *Drug Metab Rev* **2008,** *40* (3), 447-463.

4. Gibson, G. G.; Skett, P., *Introduction to drug metabolism*. Nelson Thornes: 2001.

5. Fura, A.; Shu, Y.-Z.; Zhu, M.; Hanson, R. L.; Roongta, V.; Humphreys, W. G., Discovering drugs through biological transformation: role of pharmacologically active metabolites in drug discovery. *J Med Chem* **2004,** *47* (18), 4339-4351.

6. Stella, V. J.; Charman, W. N. A.; Naringrekar, V. H., Prodrugs. *Drugs* **1985,** *29* (5), 455-473.

7. Rooseboom, M.; Commandeur, J. N. M.; Vermeulen, N. P. E., Enzyme-catalyzed activation of anticancer prodrugs. *Pharmacol Rev* **2004,** *56* (1), 53-102.

8. Gunaratna, C., Drug metabolism and pharmacokinetcs in drug discovery: a primer for bioanalytical chemists, part I. *Bioanalyt Inc* **2000**, 17-23.

9. Administration., U. S. F. a. D., Guidance for industry: Safety testing of drug metabolites. *FDA: Center for Drug Evaluation and Research* **2006**.

10. Liu, X.; Jia, L., The conduct of drug metabolism studies considered good practice (I): analytical systems and *in vivo* studies. *Curr Drug Metab* **2007,** *8* (8), 815-821.

11. Asha, S.; Vidyavathi, M., Role of human liver microsomes in *in vitro* metabolism of drugs-a review. *Appl Biochem Biotechnol* **2010,** *160* (6), 1699-722.

12. Rodrigues, A. D., Use of *in vitro* human metabolism studies in drug development. An industrial perspective. *Biochem Pharmacol* **1994,** *48* (12), 2147-56.

13. Bjornsson, T. D.; Callaghan, J. T.; Einolf, H. J.; Fischer, V.; Gan, L.; Grimm, S.; Kao, J.; King, S. P.; Miwa, G.; Ni, L.; Kumar, G.; McLeod, J.; Obach, R. S.; Roberts, S.; Roe, A.; Shah, A.; Snikeris, F.; Sullivan, J. T.; Tweedie, D.; Vega, J. M.; Walsh, J.; Wrighton, S. A., The conduct of *in vitro* and *in vivo* drug-drug interaction studies: a pharmaceutical research and manufacturers of america (PhRMA) perspective. *Drug Metab Dispos* **2003,** *31* (7), 815-32.

14. Industry, G. f. Safety testing of drug metabolites.

15. Maharsy, W., Chemotherapy induced cardiotoxicity: facts, breakthroughs, and challenges. *J Med* **2015,** *5* (1), 51-56.

16. Hrynchak, I.; Sousa, E.; Pinto, M.; Costa, V. M., The importance of drug metabolites synthesis: the case-study of cardiotoxic anticancer drugs. *Drug Metab Rev* **2017,** *49* (2), 158-196.

17. Seiter, K., Toxicity of the topoisomerase II inhibitors. *Expert Opin Drug Saf* **2005,** *4* (2), 219-34.

18. Costa, V. M.; Carvalho, F.; Duarte, J. A.; Bastos Mde, L.; Remiao, F., The heart as a target for xenobiotic toxicity: the cardiac susceptibility to oxidative stress. *Chem Res Toxicol* **2013,** *26* (9), 1285-311.

19. Ehninger, G.; Schuler, U.; Proksch, B.; Zeller, K.-P.; Blanz, J., Pharmacokinetics and Metabolism of Mitoxantrone A Review. *Clin Pharmacokinet* **1990,** *18* (5), 365-380.

20. Cheng, C. C.; Zee-Cheng, R. K. Y.; Narayanan, V. L.; Ing, R. B.; Pauli, K. D., The collaborative development of a new family of antineoplastic drugs. *Trends Pharmacol Sci* **1981,** *2*, 223-224.

21. Murdock, K.; Child, R.; Fabio, P.; Angier, R. D.; Wallace, R. E.; Durr, F. E.; Citarella, R., Antitumor agents. 1. 1, 4-Bis [(aminoalkyl) amino]-9, 10-anthracenediones. *J Med Chem* **1979,** *22* (9), 1024-1030.

22. Zee-Cheng, R. K.; Cheng, C., Structure-activity relationship study of anthraquinones: 1, 4-dihydroxy-5, 8-bis [[2-(2-hydroxyethoxy) ethyl] amino]-9, 10-anthracenedione, an analog of an established antineoplastic agent. *J Pharm Sci* **1982,** *71* (6), 708-709.

23. Ellis, G. P.; West, G. B., *Progress in Medicinal Chemistry*. Elsevier Science: 2011.

24. Beijnen, J. H.; Bult, A.; Underberg, W. J. M., Mitoxantrone Hydrochloride. *Analytical Profiles of Drug Substances* **1988,** *17*, 221-258.

25. Chang, P., Synthesis and characterization of anticancer anthraquinones: Ametantrone and mitoxantrone. Part A. *Phys Eng Sci* **1992,** *16* (4), 304-310.

26. Krapcho, A. P.; Getahun, Z.; Avery Jr, K. J., The synthesis of 1, 4-difluoro-5, 8-dihydroxyanthracene-9, 10-dione and ipso substitutions of the fluorides by diamines leading to 1, 4-bis-[(aminoalkyl) amino]-5, 8-dihydroxyanthracene-9, 10-diones. *Synth Commun* **1990,** *20* (14), 2139-2146.

27. De Leoz, M. L. A.; Chua, M. T.; Endoma-Arias, M. A. A.; Concepcion, G. P.; Cruz, L. J., A modified procedure for the preparation of mitoxantrone. *Philippine Journal of Science* **2006,** *135* (2), 83.

28. Mitoxantrone. https://monographs.iarc.fr/ENG/Monographs/vol76/mono76-12.pdf. Accessed 25 May.

29. Crespi, M. D.; Ivanier, S. E.; Genovese, J.; Baldi, A., Mitoxantrone affects topoisomerase activities in human breast cancer cells. *Biochem Biophys Res Commun* **1986,** *136* (2), 521-8.

30. Damiani, R. M.; Moura, D. J.; Viau, C. M.; Caceres, R. A.; Henriques, J. A.; Saffi, J., Pathways of cardiac toxicity: comparison between chemotherapeutic drugs doxorubicin and mitoxantrone. *Arch Toxicol* **2016,** *90* (9), 2063-76.

31. Duthie, S. J.; Grant, M. H., The role of reductive and oxidative metabolism in the toxicity of mitoxantrone, adriamycin and menadione in human liver derived Hep G2 hepatoma cells. *Br J Cancer* **1989,** *60* (4), 566-71.

32. Durr, F. E.; Wallace, R. E.; Citarella, R. V., Molecular and biochemical pharmacology of mitoxantrone. *Cancer Treat Rev* **1983,** *10 Suppl B*, 3-11.

33. Administration, U. S. F. a. D. NOVANTRONE® mitoXANTRONE for injection concentrate. https://www.accessdata.fda.gov/drugsatfda_docs/label/2010/019297s033s034lbl.pdf. Accessed 25 May.

34. Batra, V. K.; Morrison, J. A.; Woodward, D. L.; Siverd, N. S.; Yacobi, A., Pharmacokinetics of mitoxantrone in man and laboratory animals. *Drug Metab Rev* **1986,** *17* (3-4), 311-329.

35. Alberts, D. S.; Peng, Y. M.; Leigh, S.; Davis, T. P.; Woodward, D. L., Disposition of mitoxantrone in cancer patients. *Cancer Res* **1985,** *45* (4), 1879-84.

36. Chiccarelli, F. S.; Morrison, J. A.; Cosulich, D. B.; Perkinson, N. A.; Ridge, D. N.; Sum, F. W.; Murdock, K. C.; Woodward, D. L.; Arnold, E. T., Identification of human urinary mitoxantrone metabolites. *Cancer Res* **1986,** *46* (9), 4858-61.

37. Ehninger, G.; Proksch, B.; Heinzel, G.; Schiller, E.; Weible, K.-H.; Woodward, D. L., The pharmacokinetics and metabolism of mitoxantrone in man. *Invest New Drugs.* **1985,** *3* (2), 109-116.

38. Alberts, D. S.; Peng, Y. M.; Leigh, S.; Davis, T. P.; Woodward, D. L., Disposition of mitoxantrone in patients. *Cancer Treat Rev* **1983,** *10 Suppl B*, 23-7.

39. Yang, X.; Morris, M. E., Pharmacokinetics and biliary excretion of mitoxantrone in rats. *J Pharm Sci* **2010,** *99* (5), 2502-10.

40. Blanz, J.; Mewes, K.; Ehninger, G.; Proksch, B.; Waidelich, D.; Greger, B.; Zeller, K. P., Evidence for oxidative activation of mitoxantrone in human, pig, and rat. *Drug Metab Dispos* **1991,** *19* (5), 871-80.

41. Mewes, K.; Blanz, J.; Ehninger, G.; Gebhardt, R.; Zeller, K. P., Cytochrome P-450-induced cytotoxicity of mitoxantrone by formation of electrophilic intermediates. *Cancer Res* **1993,** *53* (21).

42. Rossato, L. G.; Costa, V. M.; de Pinho, P. G.; Arbo, M. D.; de Freitas, V.; Vilain, L.; de Lourdes Bastos, M.; Palmeira, C.; Remião, F., The metabolic profile of mitoxantrone and its relation with mitoxantrone-induced cardiotoxicity. *Arch Toxicol* **2013,** *87* (10), 1809-1820.

43. Richard, B.; Fabre, G.; De Sousa, G.; Fabre, I.; Rahmani, R.; Cano, J.-P., Interspecies variability in mitoxantrone metabolism using primary cultures of hepatocytes isolated from rat, rabbit and humans. *Biochem Pharmacol* **1991,** *41* (2), 255-262.

44. Mewes, K.; Blanz, J.; Ehninger, G.; Gebhardt, R.; Zeller, K. P., Cytochrome P-450-induced cytotoxicity of mitoxantrone by formation of electrophilic intermediates. *Cancer Res* **1993,** *53* (21), 5135-42.

45. Wolf, C. R.; Macpherson, J. S.; Smyth, J. F., Evidence for the metabolism of mitozantrone by microsomal glutathione transferases and 3-methylcholanthrene-inducible glucuronosyl transferases. *Biochem Pharmacol* **1986,** *35* (9), 1577-81.

46. Ehninger, G.; Proksch, B.; Hartmann, F.; Gärtner, H.-V.; Wilms, K., Mitoxantrone metabolism in the isolated perfused rat liver. *Cancer Chemother Pharmacol* **1984,** *12* (1), 50-52.

47. Panousis, C.; Kettle, A. J.; Phillips, D. R., Neutrophil-mediated activation of mitoxantrone to metabolites which form adducts with DNA. *Cancer Lett* **1997,** *113* (1-2), 173-178.

48. Shipp, N. G.; Dorr, R. T.; Alberts, D. S.; Dawson, B. V.; Hendrix, M., Characterization of experimental mitoxantrone cardiotoxicity and its partial inhibition by ICRF-187 in cultured neonatal rat heart cells. *Cancer Res* **1993,** *53* (3), 550-6.

49. Reis-Mendes, A.; Gomes, A. S.; Carvalho, R. A.; Carvalho, F.; Remiao, F.; Pinto, M.; Bastos, M. L.; Sousa, E.; Costa, V. M., Naphthoquinoxaline metabolite of mitoxantrone is less cardiotoxic than the parent compound and it can be a more cardiosafe drug in anticancer therapy. *Arch Toxicol* **2017,** *91* (4), 1871-1890.

50. Reszka, K.; Kolodziejczyk, P.; William Lown, J., Horseradish peroxidase-catalyzed oxidation of mitoxantrone: spectrophotometric and electron paramagnetic resonance studies. *J Free Radic Biol Med* **1986,** *2* (1), 25-32.

51. Kolodziejczyk, P.; Reszka, K.; Lown, J. W., Enzymatic oxidative activation and transformation of the antitumor agent mitoxantrone. *Free Radic Biol Med* **1988,** *5* (1), 13-25.

52. Reis-Mendes, A. F.; Sousa, E.; De Lourdes Bastos, M.; Costa, V. M., The role of the metabolism of anticancer drugs in their induced-cardiotoxicity. *Curr Drug Metab* **2016,** *17* (1), 75-90.

53. Venn, R. F., *Principles and practice of bioanalysis*. CRC Press: 2008.

54. Brück, T. B.; Brück, D. W., Oxidative metabolism of the anti-cancer agent mitoxantrone by horseradish, lacto-and lignin peroxidase. *Biochimie* **2011,** *93* (2), 217-226.

55. Brück, T. B.; Harvey, P. J., Oxidation of mitoxantrone by lactoperoxidase. *Biochim Biophys Acta* **2003,** *1649* (2), 154-163.

56. Shenkenberg, T. D.; Von Hoff, D. D., Mitoxantrone: a new anticancer drug with significant clinical activity. *Ann Intern Med* **1986,** *105* (1), 67-81.

57. Von Hoff, D. D.; Pollard, E.; Kuhn, J.; Murray, E.; Coltman, C. A., Jr., Phase I clinical investigation of 1,4-dihydroxy-5,8-bis (((2-[(2-hydroxyethyl)amino]ethyl) amino))-9,10-anthracenedione dihydrochloride (NSC 301739), a new anthracenedione. *Cancer Res* **1980,** *40* (5), 1516-8.

58. Paciucci, P. A.; Ohnuma, T.; Cuttner, J.; Silver, R. T.; Holland, J. F., Mitoxantrone in patients with acute leukemia in relapse. *Cancer Res* **1983,** *43* (8), 3919-22.

59. Crossley, R. J., Clinical safety and tolerance of mitoxantrone (Novantrone). *Cancer Treat Rev* **1983,** *10 Suppl B*, 29-36.

60. Smith, I. E., Mitoxantrone (novantrone): a review of experimental and early clinical studies. *Cancer Treat Rev* **1983,** *10* (2), 103-115.

61. Creamer, J. D.; Mortimer, P. S.; Powles, T. J., Mitozantrone-induced onycholysis. A series of five cases. *Clin Exp Dermatol* **1995,** *20* (6), 459-461.

62. Ballestrero, A.; Ferrando, F.; Garuti, A.; Basta, P.; Gonella, R.; Esposito, M.; Vannozzi, M. O.; Sorice, G.; Friedman, D.; Puglisi, M.; Brema, F.; Mela, G. S.; Sessarego, M.; Patrone, F., High-dose mitoxantrone with peripheral blood progenitor cell rescue: toxicity, pharmacokinetics and implications for dosage and schedule. *Br J Cancer* **1997,** *76* (6), 797-804.

63. Feldman, E. J.; Seiter, K.; Damon, L.; Linker, C.; Rugo, H.; Ries, C.; Case, D. C., Jr.; Beer, M.; Ahmed, T., A randomized trial of high- vs standard-dose mitoxantrone with cytarabine in elderly patients with acute myeloid leukemia. *Leukemia* **1997,** *11* (4), 485-9.

64. Pratt, C. B.; Vietti, T. J.; Etcubanas, E.; Sexauer, C.; Krance, R. A.; Mahoney, D. H.; Patterson, R. B., Novantrone for childhood malignant solid tumors. A pediatric oncology group phase II study. *Invest New Drugs* **1986,** *4* (1), 43-8.

65. Rossato, L. G.; Costa, V. M.; Dallegrave, E.; Arbo, M.; Silva, R.; Ferreira, R.; Amado, F.; Dinis-Oliveira, R. J.; Duarte, J. A.; de Lourdes Bastos, M.; Palmeira, C.; Remiao, F., Mitochondrial cumulative damage induced by mitoxantrone: late onset cardiac energetic impairment. *Cardiovasc Toxicol* **2014,** *14* (1), 30-40.

66. Dores-Sousa, J. L.; Duarte, J. A.; Seabra, V.; Bastos Mde, L.; Carvalho, F.; Costa, V. M., The age factor for mitoxantrone's cardiotoxicity: multiple doses render the adult mouse heart more susceptible to injury. *Toxicology* **2015,** *329*, 106-19.

67. Henderson, I. C.; Allegra, J. C.; Woodcock, T.; Wolff, S.; Bryan, S.; Cartwright, K.; Dukart, G.; Henry, D., Randomized clinical trial comparing mitoxantrone with doxorubicin in previously treated patients with metastatic breast cancer. *J Clin Oncol* **1989,** *7* (5), 560-71.

68. Aapro, M. S.; Alberts, D. S.; Woolfenden, J. M.; Mackel, C., Prospective study of left ventricular function using radionuclide scans in patients receiving mitoxantrone. *Invest New Drugs* **1983,** *1* (4), 341-7.

69. van Dalen, E. C.; van der Pal, H. J.; Bakker, P. J.; Caron, H. N.; Kremer, L. C., Cumulative incidence and risk factors of mitoxantrone-induced cardiotoxicity in children: a systematic review. *Eur J Cancer* **2004,** *40* (5), 643-52.

70. Zingler, V. C.; Nabauer, M.; Jahn, K.; Gross, A.; Hohlfeld, R.; Brandt, T.; Strupp, M., Assessment of potential cardiotoxic side effects of mitoxantrone in patients with multiple sclerosis. *Eur Neurol* **2005,** *54* (1), 28-33.

71. Paul, F.; Dorr, J.; Wurfel, J.; Vogel, H. P.; Zipp, F., Early mitoxantrone-induced cardiotoxicity in secondary progressive multiple sclerosis. *J Neurol Neurosurg Psychiatry* **2007,** *78* (2), 198-200.

72. Peak, S.; Tsao-Wei, D. D.; Chamberlain, M. C., Mitoxantrone in secondary progressive multiple sclerosis: a review of toxicity in 41 patients. **2007**.

73. Marriott, J. J.; Miyasaki, J. M.; Gronseth, G.; O'connor, P. W., Evidence Report: The efficacy and safety of mitoxantrone (Novantrone) in the treatment of multiple sclerosis Report of the Therapeutics and Technology Assessment Subcommittee of the American Academy of Neurology. *Neurology* **2010,** *74* (18), 1463-1470.

74. Fox, E. J., Management of worsening multiple sclerosis with mitoxantrone: a review. *Clin Ther* **2006,** *28* (4), 461-74.

75. Carvalho, F. S.; Burgeiro, A.; Garcia, R.; Moreno, A. J.; Carvalho, R. A.; Oliveira, P. J., Doxorubicin-Induced Cardiotoxicity: From Bioenergetic Failure and Cell Death to Cardiomyopathy. *Med Res Rev* **2014,** *34* (1), 106-135.

76. Li, S. J.; Rodgers, E. H.; Grant, M. H., The activity of xenobiotic enzymes and the cytotoxicity of mitoxantrone in MCF 7 human breast cancer cells treated with inducing agents. *Chem Biol Interact* **1995,** *97* (2), 101-18.

77. Panousis, C.; Kettle, A. J.; Phillips, D. R., Oxidative metabolism of mitoxantrone by the human neutrophil enzyme myeloperoxidase. *Biochem Pharmacol* **1994,** *48* (12), 2223-30.

78. Rossato, L. G.; Costa, V. M.; Vilas-Boas, V.; de Lourdes Bastos, M.; Rolo, A.; Palmeira, C.; Remiao, F., Therapeutic concentrations of mitoxantrone elicit energetic imbalance in H9c2 cells as an earlier event. *Cardiovasc Toxicol* **2013,** *13* (4), 413-25.

79. Rao, V. A.; Zhang, J.; Klein, S. R.; Espandiari, P.; Knapton, A.; Dickey, J. S.; Herman, E.; Shacter, E. B., The iron chelator Dp44mT inhibits the proliferation of cancer cells but fails to protect from doxorubicin-induced cardiotoxicity in spontaneously hypertensive rats. *Cancer Chemother Pharmacol* **2011,** *68* (5), 1125-1134.

80. Torres, V. M.; Simic, V. D., Doxorubicin-Induced Oxidative Injury of Cardiomyocytes - Do We Have Right Strategies for Prevention? In *Cardiotoxicity of Oncologic Treatments*, Fiuza, M., Ed. InTech: Rijeka, 2012; p Ch. 5.

81. Herman, E. H.; Zhang, J.; Hasinoff, B. B.; Clark Jr, J. R.; Ferrans, V. J., Comparison of the Structural Changes Induced by Doxorubicin and Mitoxantrone in the Heart, Kidney and Intestine and Characterization of the Fe(III)-mitoxantrone Complex. *J Mol Cell Cardiol* **1997,** *29* (9), 2415-2430.

82. Zhang, S.; Liu, X.; Bawa-Khalfe, T.; Lu, L.-S.; Lyu, Y. L.; Liu, L. F.; Yeh, E. T. H., Identification of the molecular basis of doxorubicin-induced cardiotoxicity. *Nat Med* **2012,** *18* (11), 1639-1642.

83. Aminkeng, F.; Bhavsar, A. P.; Visscher, H.; Rassekh, S. R.; Li, Y.; Lee, J. W.; Brunham, L. R.; Caron, H. N.; van Dalen, E. C.; Kremer, L. C.; van der Pal, H. J.; Amstutz, U.; Rieder, M. J.; Bernstein, D.; Carleton, B. C.; Hayden, M. R.; Ross, C. J., A coding variant in RARG confers susceptibility to anthracycline-induced cardiotoxicity in childhood cancer. *Nat Genet* **2015,** *47* (9), 1079-84.

84. Agarwal, S.; Jangir, D. K.; Mehrotra, R., Spectroscopic studies of the effects of anticancer drug mitoxantrone interaction with calf-thymus DNA. *J Photochem Photobiol B* **2013,** *120*, 177-82.

85. Chang, P.; Cheng, C. C., An Improved Practical Synthesis of Leuco-1,4,5,8-Tetrahydroxyanthraquinone. *Synth Commun* **1995,** *25* (13), 1893-1900.

86. Murdock, K. C.; Durr, F. E., 1,4-Bis(substituted-amino)-5,8-dihydroxyanthraquinones and leuco bases thereof. US4197249 A: 1980.

87. Barros, A. I. R. N. A.; Silva, A. M. S., Efficient Synthesis of Nitroflavones by Cyclodehydrogenation of 2′-Hydroxychalcones and by the Baker-Venkataraman Method. *Monatsh Chem.* **2006,** *137* (12), 1505-1528.

88. Kumar, P. H.; Rao, G. V.; Narayanaswamy, B.; Reddy, G. C., An Improved Method for the Preparation of 4,5-Diaminochrysazin. *Synth Commun* **2010,** *40* (23), 3501-3505.

89. Li, J.; Sha, Y., A Convenient Synthesis of Amino Acid Methyl Esters. *Molecules* **2008,** *13* (5), 1111.

90. Lundt, B. F.; Johansen, N. L.; Vølund, A.; Markussen, J., Removal of t-butyl and t-butoxycarbonyl protecting groups with trifluoroacetic acid. *Int J Pept Protein Res* **1978,** *12* (5), 258-268.

91. Noyori, R.; Aoki, M.; Sato, K., Green oxidation with aqueous hydrogen peroxide. *Chem Commun* **2003,** (16), 1977-1986.

92. Murahashi, S.; Mitsui, H.; Shiota, T.; Tsuda, T.; Watanabe, S., Tungstate-catalyzed oxidation of secondary amines to nitrones.. alpha.-Substitution of secondary amines via nitrones. *J Org Chem* **1990,** *55* (6), 1736-1744.

93. Gavit, R. S.; Laddha, K., Synthesis of 4, 5-dihydroxy-9, 10-dioxoanthracene-2-benzyl carboxylate ester from rhein. *Int J Pharm Sci Res* **2010,** *1* (10), 60.

94. Malik, E. M.; Baqi, Y.; Müller, C. E., Syntheses of 2-substituted 1-amino-4-bromoanthraquinones (bromaminic acid analogues)–precursors for dyes and drugs. *Beilstein J Org Chem* **2015,** *11*, 2326.